Directed Polymers in a Random Medium

Joanna Cook

Submitted for the degree of
Doctor of Philosophy

Department of Physics
University of Edinburgh
1990

Abstract

After a brief introduction to the problem of directed polymers in a random medium, several aspects of the problem are addressed in more detail.

It is possible to show that, in high enough dimension and above a certain temperature, a phase exists in which the free energy is given by the annealed free energy, with probability one. The proof of this statement is extended to obtain upper and lower bounds on the temperature of the transition between this phase and a low temperature phase and hence prove the existence of the phase transition.

The mean field solution is reviewed and a method of obtaining high dimension expansions around it is presented. The method uses the idea of "n-tree approximations" as a systematic way of including the correlations present in finite dimensions. Using this approach $1/d$ expansions are obtained for the free energy, transition temperature, transverse fluctuations and overlaps. The results are consistent with the existence of a finite upper critical dimension above which the behaviour is of a mean field nature.

Directed polymers are then considered on disordered hierarchical lattices. On these lattices the problem reduces to the study of the stable laws that occur when one combines random variables in a nonlinear way. Recursion relations for various properties of the system are obtained, which are studied using numerical and analytical techniques. It is possible to obtain a perturbative expansion for the free energy, overlaps and non-integer moments of the partition function.

Finally, a generalisation of the standard directed polymer problem is considered, in which one allows the walks to contribute positive and negative weights to the partition sum. The solution of the mean field limit of this problem is obtained indirectly, by using the relationship between the mean field directed polymer problem, the random energy model (REM) and the generalised random energy model (GREM). Numerical simulations are presented which give good confirmation of the analytical predictions. It is observed that in solving this generalised polymer problem one has also obtained a formula for the largest Lyapounov exponent of a product of large, sparse random matrices.

Declaration

This thesis contains work that I have done in collaboration with Dr. Bernard Derrida.

The results of chapters 2 and 4 have been published in

J. Cook and B. Derrida, *J. Stat. Phys.* **57** 89 (1989).

The contents of sections 3.2.1–3.2.6 have appeared in

J. Cook and B. Derrida, *Europhys. Lett.* **10** 195 (1989).

J. Cook and B. Derrida, *J. Phys. A* **23** 1523 (1990).

The work presented in chapter 5 has been submitted for publication as

J. Cook and B. Derrida, Saclay preprint S Ph T 90/055,
submitted to *J. Stat. Phys.*

Before commencing the research presented in this thesis I had been working on neural networks with the late Dr. Elizabeth Gardner. The results of this research have been published in

J. Cook, *J. Phys. A* **22** 2057 (1989).

21/6/1990.

Acknowledgements

I should like to thank Bernard Derrida, in collaboration with whom this work was done, for all his helpful support and advice.

Grateful thanks are also due to the other members of the Service de Physique Théorique de Saclay, who made my stay in Paris so pleasant. Equal acknowledgement must go to the members of the theory group of the physics department of Edinburgh University, especially my supervisor David Wallace, for their help and encouragement.

Finally, I should like to thank Alan Bray, Joachim Krug, Wolfgang Renz, Herbert Spohn and Yonathan Shapir for interesting discussions.

Contents

Chapter 1

Introduction

The problem of directed polymers in a random medium has recently become the focus of a great deal of research. The interest in this particular disordered system has yielded many new results over the last few years. This thesis seeks to explore a few of these advances.

This introductory chapter aims to set the problem of directed polymers in a random medium in context, prior to the more detailed discussion of several aspects of the problem in the following chapters.

1.1 Formulation of the problem

The problem of directed polymers in a random medium can be defined either on some regular lattice or in the continuum.

1.1.1 Directed polymers on a lattice

The directed polymer problem can be formulated on a lattice as follows. For each bond, ij, of some regular lattice one chooses a random energy, ϵ_{ij}, according to a given probability distribution $\rho(\epsilon_{ij})$. One then considers all the directed walks

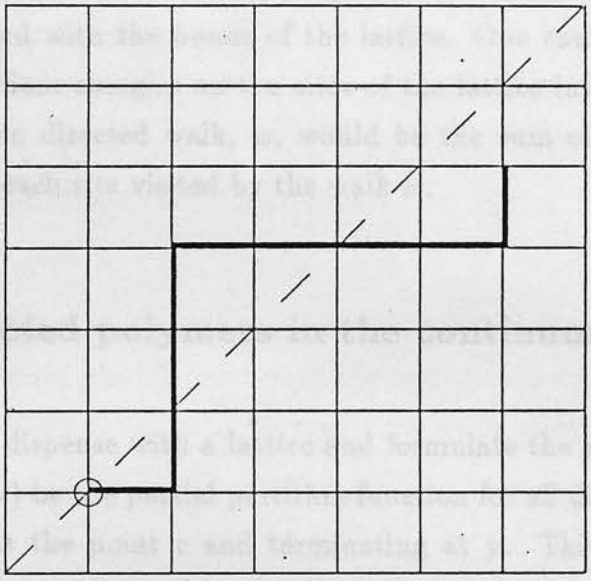

Figure 1.1: One walk, shown in bold, directed along the $(1,1)$ direction of the square lattice.

of length L emanating from a fixed origin on the lattice. A directed walk is, by definition, one stretched along a single longitudinal direction, with fluctuations in the transverse directions only. For example, suppose that one chooses the regular lattice to be the square lattice. It is then convenient to select the $(1,1)$ direction to be that along which the walks are directed. This is illustrated in Figure 1.1. The bold line shows one example of a directed walk of nine steps on a square lattice and the dotted line indicates the direction along which the walks are to be directed. One can see that the directed walk can only move up or to the right, not down or to the left. The energy, E_w, of a given directed walk, w, is defined to be the sum of the energies associated with all the bonds visited by walk w, i.e.

$$E_w = \sum_{ij \in w} \epsilon_{ij} \tag{1.1}$$

where the summation runs over all the bonds, ij, contained in the directed walk w. It is now possible to define a partition function for the problem as the sum of the Boltzmann weights of all the directed walks of length L,

$$Z_L(\mathbf{r}) = \sum_w \exp\left[-E_w/T\right]. \tag{1.2}$$

The summation includes all directed walks of length L emanating from the point $\mathbf{r}$ and T is the temperature.

In this formulation of the problem the quenched random variables (the energies, ϵ_{ij}) are associated with the bonds of the lattice. One could equally well choose to place the random energies on the sites of the lattice instead. In this case the energy of a given directed walk, w, would be the sum of the random energies associated with each site visited by the walk w.

1.1.2 Directed polymers in the continuum

It is possible to dispense with a lattice and formulate the problem in the continuum. Let $Z_t(\mathbf{r},\mathbf{y})$ be the partial partition function for all directed walks of length t commencing at the point $\mathbf{r}$ and terminating at $\mathbf{y}$. This can be written as a path integral, by combining the usual Wiener measure for random walks in $d-1$ spatial dimensions with a random potential, $V_t(\mathbf{x})$. The direction along which the polymers are directed corresponds to the time parameter in the random walk.

$$Z_t(\mathbf{r},\mathbf{y}) = \int_{\mathbf{x}(0)=\mathbf{r}}^{\mathbf{x}(t)=\mathbf{y}} \mathcal{D}\mathbf{x}(s) \exp\left[-\int_0^t ds\, \left\{\frac{1}{2\sigma}\dot{\mathbf{x}}^2(s) - V_s(\mathbf{x}(s))\right\}\right] \tag{1.3}$$

The potential $V_s(\mathbf{x})$ should have no correlations in $\mathbf{x}$ or s. However, it is convenient to choose the potential to be Gaussian with a variance

$$\langle V_s(\mathbf{x}) V_{s'}(\mathbf{x}')\rangle = K(\mathbf{x}-\mathbf{x}')\delta(s-s') \tag{1.4}$$

where $K(\mathbf{x})$ has a behaviour at $\mathbf{x}=\mathbf{0}$ and when $|\mathbf{x}| \to \infty$ that ensures a well-defined path integral. The condition that the potential be white noise (i.e. that $K(\mathbf{x}) = \eta^2\delta(\mathbf{x})$, with η a constant) will be imposed later. Throughout, $\langle\cdots\rangle$ will be used to denote an average over disorder, as distinct from an ensemble or thermal average, which will be denoted by $\overline{\cdots}$. The total partition function for all directed polymers of length t emanating from $\mathbf{r}$, $Z_t(\mathbf{r})$, can be obtained by summing over all the possible end points, $\mathbf{y}$

$$Z_t(\mathbf{r}) = \int d\mathbf{y}\, Z_t(\mathbf{r},\mathbf{y}). \tag{1.5}$$

Notice that the partial partition function, $Z_t(\mathbf{r},\mathbf{0})$, satisfies the equation for diffusion in a random potential,

$$\frac{\partial Z_t(\mathbf{r},\mathbf{0})}{\partial t} = \frac{\sigma}{2}\nabla^2 Z_t(\mathbf{r},\mathbf{0}) + V_t(\mathbf{r}) Z_t(\mathbf{r},\mathbf{0}). \tag{1.6}$$

So, $Z_t(\mathbf{r}, 0)$ could also be thought of as the wavefunction of a particle in a random potential in imaginary time.

1.2 Quantities of interest

Now that the problem of directed polymers in a random medium has been defined, one needs to consider what properties of the system will be of interest. These can be grouped into three categories: thermal properties, geometrical properties and overlaps.

The thermal properties of the system can be obtained from the partition function. To construct the phase diagram, one is interested in calculating the free energy, F

$$F = \lim_{L \to \infty} -T \frac{\langle \ln Z_L \rangle}{L} \tag{1.7}$$

where L is the length of the polymer. Notice that, as one is dealing with quenched random variables, one has to average the logarithm of the partition function, not the partition function itself. Once one has the free energy, other thermal properties, such as the specific heat, can be obtained from its derivatives with respect to temperature. Another quantity which one can consider is the sample-to-sample fluctuation of the ground state energy. This is found to scale, for large L, as the length of the polymer to an exponent ω,

$$\langle E_{GS}^2 \rangle - \langle E_{GS} \rangle^2 \sim L^{2\omega} \tag{1.8}$$

where the ground state energy of the polymer, $(-T \ln Z_L)_{T=0}$, is denoted by E_{GS}.

Although directed walks of length L always take a fixed number of steps in the direction along which they are directed, they are free to fluctuate in the transverse directions. Hence, when exploring the geometrical properties of the system, one should consider the transverse displacement, $\mathbf{R}_w$, of a given directed walk, w. This is illustrated in figure 1.2 for two directed walks, w_1 and w_2, in the geometry of figure 1.1 (i.e. the square lattice directed along the diagonal). The average transverse displacement, $\langle \overline{\mathbf{R}} \rangle$, will always be zero for reasons of symmetry. However, the fluctuations of the transverse displacement do not, in general, vanish. Two

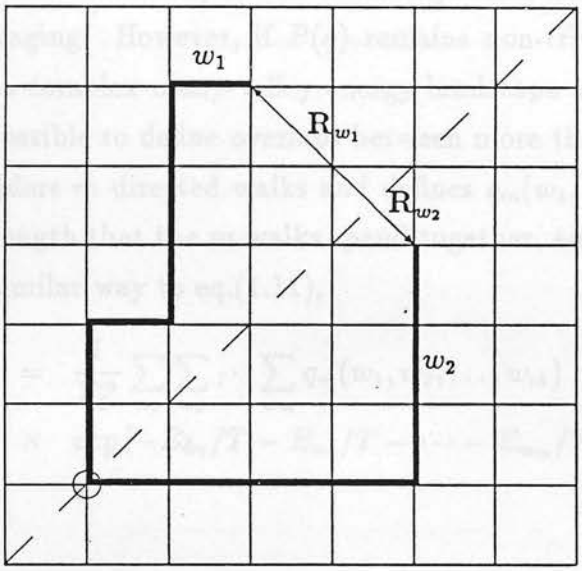

Figure 1.2: The transverse displacements, $\mathbf{R}_{w_1}$ and $\mathbf{R}_{w_2}$, of the two walks w_1 and w_2.

types of fluctuations of the transverse displacement can be defined: thermal and disorder fluctuations. The thermal fluctuations are defined as

$$\langle \overline{\mathbf{R}^2} \rangle - \langle \overline{\mathbf{R}}^2 \rangle \sim L. \tag{1.9}$$

These will always scale as the length of the polymer, L (see section 3.3.3). The disorder transverse fluctuations, on the other hand, scale with a non-trivial exponent, ν

$$\langle \overline{\mathbf{R}}^2 \rangle = \left\langle \frac{1}{Z_L^2} \left(\sum_w \mathbf{R}_w \exp\left[-E_w/T\right] \right)^2 \right\rangle \sim L^{2\nu}. \tag{1.10}$$

Lastly, one can consider the overlaps for such a system. Let $q(w_1, w_2)$ be the fraction of their lengths that two directed walks, w_1 and w_2, of length L spend together. The overlap, q, between two polymers can then be defined as

$$q = \frac{1}{Z_L^2} \sum_{w_1} \sum_{w_2} q(w_1, w_2) \exp\left[-E_{w_1}/T - E_{w_2}/T\right]. \tag{1.11}$$

This overlap is analagous to the overlaps that occur in the mean field theory of spin glasses [1], and should provide one with information about the statistical properties of the energy landscape. A useful quantity to be able to compute is the probability distribution of the overlaps, $P(q)$. If this distribution becomes

trivial (i.e. a single delta function) in the thermodynamic limit ($L \to \infty$), the overlaps are self-averaging. However, if $P(q)$ remains non-trivial this indicates that the system has a complex many-valley energy landscape and broken replica symmetry [1]. It is possible to define overlaps between more than two walks. For example, if one considers m directed walks and defines $q_m(w_1, w_2, \ldots, w_m)$ to be the fraction of their length that the m walks spend together, an overlap $q(m)$ can be constructed in a similar way to eq.(1.11),

$$\begin{aligned} q(m) &= \frac{1}{Z_L^m} \sum_{w_1} \sum_{w_2} \cdots \sum_{w_m} q_m(w_1, w_2, \ldots, w_m) \\ &\times \exp\left[-E_{w_1}/T - E_{w_2}/T - \cdots - E_{w_m}/T\right]. \end{aligned} \tag{1.12}$$

1.3 Motivations

Before embarking upon a summary of what is known about the problem of directed polymers in a random medium, it is reasonable to ask why this particular disordered system might be of interest.

The recent attention devoted to the directed polymer problem has probably been partly inspired by the many other systems to which it is closely related. To see the relationships between these different systems it is convenient to consider the continuum version of the problem, eqs.(1.3)–(1.5) [2,3]. As was pointed out in section 1.1.2, the partial partition function for directed walks commencing at a point $\mathbf{r}$ and terminating after a length t at the point $\mathbf{0}$, $Z_t(\mathbf{r}, \mathbf{0})$, satisfies an imaginary time Schrödinger equation. As the total partition function, $Z_t(\mathbf{r})$, is a linear combination of these partial partition functions this remains true for $Z_t(\mathbf{r})$

$$\frac{\partial Z_t(\mathbf{r})}{\partial t} = \frac{\sigma}{2} \nabla^2 Z_t(\mathbf{r}) + V_t(\mathbf{r}) Z_t(\mathbf{r}). \tag{1.13}$$

If $\mathbf{r}$ is taken to be one-dimensional (i.e. $\mathbf{r} = r$), then this equation can be interpreted as describing a one-dimensional interface, without overhangs, in a two-dimensional Ising model with random nearest-neighbour interactions [4,5]. The quantity t then parametrizes the distance along the interface and r gives the displacement of the interface from some reference line. σ can then be interpreted as a surface tension, favouring a flat interface, whilst $V_t(r)$ represents the effect

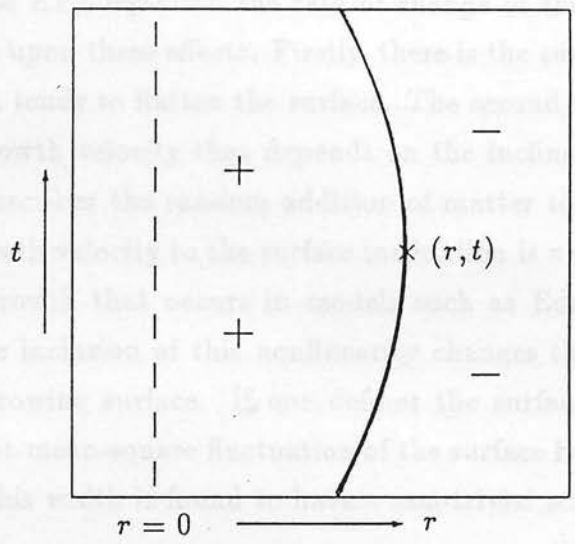

Figure 1.3: Diagram to show how eq.(1.13) can be interpreted as the equation describing an interface in a two-dimensional Ising model.

of the random bonds, which tend to roughen the interface. In this interpretation $Z_t(r)$ is a measure of the probability of finding the interface at the point (r,t), see figure 1.3. So the directed polymer problem in dimension $1+1$ is equivalent to an interface in a two-dimensional random-bond Ising model. (The spatial dimension of the polymer problem will always be specified in the form $1+1$, $2+1$, $3+1$, etc., where the first digit denotes the number of transverse directions and the "+1" indicates the direction along which the polymers are directed.)

If one makes the substitution

$$Z_t(\mathbf{r}) = \exp\left[\, h_t(\mathbf{r})/\sigma \,\right] \tag{1.14}$$

in eq.(1.13) one obtains the equation

$$\frac{\partial h_t(\mathbf{r})}{\partial t} = \frac{\sigma}{2}\nabla^2 h_t(\mathbf{r}) + \frac{1}{2}(\nabla h_t(\mathbf{r}))^2 + \sigma V_t(\mathbf{r}). \tag{1.15}$$

This equation, known as the Kardar-Parisi-Zhang (KPZ) equation [2], was introduced in an attempt to describe the profile of a growing surface. It is believed to apply to many models of surface growth, including the Eden model [6] and ballistic deposition [7]. The quantity $h_t(\mathbf{r})$ is now interpreted as the height of the

surface above some reference. r defines the position along the surface and t is now the time. In the KPZ equation the rate of change of the height of the growing surface depends upon three effects. Firstly, there is the surface tension term, as in eq.(1.13), which tends to flatten the surface. The second term in eq.(1.15) allows for a surface growth velocity that depends on the inclination of the surface and the last term describes the random addition of matter to the deposit. The term relating the growth velocity to the surface inclination is necessary to take account of the lateral growth that occurs in models such as Eden growth and ballistic deposition. The inclusion of this nonlinearity changes the characteristics of the profile of the growing surface. If one defines the surface to have a width, W, given by the root-mean-square fluctuation of the surface height around its average position, then this width is found to have a non-trivial scaling behaviour [8,9]

$$W = N^{\alpha} f(\frac{h}{N^z})$$

$$\begin{aligned} f(x) &\to \text{const.} && \text{for } x \to \infty \\ f(x) &\sim x^{\alpha/z} && \text{for } x \to 0 \end{aligned} \tag{1.16}$$

where N indicates the length of the substrate on which the growth occurs. If the nonlinear term is omitted, the equation can be solved by Fourier transforms [10], and in dimension $d'+1$ (i.e. a d'-dimensional substrate) one can show that the exponents α and z are given by

$$\alpha = \frac{2-d'}{2} \qquad \text{for } d' \leq 2 \tag{1.17}$$

$$z = 2\,. \tag{1.18}$$

However, the inclusion of the nonlinearity changes the exponents. The exponents characterising the width of the growing surface, α and z, are related to the exponents ω and ν which characterise the fluctuations of the ground state energy and disorder transverse fluctuations respectively.

$$\omega = \frac{\alpha}{z} \tag{1.19}$$

$$\nu = \frac{1}{z} \tag{1.20}$$

These relationships can be understood when one notices that the average height of the growing surface corresponds to the logarithm of the partition function of the

polymer, see eq.(1.14), and therefore scales as the polymer length. The relevant scale for the height is $h \sim N^z$. The substrate size, N, corresponds to transverse displacements of the polymer, which scale as the polymer length to an exponent ν. This gives eq.(1.20). The width of the growing surface corresponds to the sample-to-sample fluctuations of the logarithm of the partition function for the polymer, which scale as the polymer length to an exponent ω. Hence, from the scaling form, one recovers eq.(1.19). The problem of directed polymers in a random medium is therefore essentially equivalent to many models of surface growth. In studying the former, one might hope to gain valuable information about the latter problem. In particular, if one can obtain the polymer exponents ω and ν, one immediately knows the scaling behaviour of the width of the growing surface, and if one knows the free energy of the polymer problem, one knows the average growth velocity of the growing surface. (A recent review of the kinetic roughening of surfaces and its relation to the problem of directed polymers in a random medium can be found in [11].)

If one returns to the KPZ equation and makes the substitution

$$\mathbf{v}_t(\mathbf{r}) = -\nabla h_t(\mathbf{r}), \tag{1.21}$$

it is transformed into Burgers's equation [12] with an added noise term,

$$\frac{\partial \mathbf{v}_t}{\partial t} + (\mathbf{v}_t.\nabla)\mathbf{v}_t = \frac{\sigma}{2}\nabla^2\mathbf{v}_t - \sigma\nabla V_t. \tag{1.22}$$

Burgers's equation is well-known in fluid dynamics as describing vorticity-free compressible fluid flow. The added noise term acts as a random stirring force. Burgers's equation is interesting in itself, as it is one of the simplest types of non-linear evolution equations and can be solved exactly, the nonlinearity producing shock wave solutions. A variant of Burgers's equation with added noise is also believed to describe the long time limit of the Sivashinski equation for flame fronts [13].

In addition to these direct mappings of the directed polymer problem on to problems of interfaces, surface growth and fluid dynamics, there are several other interesting aspects. Directed polymers in a random medium are a simple and easily formulated example of a disordered system. One might hope to be able to learn more about disordered systems in general by studying this particular case. As will

be shown later (chapter 3), the mean field limit of the directed polymer problem can be solved [14], yielding an unexpectedly simple form for the thermal properties. It is possible to obtain the exact solution, which has broken replica symmetry, without recourse to the replica method [15]. The problem is therefore an ideal candidate with which to try to investigate whether Parisi's scheme of replica symmetry breaking [16,17] is relevant in finite dimensional systems. Although Parisi's mean field theory for spin glasses is now well accepted, its relevance to the spin glass in finite dimension remains controversial. It is believed by some [18], that a Parisi-type solution with broken replica symmetry should be valid above some finite upper critical dimension. Others [19,20], however, hold the view that a Parisi solution is only relevant in the mean field limit, there being no finite upper critical dimension. Attempts at obtaining a high dimension expansion for spin glasses are hampered by the complexity of the mean field solution itself [21,22]. A first step towards a better understanding of finite dimensional spin glasses could be to try to understand the directed polymer in finite dimension, which has a much simpler mean field solution.

The mean field directed polymer problem is related to a travelling wave equation [14]. Similar travelling wave equations occur in problems of pattern formation [23,24]. It would be interesting to have an improved understanding of these equations representing the invasion of an unstable phase by a stable phase. Also the mean field version of directed polymers in a random medium has come to the attention of probability theorists, under the guise of the "first death" problem [25]. One constructs a family tree beginning with a single progenitor who dies at time $t = 0$. Each person on the tree has a lifetime u, distributed with some given distribution function. On dying, each person is replaced by j newly-born offspring with probability p_j. One takes all the members of the tree to be independent. The r^{th} generation consists of the offspring of the $(r-1)^{\text{th}}$ generation, the progenitor being the 0^{th} generation. The "first death" problem is to calculate at what time a death first occurs in the r^{th} generation. This can be viewed as the optimisation problem of finding the shortest possible time to reach the r^{th} generation.

Recently, a generalisation of the directed polymer problem has been introduced [26] in an attempt to understand the properties of hopping conductivity in random media. Consider the Nguyen, Spivak and Shklovskii (NSS) model of hopping con-

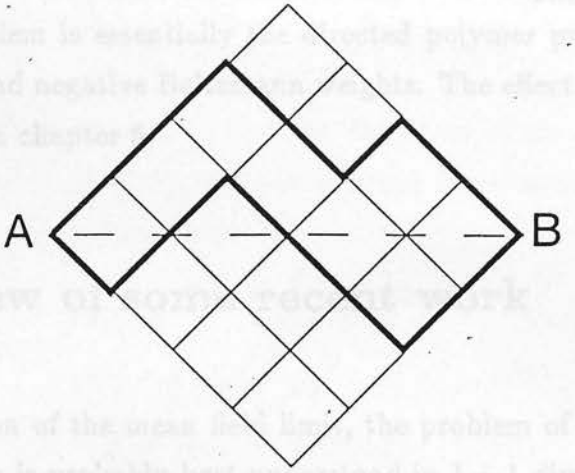

Figure 1.4: The geometry of the NSS model . Two directed walks between A and B are shown.

ductivity [27,28]. This is an Anderson tight-binding model, with the Hamiltonian

$$\mathcal{H} = \sum_i \epsilon_i a_i^\dagger a_i + V \sum_{\langle ij \rangle} (a_i^\dagger a_j + a_i a_j^\dagger) \tag{1.23}$$

on a square lattice. The on-site energies ϵ_i are assumed to be independent random variables, taking the value $+U$ with probability p and $-U$ with probability $1-p$. The hopping term in eq.(1.23) is taken to be the same for all nearest-neighbour pairs. Suppose one is interested in finding the conductivity between two sites A and B, as shown in figure 1.4. This will be proportional to the square modulus of the matrix element, I, connecting these sites (see [28]). Each step along the path from A to B introduces a factor V/U into the overall matrix element, so if one takes the limit $V \ll U$, the matrix element will be dominated by the walks directed along the line AB. Two such directed walks are shown in figure 1.4. Hence, one can write the matrix element I as

$$I = V(\frac{V}{U})^{L-1} \sum_w \prod_{i \in w} \zeta_i \tag{1.24}$$

where A and B are separated by L steps, the summation includes all directed walks from A to B and $\zeta_i = U/\epsilon_i = \pm 1$ [28]. Eq.(1.24) looks very similar to the definition of the partition function for the polymer problem (eq.(1.2)). In the

directed polymer case, each walk contributes its Boltzmann weight, $\exp[-E_w/T]$, to the sum, whereas here each walk contributes $V^L U^{1-L} \prod_{i \in w} \zeta_i$. So this hopping conductivity problem is essentially the directed polymer problem generalised to include positive and negative Boltzmann weights. The effect of this generalisation will be explored in chapter 5.

1.4 Review of some recent work

With the exception of the mean field limit, the problem of directed polymers in a random medium is probably best understood in $1+1$ dimensions. In this case a replica solution [29] and the mapping on to Burgers's equation [5] show that the exponents ω and ν take the values $1/3$ and $2/3$ respectively, the system always being in a strong coupling phase. An exponent identity, connecting ω and ν, is known to be valid in all dimensions [3,30,31]. Hence, once one knows one of these two exponents, the other can be inferred. A dynamic renormalisation group analysis of Burgers's equation with noise [32] and the KPZ equation [31] has tried to investigate the problem in dimensions above $1+1$, as has a recent functional renormalisation group approach [33,34,35]. In addition to these analytic approaches, there have been several numerical investigations of the problem aimed at evaluating the exponents ω and ν [36,37,38], or calculating the thermal properties of the system [39]. This section presents a summary of some of these approaches to the problem of directed polymers in a random medium.

1.4.1 The replica approach in 1+1 dimensions [29]

In order to obtain the free energy of the system one wants to perform the disorder average of the logarithm of the partition function. This difficulty is often avoided in disordered systems by using the replica trick [15],

$$\langle \ln Z_t \rangle = \lim_{n \to 0} \frac{\langle Z_t^n \rangle - 1}{n}. \tag{1.25}$$

In fact one can sometimes obtain more information from $\langle Z_t^n \rangle$ than just the free energy by using its cumulant expansion,

$$\langle Z_t^n \rangle = \exp\left[\sum_{i=1}^{\infty} \frac{n^i}{i!} C_i(\ln Z_t)\right] \tag{1.26}$$

where C_i is the i^{th} cumulant. Using the definition of the partition function in the continuum, eqs.(1.3)–(1.5), one can perform the Gaussian integrals over the random potential, $V_t(\mathbf{r})$, to obtain

$$\begin{aligned} \langle Z_t^n(\mathbf{r}) \rangle \;=\; & \int_{\mathbf{x}_1(0)=\mathbf{r}} \mathcal{D}\mathbf{x}_1(s) \int_{\mathbf{x}_2(0)=\mathbf{r}} \mathcal{D}\mathbf{x}_2(s) \cdots \int_{\mathbf{x}_n(0)=\mathbf{r}} \mathcal{D}\mathbf{x}_n(s) \\ & \exp\Big[-\int_0^t ds\Big\{\frac{1}{2\sigma}(\dot{\mathbf{x}}_1^2 + \dot{\mathbf{x}}_2^2 + \ldots + \dot{\mathbf{x}}_n^2) - \frac{nK(0)}{2} \\ & - \sum_{i<j} K(\mathbf{x}_i(s) - \mathbf{x}_j(s))\Big\}\Big]. \end{aligned} \tag{1.27}$$

(Notice that this path integral is not well-defined if $K(\mathbf{x}) = \delta(\mathbf{x})$.) From eq.(1.27) one can see that $\langle Z_t^n(\mathbf{r}) \rangle$ satisfies an n-particle imaginary time Schrödinger equation,

$$\frac{\partial \langle Z_t^n(\mathbf{r}) \rangle}{\partial t} = -\left(-\frac{\sigma}{2}\sum_{i=1}^{n} \nabla_i^2 - \sum_{i<j} K(\mathbf{x}_i - \mathbf{x}_j)\right) \langle Z_t^n(\mathbf{r}) \rangle. \tag{1.28}$$

In the thermodynamic limit ($t \to \infty$) the ground state will dominate, with $\langle Z_t^n(\mathbf{r}) \rangle$ behaving as

$$\langle Z_t^n(\mathbf{r}) \rangle \sim \exp\left[-E_n t\right] \tag{1.29}$$

where E_n is the ground state energy of the Schrödinger operator, $\mathcal{H}$, on the right-hand side of eq.(1.28). If we now take the random potential to have no spatial correlations, i.e. $K(\mathbf{x}) = \eta^2 \delta(\mathbf{x})$, this Schrödinger operator becomes

$$\mathcal{H} = -\frac{\sigma}{2}\sum_{i=1}^{n} \nabla_i^2 - \eta^2 \sum_{i<j} \delta(\mathbf{x}_i - \mathbf{x}_j). \tag{1.30}$$

In $1+1$ dimensions, the ground state energy and wavefunction of this operator can be found using the Bethe ansatz [29], to yield

$$E_n = -\frac{\eta^4}{24\sigma} n(n^2 - 1). \tag{1.31}$$

So, comparing eqs.(1.26),(1.29) and (1.31), one sees that the first three cumulants of the logarithm of the partition function are given by

$$\begin{aligned} \lim_{t\to\infty} \frac{1}{t} C_1(\ln Z_t) &= -\frac{\eta^4}{24\sigma} \\ \lim_{t\to\infty} \frac{1}{t} C_2(\ln Z_t) &= 0 \\ \lim_{t\to\infty} \frac{1}{t} C_3(\ln Z_t) &= \frac{\eta^4}{4\sigma}. \end{aligned} \tag{1.32}$$

One can write $\ln Z_t$ as

$$\ln Z_t = at + bt^{\omega},$$

where a is a constant of order one, b is a fluctuating quantity of order one and ω is the energy fluctuation exponent. Substituting this form for $\ln Z_t$ into eqs.(1.32) one can conclude that the exponent ω must take the value $1/3$. The other exponent, ν, can then be inferred using the exponent identity eq.(1.48), to be discussed later.

Recently there have been attempts to extract more information from this method [40,41], but one is hampered by not knowing the other eigenfunctions of the operator $\mathcal{H}$ of eq.(1.30). In higher dimension the ground state energy of this operator cannot be found using the Bethe ansatz and is not known.

1.4.2 The Burgers's equation mapping in 1+1 dimensions [5]

In section 1.3 it was noticed that the continuum version of the directed polymer problem could be mapped on to Burgers's equation with added noise

$$\frac{\partial \mathbf{v}_t}{\partial t} + (\mathbf{v}_t.\nabla)\mathbf{v}_t = \frac{\sigma}{2}\nabla^2\mathbf{v}_t - \sigma\nabla V_t. \tag{1.33}$$

In 1+1 dimensions ($\mathbf{v}_t(\mathbf{r}) = v_t(x)$), this equation possesses an invariant probability distribution, $P(\{v_t(x)\})$, given by Gaussian white noise,

$$P(\{v_t(x)\}) \propto \exp\left[-\frac{1}{2\sigma\eta^2}\int dx\, v_t^2(x)\right]. \tag{1.34}$$

One way to see this is to discretize eq.(1.33) in the form

$$\begin{aligned} v_{t+\Delta t}(x) - v_t(x) &= \frac{\sigma\Delta t}{2(\Delta x)^2}\left(v_t(x+\Delta x) - 2v_t(x) + v_t(x-\Delta x)\right) \\ &- \frac{\Delta t}{6\Delta x}\left[v_t(x+\Delta x)\left(v_t(x) + v_t(x+\Delta x)\right) - v_t(x-\Delta x)\left(v_t(x-\Delta x) + v_t(x)\right)\right] \\ &- \frac{\sigma\Delta t}{\Delta x}\left(V_t(x+\Delta x) - V_t(x)\right) \end{aligned} \tag{1.35}$$

and hence derive the Fokker-Planck equation that corresponds to this Langevin equation. One can then show that a discretized version of eq.(1.34) is a stationary

probability distribution. Once one knows this invariant distribution, one can calculate the fluctuations of the free energy of the polymer problem, by noticing that from eqs.(1.21) and (1.14)

$$v = -\sigma \frac{\partial}{\partial x} \ln Z_t(x) \tag{1.36}$$

and that in the steady state $v_t(x)$ will be Gaussian white noise of variance $\sigma\eta^2$. From this one can conclude that

$$\langle (\ln Z_t(x) - \ln Z_t(x'))^2 \rangle = \frac{\eta^2}{\sigma} |x - x'|. \tag{1.37}$$

As the transverse displacement fluctuations and ground state energy fluctuations scale as the polymer length, t, to exponents ν and ω respectively, eq.(1.37) relates these exponents, to give

$$2\omega = \nu. \tag{1.38}$$

Together with the exponent identity to be discussed in the next section this shows that in $1+1$ dimensions $\omega = 1/3$ and $\nu = 2/3$.

1.4.3 Dynamic renormalisation group analysis of the KPZ equation [31, 32]

Dynamic renormalisation group calculations have been carried out on both Burgers's equation with noise and the KPZ equation. Here the case of the KPZ equation will be discussed. (The calculation for Burgers's equation would follow in exactly the same way.) It is convenient to use the KPZ equation in $d = d' + 1$ dimensions in the form

$$\frac{\partial h_t(\mathbf{r})}{\partial t} = \frac{\sigma}{2} \nabla^2 h_t(\mathbf{r}) + \frac{\lambda}{2} (\nabla h_t(\mathbf{r}))^2 + \sigma V_t(\mathbf{r}) \tag{1.39}$$

where the parameter λ has been introduced in front of the nonlinear term ($\lambda = 1$ in eq.(1.15)). After a Fourier transform, introducing a cutoff Λ

$$h_t(\mathbf{r}) = \int_{-\infty}^{\infty} \int_{k<\Lambda} d\Omega \, d^{d'}k \, \frac{1}{(2\pi)^d} \, h(\mathbf{k}, \Omega) \, e^{i(\mathbf{k}.\mathbf{r} - \Omega t)} \tag{1.40}$$

eq.(1.39) becomes

$$\begin{aligned} h(\mathbf{k}, \Omega) &= \sigma G_0(\mathbf{k}, \Omega) V(\mathbf{k}, \Omega) \\ &- \frac{\lambda}{2} G_0(\mathbf{k}, \Omega) \int \int d\Omega' \, d^{d'}q \, \frac{1}{(2\pi)^d} \, \mathbf{q}.(\mathbf{k} - \mathbf{q}) \, h(\mathbf{q}, \Omega') \, h(\mathbf{k} - \mathbf{q}, \Omega - \Omega') \end{aligned} \tag{1.41}$$

where $V(\mathbf{k},\Omega)$ is defined in the same way as $h(\mathbf{k},\Omega)$ (see eq.(1.40)), and a bare propagator

$$G_0(\mathbf{k},\Omega) = \frac{2}{\sigma k^2 - 2i\Omega} \tag{1.42}$$

has been introduced. Eq.(1.41) can now be solved perturbatively in the strength of the nonlinearity, λ. In doing so one obtains perturbation expansions for an effective propagator, an effective nonlinearity strength and an effective width for the random potential. The one-loop terms in these expansions are found to diverge if $d' < 2$. However, the perturbation expansions can be turned into a renormalisation by integrating out wavevectors in the shell $e^{-l}\Lambda \leq q \leq \Lambda$. One then needs to rescale the wavevectors, time and heights according to :

$$\mathbf{k} \to e^{-l}\mathbf{k} \qquad t \to e^{l/\nu}t \qquad h_t(\mathbf{r}) \to e^{\omega l/\nu} h_{\exp[l/\nu]t}(e^l \mathbf{r}) \tag{1.43}$$

This enables one to obtain flow equations for the renormalisation of the surface tension, σ, the width of the random potential, η^2, and the nonlinearity strength, λ, which read to one loop:

$$\frac{d\sigma}{dl} = \sigma\left[\frac{1}{\nu} - 2 + \frac{\lambda^2\eta^2}{\sigma^3}\frac{K_{d'}(2-d')}{d'}\right] \tag{1.44}$$

$$\frac{d\eta^2}{dl} = \eta^2\left[\frac{1}{\nu} - d' - \frac{2\omega}{\nu} + \frac{\lambda^2\eta^2}{\sigma^3}K_{d'}\right] \tag{1.45}$$

$$\frac{d\lambda}{dl} = \lambda\left[\frac{\omega}{\nu} + \frac{1}{\nu} - 2\right] \tag{1.46}$$

where $K_{d'} = (2^{d'-1}\pi^{d'/2}\Gamma(d'/2))^{-1}$.

One now wants to find the fixed points of these equations, eqs.(1.44)–(1.46). One way to do this is to adjust ω and ν so that σ and η^2 are left unchanged, leaving one with the following flow equation for the nonlinearity strength,

$$\frac{d\lambda}{dl} = \frac{2-d'}{2}\lambda + K_{d'}\frac{2d'-3}{d'}\frac{\lambda^3\eta^2}{\sigma^3}. \tag{1.47}$$

The fixed points of this equation can now be investigated. There is a fixed point at $\lambda = 0$. If $d' > 2$ ($d > 2+1$) this fixed point is attractive and one expects a weak coupling phase where the nonlinearity is irrelevant. No attractive strong coupling fixed point of eq.(1.47) exists if $d \geq 2+1$. If $d' < 2$ ($d < 2+1$) the $\lambda = 0$ fixed point is repulsive and one expects that λ should flow to a strong coupling fixed point, controlled by the nonlinearity of the KPZ equation. If $d = 1+1$, eq.(1.47)

possesses such an attractive strong coupling fixed point, at which the exponents take the values $\omega = 1/3$ and $\nu = 2/3$. One must remember that these results are perturbative in the nonlinearity strength, λ, and so will only hold provided that λ is small enough.

From eq.(1.46) one can see that at any strong coupling fixed point one has an exponent identity

$$\omega + 1 = 2\nu. \tag{1.48}$$

This identity is a consequence of an invariance of the KPZ equation. The KPZ equation is invariant under an infinitesimal tilting of the surface through an angle $\mathbf{a}$

$$h \to h + \mathbf{a}.\mathbf{r} \qquad \mathbf{r} \to \mathbf{r} - \lambda t\mathbf{a} \qquad t \to t. \tag{1.49}$$

This invariance is preserved under the renormalisation and this causes corrections to equation (1.46) to vanish to all orders in perturbation theory [31], so that the flow equation for λ, eq.(1.46), is, in fact, exact. The identity eq.(1.48) is, therefore, exact in all dimensions. This identity can also be obtained by assuming a continuum elastic description for the polymers [3] or by a mode-coupling approximation on the KPZ equation [30].

1.4.4 Functional renormalisation of the replicated system [33,34,35]

Another method used to try to extract information about the exponents ω and ν is that of functional renormalisation. In this approach one assumes that the random potential of the continuum formulation is Gaussian with a variance given by eq.(1.4) and one examines the flow of the function $K(\mathbf{x})$ under a renormalisation.

The first step in the calculation is to evaluate the effective action of the replicated Hamiltonian, eq.(1.27), to one-loop order. This effective action can be expressed in terms of an effective Gaussian variance or replica interaction strength, K_{eff}. The second step is then to perform a renormalisation on K_{eff}, integrating out the Fourier modes with frequencies between $\mathrm{e}^{-l}\Lambda$ and Λ (Λ is the cutoff in the Fourier space conjugate to the length of the polymer t), and then carrying out the

compensatory rescaling, $t \rightarrow e^l t$. Under this rescaling the quantity $\sigma^2 K(\mathbf{x})$ scales as

$$\sigma^2 K(\mathbf{x}) \rightarrow e^{(3-4\nu)l}\, \sigma^2 K(e^{\nu l}\, \mathbf{x}). \tag{1.50}$$

Hence one can obtain an approximate flow equation for the renormalisation of the variance of the random potential. This is given by

$$\begin{aligned} \frac{\partial(\sigma^2 K)}{\partial l} &= (3-4\nu)\sigma^2 K + x\nu\sigma^2 K' + \frac{1}{2}(\sigma^2 K'')^2 - \sigma^4 K''(0)K'' \\ &+ \frac{(d-2)}{2x^2}(\sigma^2 K')^2 - \frac{(d-2)}{x}\sigma^4 K''(0)K', \end{aligned} \tag{1.51}$$

where the prime denotes differentiation with respect to the modulus of $\mathbf{x}$, x. The result is given here for the product $\sigma^2 K$, as this corresponds to the quantity considered in [33–35].

The aim is now to determine the fixed point (FP) functions of eq.(1.51). For large values of x one can neglect the nonlinearities and consider only the linear terms in eq.(1.51). The resulting linear equation has two independent solutions, which, for large x, are of the form

$$\sigma^2 K_{FP}(x) \approx x^{(3/\nu-3-d)} \exp\left[\frac{\nu x^2}{2\sigma^2 K''(0)}\right] \quad \text{and} \quad \sigma^2 K_{FP}(x) \approx x^{4-3/\nu}. \tag{1.52}$$

Halpin-Healy [33] has adopted the procedure of matching the algebraic decays of these two solutions to obtain the exponent ν,

$$\nu = \frac{6}{(7+d)}, \tag{1.53}$$

which reproduces the correct answer when $d = 1+1$, but vanishes as $d \rightarrow \infty$, instead of giving the known result $\nu = 1/2$. One interpretation of these results [35] is that eq.(1.53) should be a valid approximation to ν when $\nu \geq 1/2$ ($d \leq 4+1$) and that above this upper critical dimension the exponent sticks at the value $1/2$ in both weak and strong coupling phases.

1.4.5 Numerical simulations

As the analytic approaches of sections 1.4.1 – 1.4.4 have yielded little information about the strong coupling phase outside the mean field limit and dimension $d = 1+1$, numerical calculations have proved particularly valuable.

Dimension	ω	ν	Reference
2+1	0.22 ± 0.02	0.66 ± 0.06 †	Wolf and Kertész [36]
3+1	0.146 ± 0.015	0.61 ± 0.08 †	
2+1	0.250 ± 0.005	0.63 ± 0.02 †	Kim and Kosterlitz [37]
3+1	0.20 ± 0.01		
2+1	0.240 ± 0.001	0.623 ± 0.009 †	Forrest and Tang [38]
3+1	0.180 ± 0.005	0.60 ± 0.03 †	
2+1	0.225 ± 0.005	0.613 ± 0.005	Renz [42]
3+1	0.165 ± 0.010	0.585 ± 0.010	
4+1	0.1 ± 0.1	0.55 ± 0.02	

Table 1.1: Some recent results on the exponents ω and ν († indicates that the errors have been estimated from errors given on the exponents of the growth problem).

The principal effort has been directed at trying to determine the exponents ω and ν. Some of the current best estimates of these exponents are given in table 1.1. It was pointed out in section 1.3 that there exists a mapping from the continuum directed polymer problem to the KPZ equation, eq.(1.15), believed to describe many models of surface growth. This link allows one to obtain the exponents ω and ν from the knowledge of the exponents characterising a growing surface (see eqs.(1.19)–(1.20)). The estimates of ω and ν due to Wolf and Kertész [36], Kim and Kosterlitz [37] and Forrest and Tang [38] were obtained using this approach. (Wolf and Kertész simulated a noise-reduced Eden model, Kim and Kosterlitz a restricted solid-on-solid model and Forrest and Tang a hypercubic stacking model.) The data due to Renz [42] were obtained directly from a study of the directed polymer problem. If $Z_L(\mathbf{r})$ is the partition function for directed polymers of length L emanating from $\mathbf{r}$, one can write a transfer matrix equation connecting the set of partition functions for all the sites $\{\mathbf{r}\}$ on the lattice, $\{Z_L(\mathbf{r})\}$, to that at the next time step $\{Z_{L+1}(\mathbf{r})\}$. This allows one to study the directed polymer problem using transfer matrix methods. Renz exploited this approach to determine the exponents up to dimension $d = 4 + 1$. From their numerical data, Wolf and Kertész and Kim and Kosterlitz have made conjectures on the behaviour of ω and ν with dimension. These are

$$\text{Wolf and Kertész [36]}: \quad \omega = \frac{1}{2d-1} \qquad \nu = \frac{d}{2d-1} \tag{1.54}$$

$$\text{Kim and Kosterlitz [37]} : \omega = \frac{1}{d+1} \qquad \nu = \frac{d+2}{2(d+1)} \tag{1.55}$$

These both agree with the known results in the mean field and $d = 1+1$. However, neither agrees with the recent accurate results of Forrest and Tang [38].

The transfer matrix method has also been used to investigate the thermal properties of directed polymers in a random medium. Derrida and Golinelli [39] evaluated the specific heat and third derivative of the logarithm of the partition function with respect to inverse temperature by transfer matrix techniques. Their results clearly show a phase transition when $d = 3 + 1$, with the expected behaviour observed in the high temperature phase (the nature of the high temperature phase will be discussed in the next chapter), and no transition in dimension $d = 1 + 1$, as expected. The data in dimension $d = 2+1$ indicate a possible phase transition, although the nonlinearity is found to be marginally relevant in the dynamical renormalisation treatment in this dimensionality [31].

1.4.6 Outline of the work to be presented in the following chapters

In addition to the work outlined above, several other results have been obtained on the directed polymer problem and these will be discussed in the following chapters. The nature of the high temperature or weak coupling phase is well understood [43,44] and it is possible to prove the existence of a phase transition for the system in dimension $d \geq 3+1$ [44]. This is discussed in chapter 2. It has been mentioned earlier that the mean field limit of the problem can be solved exactly [14]. This solution, and the high dimension expansion [45,46] that can be performed around it, will be dealt with in chapter 3. One can often gain insight into a statistical mechanical system by the use of real space renormalisation group techniques. This approach has been used, by taking the regular lattice on which the directed polymers exist to be a hierarchical lattice [47,44]. The results obtained on these lattices, on which real space renormalisation is exact, are presented in chapter 4. Finally the problem of directed polymers in a random medium is generalised, as was briefly discussed in section 1.3, to allow positive and negative "Boltzmann

weights". The mean field solution [48] of this generalised model is discussed in chapter 5.

Chapter 2

Bounds on the transition temperature

It has been shown by Imbrie and Spencer [43], that, for the problem of directed polymers in a random medium in sufficiently large dimension and above a certain temperature, there exists a phase characterised by two properties. Firstly it is diffusive, i.e. the disorder transverse fluctuation exponent ν, eq.(1.10), is equal to 1/2 and secondly, with probability one, its free energy is equal to the annealed free energy, i.e.

$$\lim_{L\to\infty} \frac{\ln Z_L}{L} = \lim_{L\to\infty} \frac{\ln \langle Z_L \rangle}{L} \quad \text{with probability 1.} \tag{2.1}$$

In this chapter a slightly different demonstration of eq.(2.1) is given [44]. By extending this calculation, one can obtain bounds on the transition temperature between the low temperature, or strong coupling, phase and the high temperature, or weak coupling, phase in dimension $d \geq 3 + 1$ and hence prove the existence of the transition [44].

2.1 Nature of the high temperature phase

Consider the directed polymer problem defined on some regular lattice, as described in section 1.1.1. To determine the nature of the high temperature phase one needs to evaluate the ratio $\langle Z_L^2 \rangle / \langle Z_L \rangle^2$. This can be written as

$$\frac{\langle Z_L^2 \rangle}{\langle Z_L \rangle^2} = \sum_{n=0}^{L} P_n \left(\frac{\langle \exp\left[-2\epsilon/T\right] \rangle}{\langle \exp\left[-\epsilon/T\right] \rangle^2} \right)^n \tag{2.2}$$

where P_n is the probability that two directed walks have exactly n sites in common. (Here the site randomness version of the problem is considered, but the calculation would follow similarly for bond randomness.) When the two walks occupy the same site they contribute $\langle \exp[-2\epsilon/T] \rangle$ to $\langle Z_L^2 \rangle$, whereas when they occupy different sites they contribute $\langle \exp[-\epsilon/T] \rangle^2$. In the limit $L \to \infty$ the quantity P_n will always take the form

$$\begin{aligned} P_n &= A^{n-1}(1-A) \\ P_0 &= 0 \end{aligned} \tag{2.3}$$

where A is the probability that the two directed walks meet at least twice. The two walks must always meet at least once, as they start from the same point, so $P_0 = 0$. A is a lattice-dependent quantity, and is less than one for all regular lattices in dimension $d \geq 3+1$ [49]. Using eqs.(2.2)–(2.3), one can show that, if $d \geq 3+1$ and the temperature exceeds some value T_2,

$$\lim_{L\to\infty} \frac{\langle Z_L^2 \rangle}{\langle Z_L \rangle^2} = B \tag{2.4}$$

where

$$B = \frac{(1-A)\langle \exp[-2\epsilon/T] \rangle / \langle \exp[-\epsilon/T] \rangle^2}{1 - A\langle \exp[-2\epsilon/T] \rangle / \langle \exp[-\epsilon/T] \rangle^2}. \tag{2.5}$$

The temperature T_2 is given by the temperature at which B diverges. So, T_2 is the solution of

$$\frac{\langle \exp[-2\epsilon/T_2] \rangle}{\langle \exp[-\epsilon/T_2] \rangle^2} = \frac{1}{A}. \tag{2.6}$$

Notice that B diverges at T_2 and decreases as the temperature is raised, towards the limiting value of $B = 1$. If the dimensionality is less than or equal to $2+1$, $A = 1$ and B will diverge at all temperatures.

Given eq.(2.4), it is clear that for any constant, C, the following must hold

$$\lim_{L\to\infty} \left\langle \left(\frac{Z_L}{\langle Z_L \rangle} - C \right)^2 \right\rangle = B - 2C + C^2. \tag{2.7}$$

One can now make use of Chebyschev's inequality and conclude that

$$\text{Prob}\left[\left| \frac{Z_L}{\langle Z_L \rangle} - C \right| < D \right] \geq 1 - \frac{B - 2C + C^2}{D^2}. \tag{2.8}$$

Providing that $D < C$, the fact that $|C - Z_L/\langle Z_L \rangle| < D$ implies that

$$\lim_{L\to\infty} \frac{\ln Z_L}{L} = \lim_{L\to\infty} \frac{\ln \langle Z_L \rangle}{L}. \tag{2.9}$$

One can see this by noting that $|C - Z_L/\langle Z_L\rangle| < D$ means that $C - D \leq Z_L/\langle Z_L\rangle \leq C + D$. So, taking the logarithm, dividing by L and letting $L \to \infty$ gives one eq.(2.9). By maximising the right-hand side of eq.(2.8), one can maximise the probability that eq.(2.9) is true. This is done by letting D approach C from below and setting $C = B$. One then sees that eq.(2.9) is true with a probability of at least $1/B$.

So far this has been valid for any regular lattice in sufficiently high dimension, the lattice-dependence being contained in A. Let us now consider a particular example. Suppose the problem is defined on a $d = d' + 1$ dimensional lattice, such that at each step the polymer occupies one site of a d'-dimensional hypercubic lattice. For a polymer of length L one therefore has a series of L d'-dimensional hypercubic lattices. If the polymer occupies the site $\mathbf{r}$ on the d'-dimensional lattice at step l, it is allowed to visit any of the $2d'$ neighbours of site $\mathbf{r}$ on the d'-dimensional lattice at step $l+1$. The random energies, ϵ, are placed on the sites of the $d-$dimensional lattice. In this geometry one can calculate A using random walk theory [49], to yield

$$\frac{1}{1-A} = \frac{1}{(2\pi)^{d'}} \int dq_1 \cdots \int dq_{d'} \frac{1}{1 - (1/d'^2)(\sum_{\mu=1}^{d'} \cos q_\mu)^2}. \qquad (2.10)$$

So for this lattice, one can show that eq.(2.9) is true with at least a probability $1/B$, where B is given by eq.(2.5) and eq.(2.10).

In fact one can improve on this, by showing that the free energy is given by the annealed free energy with a probability arbitrarily close to one. This can be achieved by removing the first steps of the polymers. For clarity only the specific case defined above will be considered. If $Y(l,n)$ is the partition function of the directed walks of l steps commencing anywhere within a finite d'-dimensional hypercube of linear size $2n$ and one assumes that the support of the energy distribution, $\rho(\epsilon)$, is bounded, with $|\epsilon| < a$, one has the inequality

$$\exp\left[-na/T\right] Y(L-n, \frac{n}{d'}) \; < \; Z_L \; < (2d')^n \exp\left[na/T\right] Y(L-n, n). \qquad (2.11)$$

The upper bound is obtained by noting that $\exp[na/T]$ cannot be smaller than the energy contribution of the first n steps of each walk. Also, after n steps each walk commencing at the origin has to be contained within the d'-dimensional

hypercube of linear size $2n$ centred at the origin and the number of walks reaching each point of this hypercube is certainly less than $(2d')^n$. The lower bound can be derived similarly: the energy contribution of the first n steps of the walks is not smaller than $\exp[-na/T]$ and there is at least one walk reaching each point of the hypercube of linear size $2n/d'$ centred at the origin.

Now $\langle Y^2(L,n)\rangle/\langle Y(L,n)\rangle^2$ can be computed in the same way as $\langle Z_L^2\rangle/\langle Z_L\rangle^2$, to give, for $T > T_2$,

$$\lim_{L\to\infty} \frac{\langle Y^2(L,n)\rangle}{\langle Y(L,n)\rangle^2} = B_n \tag{2.12}$$

where

$$B_n = 1 - Q_n + \frac{\langle \exp[-2\epsilon/T]\rangle/\langle \exp[-\epsilon/T]\rangle^2}{1 - A\langle \exp[-2\epsilon/T]\rangle/\langle \exp[-\epsilon/T]\rangle^2} Q_n \tag{2.13}$$

and Q_n is the probability that two directed walks starting at two randomly selected points in a d'-dimensional hypercube of linear size $2n$ will ever meet. If $d \geq 3+1$ the further apart the starting points are, the smaller the probability that the two directed walks will ever meet. So, by making n large enough, one can make Q_n as small as required, and hence make B_n as close to one as one wishes. So, using reasoning parallel to that behind eq.(2.4) and eqs.(2.7)–(2.9), one can show that for $T > T_2$ (see eq.(2.6))

$$\lim_{L\to\infty} \frac{\ln Y(L,n)}{L} = \lim_{L\to\infty} \frac{\ln \langle Y(L,n)\rangle}{L} \qquad \text{with prob. at least} \quad 1/B_n \tag{2.14}$$

It only remains to notice that

$$\langle Y(L,n)\rangle = (2n)^{d'} \langle Z_L\rangle \tag{2.15}$$

and use the inequality eq.(2.11) and eq.(2.14) to prove, by taking n to be as large as desired, that, for $d \geq 3+1$ and $T > T_2$ (see eq.(2.6))

$$\lim_{L\to\infty} \frac{\ln Z_L}{L} = \lim_{L\to\infty} \frac{\ln \langle Z_L\rangle}{L} \qquad \text{with probability 1.} \tag{2.16}$$

So, one has demonstrated that the free energy in the high temperature phase is given, with probability one, by the annealed free energy.

Knowing the analytic form of the free energy, one can compute other thermal properties in the high temperature phase, such as the specific heat and entropy, with probability one. For example, differentiating the free energy with respect to

temperature, one sees that the entropy, S, is given for the geometry defined above by

$$S = \ln(2d') + \ln\langle \exp[-\epsilon/T] \rangle + \frac{\langle \epsilon \exp[-\epsilon/T] \rangle}{T\langle \exp[-\epsilon/T] \rangle} \quad \text{with probability 1 .} \quad (2.17)$$

2.2 Obtaining the bounds

In the preceding section, the nature of the high temperature phase has been established and it has been shown that a high temperature phase exists above a temperature T_2, given by eq.(2.6), when the dimension $d \geq 3 + 1$. Notice that this does not imply that there is a phase transition at T_2. It is perfectly possible for the high temperature phase, characterised by eq.(2.16), to extend below this temperature.

It has been shown above that the entropy of this high temperature phase is given, for the particular case under discussion, by eq.(2.17). The entropy of any lattice model cannot be negative. One can therefore conclude that a phase with free energy given by eq.(2.16) cannot exist below the temperature, T_1, at which the entropy given by eq.(2.17) vanishes.

So, in dimension $d \geq 3 + 1$ one has bounds on the transition temperature, T_c, between a low temperature phase and the high temperature phase characterised by eq.(2.16). For $d \geq 3 + 1$

$$T_1 \leq T_c \leq T_2 \quad (2.18)$$

where T_2 is given by eq.(2.6) and T_1 is the temperature at which the annealed entropy vanishes. One has therefore proved the existence of a phase transition in $d \geq 3 + 1$ dimensions. In dimension $d = 2 + 1$ one can only conclude that if a transition to this high temperature phase exists, it must lie above T_1.

It has been assumed above that there exists a $T_1 > 0$ for all choices of $\rho(\epsilon)$. This will be so for most, but not all, distributions. Clearly if one chooses a single delta function for $\rho(\epsilon)$, and so has no disorder, the annealed entropy will not vanish. Also, if one considers a percolation distribution, $\rho(\epsilon) = p\delta(\epsilon + J) + (1 - p)\delta(\epsilon - J)$,

for values of p above the percolation threshold the annealed entropy will not vanish and one has no lower bound on the transition temperature.

The proof leading to eq.(2.18) can, in principle, be extended to any lattice realisation of the directed polymer problem. Changing the lattice and particular distribution of random energies would merely alter the precise values of T_1 and T_2. As an example, consider the geometry defined in section 2.1 and take the random energies to have a Gaussian distribution of unit width. One can then obtain explicit values for T_1 and T_2 in different dimensions [49]. One finds that

$$\begin{aligned} 0.6 &\leq T_c && \text{if } d = 2+1 \\ 0.528 &\leq T_c \leq 0.963 && \text{if } d = 3+1 \\ (2\ln(2d'))^{-1/2} &\leq T_c \leq (\ln(2d'))^{-1/2} && \text{for } d = d'+1 \text{ large} \end{aligned} \tag{2.19}$$

In the limit $d \to \infty$ (mean field) one finds that the true value of T_c is equal to the lower bound [14].

Chapter 3

The mean field limit and the 1/d expansion

The problem of directed polymers in a random medium can be solved exactly in the mean field limit [14], yielding relatively simple expressions for the thermal properties of the system. The solution can be obtained without recourse to the replica method, despite the fact that the low temperature phase is characterised by broken replica symmetry. Using the novel idea of " n-tree " approximations [45,46], it is possible to expand about this mean field limit and obtain $1/d$ expansions for many properties of the system. This chapter is principally concerned with the method and results of the $1/d$ expansion for the directed polymer problem. As a prelude to this, the mean field solution itself is first considered.

3.1 The mean field limit

A mean field version of the problem of directed polymers in a random medium can be solved exactly [14], for any distribution of disorder, by taking the regular lattice to be a branch of a tree (see fig. 3.1). Let the tree have a coordination number $K+1$ ($K=2$ in fig. 3.1). As usual, for each bond, ij, of the lattice one chooses a random energy, ϵ_{ij}, according to a given distribution $\rho(\epsilon_{ij})$. (The discussion will be restricted to bond randomness, although site randomness could be treated similarly.) This mean field problem can be solved using an analogy with travelling waves [14,46], or by a replica method [50]. Both of these approaches are outlined below. The solution can also be obtained by using results known on the

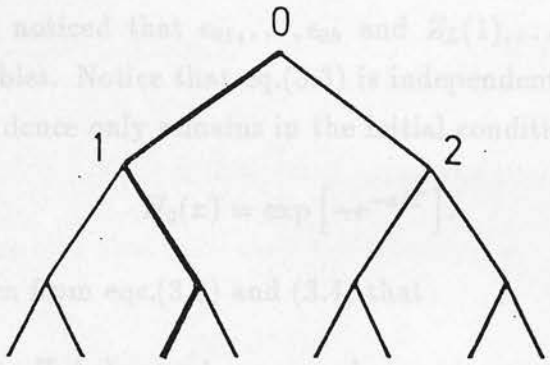

Figure 3.1: A directed walk, shown in bold, on a tree with $K = 2$.

generalised random energy model (GREM)[51]. The close relationship between the mean field directed polymer problem and the GREM will be discussed in chapter 5.

3.1.1 Travelling wave approach

Consider the mean field problem as defined above. If $Z_L(0)$ is the partition function of the K^L directed walks of length L starting at 0, defined by eq.(1.1) and eq.(1.2), one can write a recursion relation connecting Z_L and Z_{L+1} :

$$Z_{L+1}(0) = \sum_{i=1}^{K} \mathrm{e}^{-\epsilon_{0i}/T} Z_L(i) \tag{3.1}$$

where $Z_L(i)$ is the partition function of the walks in the i^{th} branch and ϵ_{0i} is the energy of the bond connecting the origin to the i^{th} branch. The energies, ϵ_{ij}, are independent random variables and so the partition function itself is random. It is therefore natural to consider a generating function of Z_L, $H_L(x)$, defined by:

$$H_L(x) = \left\langle \exp\left[-\mathrm{e}^{-x/T} Z_L\right] \right\rangle . \tag{3.2}$$

Using $H_L(x)$ the recursion eq.(3.1) takes the simple form

$$H_{L+1}(x) = \left[\int \rho(\epsilon) H_L(x+\epsilon)\, d\epsilon\right]^K \tag{3.3}$$

where it has been noticed that $\epsilon_{01}, \ldots, \epsilon_{0k}$ and $Z_L(1), \ldots, Z_L(K)$ are independent random variables. Notice that eq.(3.3) is independent of temperature. The temperature dependence only remains in the initial condition,

$$H_0(x) = \exp\left[-e^{-x/T}\right]. \tag{3.4}$$

It can easily be seen from eqs.(3.2) and (3.4) that

$$\begin{aligned} H_L(x) &\to 1 \qquad \text{when} \quad x \to +\infty \\ H_L(x) &\to 0 \qquad \text{when} \quad x \to -\infty. \end{aligned} \tag{3.5}$$

Hence $H_L(x)$ has the shape of a wave front. Equation (3.3) is a travelling wave equation, belonging to a class of nonlinear equations of the diffusion-reaction type, and has properties similar to those of the K.P.P. (Kolmogorov-Petrovsky-Piscounov) equation [52],

$$\frac{\partial H}{\partial L} = \frac{\partial^2 H}{\partial x^2} + H^2 - H\,. \tag{3.6}$$

Finding the solution of the travelling wave equation, eq.(3.3) or eq.(3.6), for large L, is not simple. However, it has been shown, by Hammersley [25] for eq.(3.3) and by Bramson [52] for eq.(3.6), that for large L, the solutions of these equations become travelling waves, W, which move with velocity v,

$$H_L(x) = W(x - vL - c(L)) \tag{3.7}$$

where $c(L)/L \to 0$ as $L \to \infty$.

In general the exact form of W is not known, but the analytic expression of the velocity is easy to obtain. The velocity of the wave, v, depends upon the initial condition. For an initial condition of the form

$$\begin{aligned} H_0(x) &= 1 - \exp\left[-\gamma x\right] \qquad x \to +\infty \\ &= 0 \qquad\qquad\qquad\quad x \to -\infty \end{aligned} \tag{3.8}$$

with $H_0(x)$ a monotonic function, it has been shown [52,25] that the velocity is given by

$$\begin{aligned} v &= G_1(\gamma) && \text{if } \gamma \leq \gamma_{\min} \\ &= G_1(\gamma_{\min}) = v_{\min} && \text{if } \gamma \geq \gamma_{\min} \end{aligned} \tag{3.9}$$

where

$$G_1(\gamma) = \frac{1}{\gamma} \ln \left[K \int \rho(\epsilon) \mathrm{e}^{-\gamma\epsilon} d\epsilon \right] \tag{3.10}$$

and $\gamma_{\min}$ is the value of γ that minimises the velocity, i.e.

$$\frac{d}{d\gamma} G_1(\gamma) \Big|_{\gamma_{\min}} = 0. \tag{3.11}$$

($G_1(\gamma)$ has a single minimum: this can be shown by using the fact that the second derivative of $\gamma G_1(\gamma)$ with respect to γ is always positive.) From eqs.(3.9)–(3.11), one sees that the exponential decay, γ, of the initial condition controls the velocity of the travelling waves. If $\gamma < \gamma_{\min}$ the velocity varies continuously with γ, whereas if $\gamma \geq \gamma_{\min}$ the velocity remains fixed at its minimal value, $v_{\min}$.

These properties of the travelling waves (eqs.(3.7)–(3.11)) can be mapped on to properties of the partition function. From eq.(3.2), one sees that the distribution of $\ln Z_L$ is concentrated near the place where the wave front is located. This implies, from eq.(3.7), that $-v$ can be identified with the free energy per unit length of the system, and so

$$\begin{aligned} \lim_{L\to\infty} \frac{T}{L} \langle \ln Z_L \rangle &= G_1(1/T) && T \geq T_c \\ &= G_1(\gamma_{\min}) && T \leq T_c \end{aligned} \tag{3.12}$$

where

$$T_c \gamma_{\min} = 1. \tag{3.13}$$

From eq.(3.12), one sees that the entropy vanishes in the whole of the low temperature phase, so that the system is completely frozen. One can conclude from eq.(3.7) that the width of the probability distribution of $\ln Z_L$ must be of order one and this means that the energy fluctuation exponent, defined by eq.(1.8), $\omega = 0$. It is not, however, possible to obtain an explicit expression for the ground state energy fluctuations, as this would require the knowledge of the shape of the travelling wave.

3.1.2 Replica approach

One can consider the same mean field problem using a replica approach. The free energy will be calculated using the replica trick [15],

$$\lim_{L\to\infty}\lim_{n\to 0}\frac{\ln\langle Z_L^n\rangle}{nL}=\lim_{L\to\infty}\frac{\langle\ln Z_L\rangle}{L}. \tag{3.14}$$

$\langle Z_L^n\rangle$ can be thought of as the average of the partition function for n walks or n replicas of the system. Following the Parisi scheme [16,17], one assumes that the arrangements of the n walks which give the leading contribution to $\langle Z_L^n\rangle$, for large L, are organised as follows:

- the n walks remain together initially for a length Lq_1
- the walks then split into m_1 groups of n/m_1 walks each and remain so for a length $L(q_2-q_1)$
- ...
- the walks then split into m_j groups of n/m_j walks each, remaining so for a length $L(q_{j+1}-q_j)$
- ...
- the walks finally separate into $m_M=n$ individual walks, a length L from the starting point.

Therefore one has

$$q_0 = 0\le q_1\le\cdots\le q_j\le\cdots\le q_M=1 \tag{3.15}$$

$$1 = m_0\le m_1\le\cdots\le m_j\le\cdots\le m_M=n\,. \tag{3.16}$$

Then for large L, $\langle Z_L^n\rangle$ is dominated by

$$\langle(Z_L)^n\rangle\approx\max_{\{q_j\}}\max_{\{m_j\}}\prod_j\exp\left\{L(q_{j+1}-q_j)m_j\ln\left[K\int\rho(\epsilon)\exp\left(-n\epsilon/m_jT\right)d\epsilon\right]\right\} \tag{3.17}$$

To evaluate $\langle Z_L^n\rangle$ for large L, one has to find the set $\{q_j\}$, $\{m_j\}$ which maximises the exponent in eq.(3.17). In the limit $n\to 0$, required in eq.(3.14), following Parisi [16,17], eq.(3.16) is inverted to give

$$1=m_0\ge m_1\ge\cdots\ge m_j\ge\cdots\ge m_M=n=0 \tag{3.18}$$

and the limit $M\to\infty$ is taken by defining a function, $x(q_j)$, such that

$$m_j=\frac{n}{x(q_j)}, \tag{3.19}$$

with q_j becoming a variable that is continuous on the interval $[0,1]$ and $0 \leq x(q) \leq 1$. Then using eq.(3.14) and eq.(3.17) one obtains

$$\lim_{L\to\infty} \frac{1}{L}\langle \ln Z_L \rangle = \text{extr.} \int_0^1 \frac{dq}{x(q)} \ln \left[K \int \rho(\epsilon) \exp\left(-\epsilon x(q)/T\right) \right] \tag{3.20}$$

where "extr." indicates that one must take the extremum over all possible functions $x(q)$.

As there is no explicit q-dependence in eq.(3.20), $x(q)$ must be a constant. Hence one finds that

$$\begin{aligned} x(q) &= 1 && T \geq T_c \\ &= T\gamma_{\min} = \frac{T}{T_c} && T \leq T_c \end{aligned} \tag{3.21}$$

where $\gamma_{\min}$ is defined by

$$\left(\frac{dG_1(\gamma)}{d\gamma} \right)_{\gamma_{\min}} = 0 \tag{3.22}$$

with

$$G_1(\gamma) = \frac{1}{\gamma} \ln \left[K \int \rho(\epsilon) \mathrm{e}^{-\epsilon\gamma} d\epsilon \right]. \tag{3.23}$$

So one can conclude from eqs.(3.20) and (3.21) that

$$\begin{aligned} \lim_{L\to\infty} \frac{1}{L}\langle \ln Z_L \rangle &= \frac{1}{T} G_1(1/T) && T \geq T_c \\ &= \frac{1}{T} G_1(\gamma_{\min}) && T \leq T_c. \end{aligned} \tag{3.24}$$

This is the same as eqs.(3.10)–(3.13), which were derived using the travelling wave analogy.

One can also determine the overlaps from this replica calculation. (These were defined in section 1.2, eq.(1.11).) The probability distribution of the overlap between two walks, $P(q)$, can be calculated using the identification [53,54]

$$P(q) = \frac{dx(q)}{dq} \tag{3.25}$$

Hence, from eq.(3.21), one can see that, for $T \leq T_c$, $P(q)$ is composed of two delta functions

$$P(q) = T\gamma_{\min}\delta(q) + (1 - T\gamma_{\min})\delta(q-1) \qquad T \leq T_c. \tag{3.26}$$

Above T_c, $P(q)$ is a single delta function at $q = 0$.

$$P(q) = \delta(q) \qquad T \geq T_c \tag{3.27}$$

In the low temperature phase $P(q)$ is not a single delta function, q is not self-averaging and one can conclude that the phase has broken replica symmetry. This is analogous to the overlaps in the low temperature phase of the mean field spin glass [1].

One can, in addition, extract some information about the valley structure of the energy landscape from eq.(3.26). The replica symmetry breaking indicates a many-valley energy landscape. Assume one has a certain number of valleys, each valley α having a weight Ω_α. If two walks fall in the same valley they have an overlap of unity and if they are in different valleys they have a zero overlap. Hence, from eq.(3.26), it follows that

$$\left\langle \sum_\alpha \Omega_\alpha^2 \right\rangle = 1 - T\gamma_{\min} \qquad T \leq T_c. \tag{3.28}$$

(This result will be useful in the $1/d$ expansion of the transverse fluctuations, see section 3.2.3.)

3.2 The n-tree approximation and the 1/d expansion

In this section the method of " n-tree " approximations will be presented and it will be shown how this can be used to develop $1/d$ expansions for various properties of the directed polymer on a d-dimensional hypercubic lattice [45,46]. The geometry considered is as follows. For each bond of the d-dimensional hypercubic lattice one chooses a random energy, ϵ_{ij}, according to a given probability distribution $\rho(\epsilon_{ij})$. The walks will be directed along the $(1, 1, \ldots, 1)$ direction of the lattice. This means that at each step one coordinate must increase by one, so that if the walks commence at the point $\mathbf{r} = (x_1, x_2, \ldots, x_d)$ they can end after L steps at any point $\mathbf{r}' = (x_1 + n_1, x_2 + n_2, \ldots, x_d + n_d)$ with $n_1 + n_2 + \cdots + n_d = L$.

The idea of n-trees is introduced and the free energies of the first few ($n = 1, 2, 3$) n-tree approximations to the polymer problem are derived in section 3.2.1. Then, in section 3.2.2, it is explained how these n-tree approximations can be turned into high dimension expansions for some of the thermal properties of the system. Sections 3.2.3 and 3.2.4 deal with the $1/d$ expansions for the transverse fluctuations and overlaps respectively. For ease of calculation the results presented in sections 3.2.2–3.2.4 assume an exponential distribution for the random energies. The generalisation of these results to other distributions is considered in section 3.2.5. Finally, in section 3.2.6, the validity of the n-tree approach to obtaining $1/d$ expansions is tested, by applying the method to some problems for which the results can be obtained by other means.

3.2.1 The n-tree approximation method

Consider the partition function $Z_L(\mathbf{r})$, for directed walks of length L emanating from the point $\mathbf{r}$ in the geometry defined above. A recursion relation can be constructed for $Z_L(\mathbf{r})$,

$$Z_{L+1}(\mathbf{r}) = \sum_{i=1}^{d} a_i(\mathbf{r}) Z_L(\mathbf{r} + \mathbf{e}_i) \tag{3.29}$$

with

$$a_i(\mathbf{r}) = \exp\left[-\epsilon_{\mathbf{r},\mathbf{r}+\mathbf{e}_i}/T\right] \tag{3.30}$$

where $\mathbf{e}_i$ are the unit vectors of the lattice in the directions in which a step is allowed, and the initial condition is

$$Z_0(\mathbf{r}) = 1. \tag{3.31}$$

Equation (3.29) is very similar to the recursion, eq.(3.1), which was valid for the tree. The main difference is that, in eq.(3.29), the $Z_L(\mathbf{r} + \mathbf{e}_i)$ are correlated. For example, $Z_L(\mathbf{r} + \mathbf{e}_i)$ and $Z_L(\mathbf{r} + \mathbf{e}_j)$ are correlated because they both depend on $Z_{L-1}(\mathbf{r} + \mathbf{e}_i + \mathbf{e}_j)$.

The n-tree approximations cope with these correlations in a systematic way. These approximations become exact in the limit $n \to \infty$. To obtain the n-tree approximation to the problem, one iterates eq.(3.29) n times exactly and then neglects

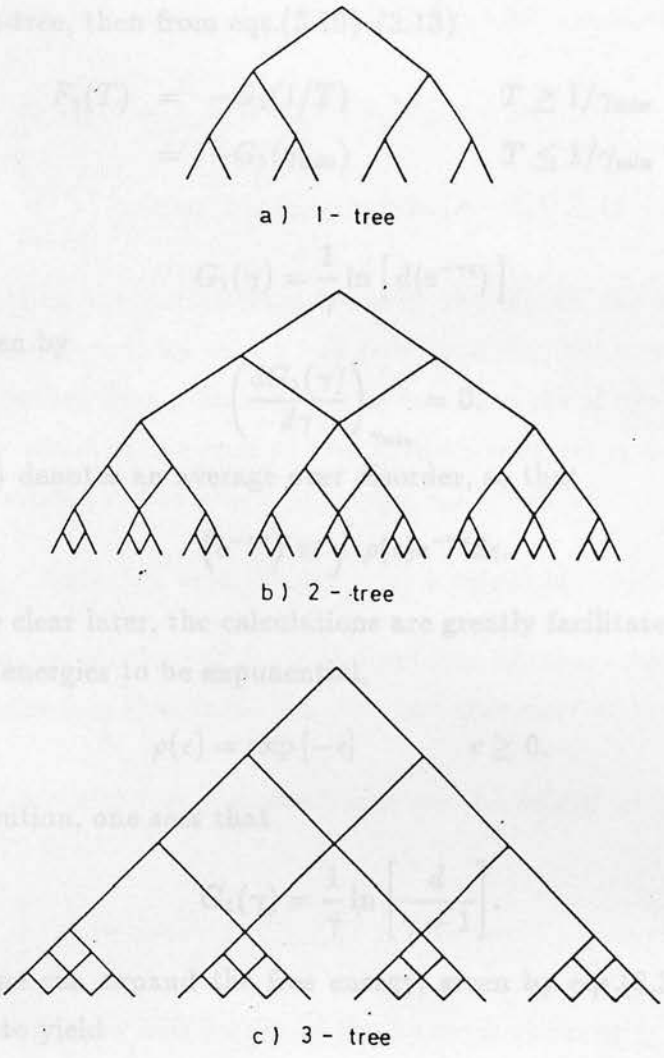

Figure 3.2: (a) the 1-tree, (b) the 2-tree, (c) the 3-tree drawn for $d = 2$.

the remaining correlations. In other words, one takes account of the correlations on the first n steps of the lattice exactly and then constructs a tree from this motif, by neglecting other correlations. Diagrams of the 1-tree, 2-tree and 3-tree are shown, for $d = 2 = 1 + 1$, in figure 3.2.

The 1-tree approximation

The first approximation, a 1-tree, neglects all correlations on the right-hand side of eq.(3.29). This gives the mean field problem of eq.(3.1), with $K = d$, the solution

of which has been discussed in section 3.1. If $F_n(T)$ is the free energy per unit length of the n-tree, then from eqs.(3.10)–(3.13)

$$\begin{aligned} F_1(T) &= -G_1(1/T) && T \geq 1/\gamma_{\min} \\ &= -G_1(\gamma_{\min}) && T \leq 1/\gamma_{\min} \end{aligned} \tag{3.32}$$

where

$$G_1(\gamma) = \frac{1}{\gamma} \ln \left[d \langle \mathrm{e}^{-\gamma\epsilon} \rangle \right] \tag{3.33}$$

and $\gamma_{\min}$ is given by

$$\left(\frac{dG_1(\gamma)}{d\gamma} \right)_{\gamma_{\min}} = 0. \tag{3.34}$$

As before, $\langle \cdots \rangle$ denotes an average over disorder, so that

$$\left\langle \mathrm{e}^{-\gamma\epsilon} \right\rangle \equiv \int \rho(\epsilon) \mathrm{e}^{-\gamma\epsilon} d\epsilon. \tag{3.35}$$

As will become clear later, the calculations are greatly facilitated by choosing the distribution of energies to be exponential,

$$\rho(\epsilon) = \exp\left[-\epsilon\right] \qquad \epsilon \geq 0. \tag{3.36}$$

For this distribution, one sees that

$$G_1(\gamma) = \frac{1}{\gamma} \ln \left[\frac{d}{\gamma + 1} \right]. \tag{3.37}$$

If d is large, one can expand the free energy, given by eqs.(3.32) and (3.37), in powers of $1/d$, to yield

$$\begin{aligned} F_1(T) &= \frac{1}{\mathrm{e}d} + \frac{1}{\mathrm{e}^2 d^2} + \frac{3}{2\mathrm{e}^3 d^3} + O(d^{-4}) && T \leq T_c \\ &= T \ln\left[(1+T)/Td\right] && T \geq T_c \end{aligned} \tag{3.38}$$

and one finds that the transition temperature, T_c, is given by

$$T_c = \frac{1}{\gamma_{\min}} = \frac{1}{\mathrm{e}d} + \frac{2}{\mathrm{e}^2 d^2} + \frac{9}{2\mathrm{e}^3 d^3} + O(d^{-4}). \tag{3.39}$$

The 2-tree approximation

All of the correlations in eq.(3.29) have been neglected in the 1-tree approximation. To extend the theory beyond the mean field limit one must consider the

correlations neglected so far. The 2-tree approximation starts to do this. The 2-tree approximation is obtained by iterating eq.(3.29) twice, to give

$$Z_{L+2}(\mathbf{r}) = \sum_{i=1}^{d} a_i(\mathbf{r}) a_i(\mathbf{r}+\mathbf{e}_i) Z_L(\mathbf{r}+2\mathbf{e}_i)$$
$$+ \sum_{i=1}^{d-1} \sum_{j>i}^{d} [a_i(\mathbf{r}) a_j(\mathbf{r}+\mathbf{e}_i) + a_j(\mathbf{r}) a_i(\mathbf{r}+\mathbf{e}_j)]\, Z_L(\mathbf{r}+\mathbf{e}_i+\mathbf{e}_j) \qquad (3.40)$$

and now neglecting the correlations between the Z_L on the right-hand side of eq.(3.40). Again one ends up with a tree (see fig. 3.2b), but now it has $d + d(d-1)/2$ branches, rather than d branches. The branches are of two types: d branches have an energy which is the sum of two random energies $\epsilon_i + \epsilon_j$, and the other $d(d-1)/2$ branches have an effective energy, ϵ_{eff}, given by

$$\epsilon_{\text{eff}} = -T \ln [a_i(\mathbf{r}) a_j(\mathbf{r}+\mathbf{e}_i) + a_j(\mathbf{r}) a_i(\mathbf{r}+\mathbf{e}_j)]. \qquad (3.41)$$

The effective energy on these $d(d-1)/2$ branches depends upon the temperature and represents the fact that these branches are composed of two paths.

As a tree structure still remains, the 2-tree can be solved as before (eqs.(3.32)–(3.34)). If one defines

$$G_2(\gamma) = \frac{1}{2\gamma} \ln \left[d \left\langle e^{-\gamma(\epsilon_1+\epsilon_2)} \right\rangle + \frac{d(d-1)}{2} \left\langle \left(e^{-(\epsilon_1+\epsilon_2)/T} + e^{-(\epsilon_3+\epsilon_4)/T} \right)^{\gamma T} \right\rangle \right], \qquad (3.42)$$

then the free energy per unit length of the 2-tree is given by

$$\begin{aligned} F_2(T) &= -G_2(1/T) && T \geq T_c \\ &= -G_2(\gamma_{\min}) && T \leq T_c \end{aligned} \qquad (3.43)$$

with $\gamma_{\min}$ the solution of

$$\left(\frac{dG_2(\gamma)}{d\gamma} \right)_{\gamma_{\min}} = 0. \qquad (3.44)$$

The extra factor of $1/2$ in eq.(3.42) appears because when one iterates eq.(3.40) L times the polymer is of length $2L$, not L. One sees that $\gamma_{\min}$ now depends upon the temperature, because the effective energy on $d(d-1)/2$ of the branches is temperature-dependent. T_c is still given by eq.(3.13), i.e. is the solution of $T_c = 1/\gamma_{\min}(T_c)$.

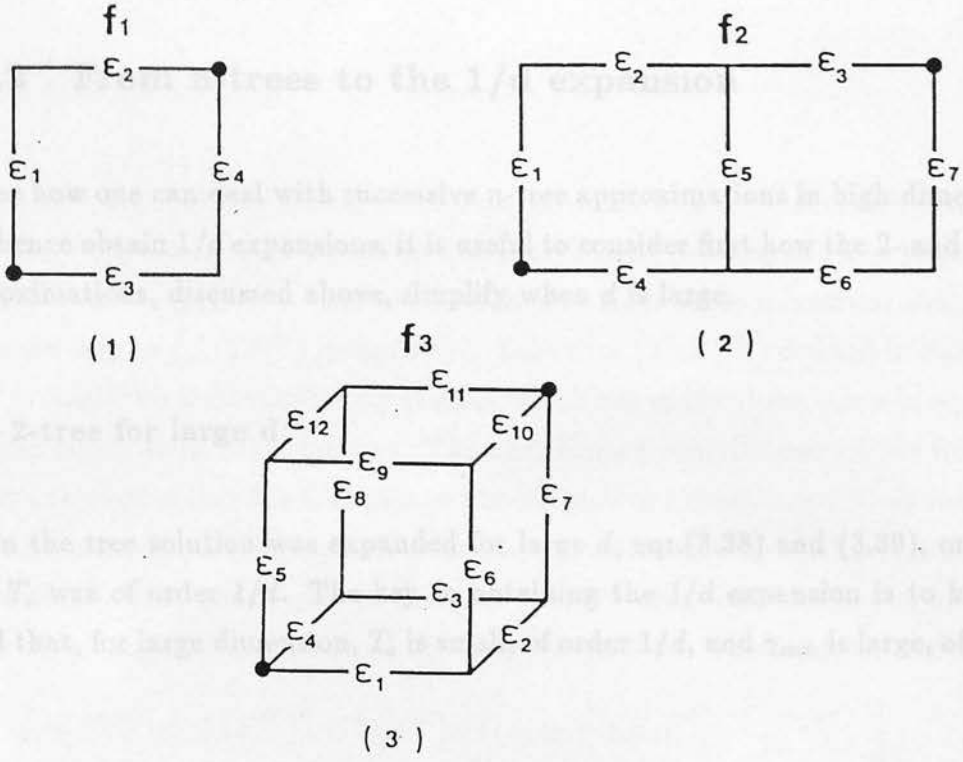

Figure 3.3: f_i is the sum of the weights of all the directed walks connecting the two marked points on the diagram i.

The 3-tree approximation

To get successively better approximations to the d-dimensional lattice one can consider in turn a 3-tree, 4-tree, etc.. For example, for the 3-tree

$$G_3(\gamma) = \frac{1}{3\gamma} \ln \left[d \left\langle e^{-\gamma\epsilon} \right\rangle^3 + d(d-1) \left\langle f_2(T)^{\gamma T} \right\rangle + \frac{d(d-1)(d-2)}{6} \left\langle f_3(T)^{\gamma T} \right\rangle \right] \tag{3.45}$$

where

$$f_2(T) = a_1 a_2 a_3 + a_4 a_5 a_3 + a_4 a_6 a_7 \tag{3.46}$$

and

$$f_3(T) = a_1 a_2 a_7 + a_1 a_6 a_{10} + a_4 a_3 a_7 + a_4 a_8 a_{11} + a_5 a_9 a_{10} + a_5 a_{12} a_{11} \tag{3.47}$$

where $a_i = \exp\left[-\epsilon_i/T\right]$. One can see that $f_2(T)$ and $f_3(T)$ are the partition functions associated with the directed walks linking the two marked points on diagrams 2 and 3 of figure 3.3 respectively. It is clear that as the number of energies that must be averaged over increases, the problem becomes much harder. So, although the aim would be to proceed to successive n-tree approximations, the complexity of the calculations that would be involved makes this approach impossible. However, for large dimension the problem is tractable.

3.2.2 From n-trees to the 1/d expansion

To see how one can deal with successive n-tree approximations in high dimension, and hence obtain $1/d$ expansions, it is useful to consider first how the 2- and 3-tree approximations, discussed above, simplify when d is large.

The 2-tree for large d

When the tree solution was expanded for large d, eqs.(3.38) and (3.39), one saw that T_c was of order $1/d$. The key to obtaining the $1/d$ expansion is to keep in mind that, for large dimension, T_c is small, of order $1/d$, and $\gamma_{\min}$ is large, of order d.

It is the fact that the relevant temperatures are small ($\sim 1/d$) that simplifies the situation. To see this, consider eq.(3.42). One needs to calculate

$$\left\langle f_1(T)^{\gamma T} \right\rangle = \left\langle \left(e^{-(\epsilon_1+\epsilon_2)/T} + e^{-(\epsilon_3+\epsilon_4)/T} \right)^{\gamma T} \right\rangle , \tag{3.48}$$

corresponding to diagram 1 of fig. 3.3. As T is at most of order $1/d$ in the low temperature phase, the leading contribution to eq.(3.48) will result from the region in the space of $\epsilon_1, \epsilon_2, \epsilon_3, \epsilon_4$ where one of the two terms on the right-hand side of eq.(3.48) is much larger than the other. One can rewrite eq.(3.48) as

$$\left\langle f_1(T)^{\gamma T} \right\rangle = 2 \left\langle e^{-\gamma \epsilon} \right\rangle^2 + \left\{ \left\langle \left(e^{-(\epsilon_1+\epsilon_2)/T} + e^{-(\epsilon_3+\epsilon_4)/T} \right)^{\gamma T} \right\rangle - 2 \left\langle e^{-\gamma \epsilon} \right\rangle^2 \right\} . \tag{3.49}$$

Using eq.(3.36), one sees that the first term on right-hand side of eq.(3.49) is $2(\gamma+1)^{-2}$, whilst the second is only of order γ^{-4}. For example, it is easy to show that at $T = 0$ the second term is $-2(3\gamma+4)(\gamma+1)^{-2}(\gamma+2)^{-3}$. Using the rearrangement of eq.(3.49), one can recast $G_2(\gamma)$ in the form

$$G_2(\gamma) = \frac{1}{2\gamma} \ln \left[d^2 \left\langle e^{-\gamma \epsilon} \right\rangle^2 + \frac{d(d-1)}{2} \left\{ \left\langle \left(e^{-(\epsilon_1+\epsilon_2)/T} + e^{-(\epsilon_3+\epsilon_4)/T} \right)^{\gamma T} \right\rangle - 2 \left\langle e^{-\gamma \epsilon} \right\rangle^2 \right\} \right] . \tag{3.50}$$

The 3-tree for large d

To see how the high dimension simplification works in a more complex case, consider $G_3(\gamma)$, given in eq.(3.45). This was complicated because one had to evaluate $\left\langle f_2(T)^{\gamma T}\right\rangle$ and $\left\langle f_3(T)^{\gamma T}\right\rangle$. However, when d is large these quantities simplify in the same way as $\left\langle f_1(T)^{\gamma T}\right\rangle$ in eq.(3.49). Take first $\left\langle f_2(T)^{\gamma T}\right\rangle$ defined in eq.(3.46). As T is small this is dominated by cases in which one of the three terms in eq.(3.46) is much larger than the other two. The next largest contribution comes from the situations when either the first pair or the last pair are much larger than the other term. Smaller again is the contribution due to cases when the first and last terms are of similar size, much greater than the middle term, and smallest of all is the effect of having all three terms of the same magnitude. Thus one can write

$$\begin{aligned}
\left\langle f_2(T)^{\gamma T}\right\rangle &= 3\left\langle a^{\gamma T}\right\rangle^3 + 2\left\langle a^{\gamma T}\right\rangle\left\{\left\langle (a_1a_2+a_3a_4)^{\gamma T}\right\rangle - 2\left\langle a^{\gamma T}\right\rangle^2\right\} \\
&+ \left\{\left\langle (a_1a_2a_3+a_4a_5a_6)^{\gamma T}\right\rangle - 2\left\langle a^{\gamma T}\right\rangle^3\right\} + \left\{\left\langle (a_1a_2a_3+a_4a_5a_3+a_4a_6a_7)^{\gamma T}\right\rangle\right. \\
&- \left[\left\langle (a_1a_2a_3+a_4a_5a_6)^{\gamma T}\right\rangle - 2\left\langle a^{\gamma T}\right\rangle^3\right] - 2\left\langle a^{\gamma T}\right\rangle\left[\left\langle (a_1a_2+a_3a_4)^{\gamma T}\right\rangle - 2\left\langle a^{\gamma T}\right\rangle^2\right] \\
&- \left.3\left\langle a^{\gamma T}\right\rangle^3\right\}. \qquad (3.51)
\end{aligned}$$

The leading term is now $3(\gamma+1)^{-3}$, using eq.(3.36), the second of order γ^{-5}, the third of order γ^{-6} and the last of order γ^{-7}. Similarly, one can rewrite $\left\langle f_3(T)^{\gamma T}\right\rangle$ as

$$\begin{aligned}
\left\langle f_3(T)^{\gamma T}\right\rangle &= 6\left\langle a^{\gamma T}\right\rangle^3 + 6\left\langle a^{\gamma T}\right\rangle\left\{\left\langle (a_1a_2+a_3a_4)^{\gamma T}\right\rangle - 2\left\langle a^{\gamma T}\right\rangle^2\right\} \\
&+ 9\left\{\left\langle (a_1a_2a_3+a_4a_5a_6)^{\gamma T}\right\rangle - 2\left\langle a^{\gamma T}\right\rangle^3\right\} \\
&+ 6\left\{\left\langle (a_1a_2a_3+a_4a_5a_3+a_4a_6a_7)^{\gamma T}\right\rangle - \left[\left\langle (a_1a_2a_3+a_4a_5a_6)^{\gamma T}\right\rangle - 2\left\langle a^{\gamma T}\right\rangle^3\right]\right. \\
&- \left.2\left\langle a^{\gamma T}\right\rangle\left[\left\langle (a_1a_2+a_3a_4)^{\gamma T}\right\rangle - 2\left\langle a^{\gamma T}\right\rangle^2\right] - 3\left\langle a^{\gamma T}\right\rangle^3\right\} + O(\gamma^{-8}). \qquad (3.52)
\end{aligned}$$

In eq.(3.52), the first term, of order γ^{-3}, results from cases when one of the six walks comprising $f_3(T)$ dominates eq.(3.47). The second and third terms (of order γ^{-5} and γ^{-6}) represent cases when two of the six terms are of similar size, much larger than the rest and when these two dominant walks have one or no bonds in common respectively. The fourth term is the effect of having three of the terms much larger than the other three, with one of the three dominant walks sharing

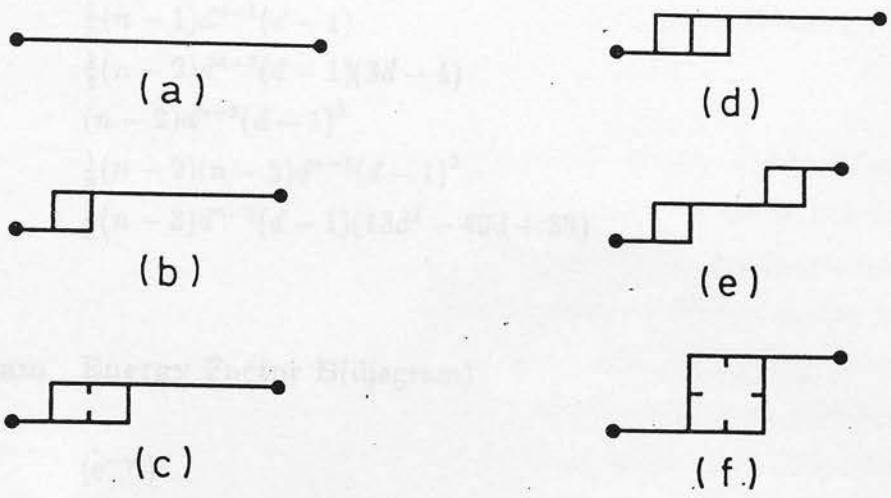

Figure 3.4: The first six diagrams connecting points n steps apart.

one bond with each of the other two dominant walks. Further contributions to $\left\langle f_3(T)^{\gamma T}\right\rangle$ are of order γ^{-8} or smaller.

Using the rearrangements of eqs.(3.51) and (3.52), one can rewrite $G_3(\gamma)$ as

$$\begin{aligned} G_3(\gamma) &= \frac{1}{3\gamma}\log\Big[d^3\left\langle e^{-\gamma\epsilon}\right\rangle^3 \\ &+ d^2(d-1)\left\langle e^{-\gamma\epsilon}\right\rangle\left\{\left\langle\left(e^{-(\epsilon_1+\epsilon_2)/T}+e^{-(\epsilon_3+\epsilon_4)/T}\right)^{\gamma T}\right\rangle - 2\left\langle e^{-\gamma\epsilon}\right\rangle^2\right\} \\ &+ \frac{d(d-1)(3d-4)}{2}\left\{\left\langle\left(e^{-(\epsilon_1+\epsilon_2+\epsilon_3)/T}+e^{-(\epsilon_4+\epsilon_5+\epsilon_6)/T}\right)^{\gamma T}\right\rangle - 2\left\langle e^{-\gamma\epsilon}\right\rangle^3\right\} \\ &+ O(\gamma^{-4})\Big]. \end{aligned} \tag{3.53}$$

The n-tree approximation for large d

Comparing eq.(3.50) and eq.(3.53), for large dimension, each of the terms in the argument of the logarithm on the right-hand side of the equations can be identified with a diagram in figure 3.4, and this allows one to obtain an expression for $G_n(\gamma)$ valid for arbitrary n. The first term in eq.(3.50) and eq.(3.53) represents a single walk of two and three steps respectively and can be identified with diagram a of

Diagram	Embedding Count A(Diagram)
a	d^n
b	$\frac{1}{2}(n-1)d^{n-1}(d-1)$
c	$\frac{1}{2}(n-2)d^{n-2}(d-1)(3d-4)$
d	$(n-2)d^{n-2}(d-1)^2$
e	$\frac{1}{8}(n-2)(n-3)d^{n-2}(d-1)^2$
f	$\frac{1}{2}(n-3)d^{n-3}(d-1)(13d^2-40d+33)$

Diagram	Energy Factor B(diagram)
a	$\langle e^{-\gamma\epsilon}\rangle^n$
b	$\langle e^{-\gamma\epsilon}\rangle^{n-2}\left[\left\langle\left(e^{-(\epsilon_1+\epsilon_2)/T}+e^{-(\epsilon_3+\epsilon_4)/T}\right)^{\gamma T}\right\rangle-2\langle e^{-\gamma\epsilon}\rangle^2\right]$
c	$\langle e^{-\gamma\epsilon}\rangle^{n-3}\left[\left\langle\left(e^{-(\epsilon_1+\epsilon_2+\epsilon_3)/T}+e^{-(\epsilon_4+\epsilon_5+\epsilon_6)/T}\right)^{\gamma T}\right\rangle-2\langle e^{-\gamma\epsilon}\rangle^3\right]$
d	$\langle e^{-\gamma\epsilon}\rangle^{n-3}\left[\left\langle\left(e^{-(\epsilon_1+\epsilon_2+\epsilon_3)/T}+e^{-(\epsilon_4+\epsilon_5+\epsilon_3)/T}+e^{-(\epsilon_4+\epsilon_6+\epsilon_7)/T}\right)^{\gamma T}\right\rangle\right.$ $-\left\langle\left(e^{-(\epsilon_1+\epsilon_2+\epsilon_3)/T}+e^{-(\epsilon_4+\epsilon_5+\epsilon_6)/T}\right)^{\gamma T}\right\rangle-2\langle e^{-\gamma\epsilon}\rangle^3\Big\}$ $\left.-2\langle e^{-\gamma\epsilon}\rangle\left\{\left\langle\left(e^{-(\epsilon_1+\epsilon_2)/T}+e^{-(\epsilon_3+\epsilon_4)/T}\right)^{\gamma T}\right\rangle-2\langle e^{-\gamma\epsilon}\rangle^2\right\}-3\langle e^{-\gamma\epsilon}\rangle^3\right]$
e	$\langle e^{-\gamma\epsilon}\rangle^{n-4}\left[\left\langle\left(e^{-(\epsilon_1+\epsilon_2)/T}+e^{-(\epsilon_3+\epsilon_4)/T}\right)^{\gamma T}\right\rangle-2\langle e^{-\gamma\epsilon}\rangle^2\right]^2$
f	$\langle e^{-\gamma\epsilon}\rangle^{n-4}\left[\left\langle\left(e^{-(\epsilon_1+\epsilon_2+\epsilon_3+\epsilon_4)/T}+e^{-(\epsilon_5+\epsilon_6+\epsilon_7+\epsilon_8)/T}\right)^{\gamma T}\right\rangle-2\langle e^{-\gamma\epsilon}\rangle^4\right]$

Table 3.1: The embedding counts, A, and energy factors, B, of the diagrams of fig. 3.4 for the diagrammatic expansion ($n \geq 3$).

fig. 3.4. Its contribution is a product of the embedding count, $A(a)$, times the energy factor, $B(a)$, given in table 3.1. The next term in eq.(3.50) and eq.(3.53) corresponds to diagram b, in which two walks bifurcate and rejoin immediately afterwards. The contribution is again the product $A(b)B(b)$ of table 3.1. Notice that an extra factor of two appears when $n = 3$, as the bifurcation can occur at the

first or second step. These two diagrams constitute all the possible arrangements of walks linking two points two steps apart. The third term in eq.(3.53) can be identified with diagram c, in which two walks split and rejoin three steps later. Again its contribution is given by $A(c)B(c)$ in table 3.1.

Hence, to be able to evaluate $G_n(\gamma)$, one need only consider all the different ways of linking two points n steps apart, starting by utilising as few bonds as possible and gradually increasing the number of bonds used by the walks to obtain higher orders in the expansion. For each diagram one has to determine the number of ways of embedding it in the lattice, A(diagram), and the corresponding energy factor, B(diagram). The diagrams of fig. 3.4 have previously been used to calculate the high dimension expansion of the directed bond percolation threshold [55].

Using table 3.1, $G_n(\gamma)$ can be written as

$$\begin{aligned} G_n(\gamma) &= \frac{1}{n\gamma}\ln\Big[d^n\left\langle \mathrm{e}^{-\gamma\epsilon}\right\rangle^n \\ &+ \frac{(n-1)}{2}d^{n-1}(d-1)\left\langle \mathrm{e}^{-\gamma\epsilon}\right\rangle^{n-2}\left\{\left\langle\left(\mathrm{e}^{-(\epsilon_1+\epsilon_2)/T}+\mathrm{e}^{-(\epsilon_3+\epsilon_4)/T}\right)^{\gamma T}\right\rangle - 2\left\langle \mathrm{e}^{-\gamma\epsilon}\right\rangle^2\right\} \\ &+ (n-2)d^{n-2}\frac{(d-1)(3d-4)}{2}\left\langle \mathrm{e}^{-\gamma\epsilon}\right\rangle^{n-3}\left\{\left\langle\left(\mathrm{e}^{-(\epsilon_1+\epsilon_2+\epsilon_3)/T}\right.\right.\right. \\ &+ \left.\left.\left.\mathrm{e}^{-(\epsilon_4+\epsilon_5+\epsilon_6)/T}\right)^{\gamma T}\right\rangle - 2\left\langle \mathrm{e}^{-\gamma\epsilon}\right\rangle^3\right\} + O(\gamma^{-4})\Big] \\ &= \frac{1}{n\gamma}\ln\left(\sum_{\text{diagrams}} A(\text{diagram})\ B(\text{diagram})\right). \end{aligned} \tag{3.54}$$

In general, a diagram will contribute at order γ^{-p} in the argument of the logarithm in eq.(3.54) if this diagram contains p extra bonds compared with diagram a. So, to expand eq.(3.54) to a given order in $1/\gamma = O(1/d)$, one needs to consider a finite number of diagrams. Having obtained $G_n(\gamma)$, the free energy per unit length then follows as before (e.g. eqs.(3.10)-(3.13))

$$\begin{aligned} F_n(T) &= -G_n(1/T) \qquad T \geq T_c \\ &= -G_n(\gamma_{\min}) \qquad T \leq T_c \end{aligned} \tag{3.55}$$

with

$$\left.\frac{dG_n(\gamma)}{d\gamma}\right|_{\gamma_{\min}} = 0 \tag{3.56}$$

and T_c given by eq.(3.13).

Using the expansion for $G_n(\gamma)$, computed from table 3.1 (eq.(3.54)), with the energy distribution eq.(3.36), one can show that in the low temperature phase

$$F_n(T) = \frac{1}{ed} + \frac{1}{e^2d^2} + \frac{3}{2e^3d^3} - \frac{1}{e^3d^3}\left(\frac{n-1}{n}\right)[g(Ted) - 3] + O(d^{-4})$$
$$\text{with} \qquad g(t) = t\int_0^\infty du(2+tu)\left[(1+e^{-u})^t - 1\right] \tag{3.57}$$

and in the high temperature phase (to all orders in $1/d$)

$$F_n(T) = T\ \ln\left(\frac{T+1}{Td}\right) \qquad T \geq T_c. \tag{3.58}$$

Notice, eq.(3.38) and eq.(3.57), that the first correction to the tree calculation for $T \leq T_c$ occurs at order d^{-3}, not d^{-2}, because the first corrective diagram includes two extra bonds. Also, one sees from eq.(3.58) that in the high temperature phase the quenched and annealed free energies are equal [43,44]. From eq.(3.57) the specific heat per unit length, $C_n(T)$, in the low temperature phase can be shown to be

$$C_n(T) = \frac{T}{ed}\left(\frac{n-1}{n}\right)g''(Ted) + O\left(\frac{1}{d^3}\right)$$
$$\simeq \frac{T}{ed}\left(\frac{n-1}{n}\right)\frac{\pi^2}{3} \qquad \text{for } T \text{ small.} \tag{3.59}$$

The low temperature phase is no longer frozen as it was in the mean field limit [14]. Instead one finds a specific heat linear in temperature at low temperature. The transition temperature, T_c, can be calculated using eqs.(3.36),(3.54) and (3.13) to yield

$$T_c = \frac{1}{ed} + \frac{2}{e^2d^2} + \frac{1}{e^3d^3}\left[\frac{9}{2} + \left(\frac{n-1}{n}\right)g'(1)\right] + O(d^{-4}) \tag{3.60}$$

where $g'(1) = 7.527827...$ (see eq.(3.57)).

These results, eqs.(3.57)–(3.60), were obtained using diagrams a and b of figure 3.4. One can go to higher orders in $1/d$ by including the next diagrams. For example, if one includes all the diagrams of figure 3.4, one obtains for the ground state energy per unit length

$$E_{GS} = \frac{1}{ed} + \frac{1}{(ed)^2} + \frac{1}{(ed)^3}\left[\frac{9}{2} - \frac{3}{n}\right] + \frac{1}{(ed)^4}\left[\frac{110}{3} - 3e + \frac{1}{n}(3e - 64)\right]$$
$$+ \frac{1}{(ed)^5}\left[\frac{11297}{24} - 74e + \frac{1}{n}(144e - 1369) + \frac{1}{n^2}\frac{81}{2}\right] + O\left(\frac{1}{d^6}\right). \tag{3.61}$$

(Notice that eq.(3.61) is only valid for $n \geq 3$, because the embedding counts of table 3.1 are only valid for $n \geq 3$.)

Diagram	Energy factor B(diagram) at T=0
a	$\dfrac{1}{(\gamma+1)^n}$
b	$\dfrac{-(6\gamma+8)}{(\gamma+1)^n(\gamma+2)^3}$
c	$\dfrac{-(20\gamma^2+50\gamma+32)}{(\gamma+1)^n(\gamma+2)^5}$
d	$\dfrac{71\gamma^4+555\gamma^3+1581\gamma^2+1937\gamma+864}{(\gamma+1)^n(\gamma+2)^5(\gamma+3)^3}$
e	$\dfrac{(6\gamma+8)^2}{(\gamma+1)^n(\gamma+2)^6}$
f	$\dfrac{-(70\gamma^3+252\gamma^2+308\gamma+128)}{(\gamma+1)^n(\gamma+2)^7}$

Table 3.2: The energy factors, B, of table 3.1 calculated at $T = 0$ for the exponential distribution eq.(3.36).

The calculation of the ground state energy in powers of $1/d$ is technically simpler than that of the free energy, because all the energy factors B, of table 3.1, can be calculated explicitly in the limit $T \to 0$ (see table 3.2) for the exponential distribution eq.(3.36).

All the results, eqs.(3.54)–(3.61), obtained so far are $1/d$ expansions valid for the n-tree problems. As the n-tree problem is identical to the hypercubic lattice in the limit $n \to \infty$, one expects these results to be valid for the hypercubic lattice in the limit $n \to \infty$. So the $1/d$ expansion of the free energy, the specific heat and the ground state energy for the hypercubic lattice are given by putting $n = \infty$ in eqs.(3.57), (3.59) and (3.61).

For these results to be correct, one needs the limits $n \to \infty$ and $d \to \infty$ to commute. It has not been possible to prove that these two limits commute. However, the coefficients in all the $1/d$ expansions that have been obtained by this method are always simple rational functions of n which have a finite limit when $n \to \infty$. So there is no indication that the limit $n \to \infty$ is singular for large d. Moreover, in section 3.2.6, some cases will be discussed which can be solved without the n-tree approximation and in these systems the exchange of these limits $n \to \infty$ and $d \to \infty$ gives the correct answer.

3.2.3 The fluctuations of the transverse displacement

As was noted in section 1.2, one can define two types of transverse fluctuation for directed polymers: thermal and disorder fluctuations (eq.(1.9) and eq.(1.10)). It is possible to relate these two types of fluctuation if one has a tree structure as the underlying lattice. By the use of a chemical potential, one can obtain the thermal fluctuations as a derivative of the free energy. (This is the reason why the thermal fluctuations, eq.(1.9), necessarily scale as the length of the polymer.) In this section these two points are discussed and used to obtain a $1/d$ expansion for the disorder transverse fluctuations at $T = 0$, eq.(3.75).

The relation between thermal and disorder fluctuations on a tree

Although the notion of transverse displacement has no *a priori* meaning in a tree problem, one can identify each direction i, $1 \leq i \leq d$, of a tree of d branches with one direction on a d-dimensional hypercubic lattice and say that a walk on a tree has a transverse displacement R_i if it takes $R_i + L/d$ steps along the i^{th} branch.

Let us now attempt to evaluate the fluctuations, eq.(1.9) and eq.(1.10), for the mean field problem in the low temperature phase. It has been shown, eq.(3.26), that in the low temperature phase, the overlaps are either zero or one. This implies that there are well defined energy valleys and that the thermal fluctuations inside a valley vanish. Therefore it is legitimate to think of a landscape composed of a number of valleys. Each valley α is characterised by some transverse displacement,

$R_1 = c_\alpha$, in direction 1 and by a weight Ω_α. The overlap between two walks inside the same valley is one, so all the walks inside the same valley α have the same transverse displacement c_α. Moreover, since the overlap between two different valleys is zero, the displacements, c_α and c_β, for two different valleys are uncorrelated. Therefore one expects that the c_α satisfy

$$\langle c_\alpha \rangle = 0 \; ; \qquad \langle c_\alpha c_\beta \rangle = \langle c_\alpha \rangle \langle c_\beta \rangle \qquad \text{if } \alpha \neq \beta \; . \tag{3.62}$$

Since the only thermal fluctuations are due to the relative weights, Ω_α, of the valleys, one has

$$\begin{aligned} \overline{R_1} &= \sum_\alpha c_\alpha \Omega_\alpha \\ \overline{R_1^2} &= \sum_\alpha c_\alpha^2 \Omega_\alpha . \end{aligned} \tag{3.63}$$

To obtain the thermal and the disorder fluctuations, one now needs to average over disorder. The weights Ω_α satisfy

$$\sum_\alpha \Omega_\alpha = 1 \tag{3.64}$$

$$\left\langle \sum_\alpha \Omega_\alpha^2 \right\rangle = 1 - T\gamma_{\min} . \tag{3.65}$$

Equation (3.64) expresses the fact that the weights of the valleys must add up to unity and eq.(3.65) was obtained in section 3.1.2 (eq.(3.28)). If the c_α and the Ω_α are not correlated, one sees that

$$\begin{aligned} \left\langle \overline{R_1} \right\rangle &= 0 \\ \left\langle \overline{R_1^2} \right\rangle &= \left\langle \sum_\alpha \Omega_\alpha \right\rangle \left\langle c_\alpha^2 \right\rangle = \left\langle c_\alpha^2 \right\rangle \\ \left\langle \overline{R_1}^2 \right\rangle &= \left\langle \sum_\alpha \Omega_\alpha^2 \right\rangle \left\langle c_\alpha^2 \right\rangle = (1 - T\gamma_{\min}) \left\langle c_\alpha^2 \right\rangle \end{aligned} \tag{3.66}$$

which give, for the thermal fluctuations

$$\left\langle \overline{R_1^2} \right\rangle - \left\langle \overline{R_1}^2 \right\rangle = \left\langle c_\alpha^2 \right\rangle T\gamma_{\min} \qquad T \leq T_c \tag{3.67}$$

and for the disorder fluctuations

$$\left\langle \overline{R_1}^2 \right\rangle = \left\langle c_\alpha^2 \right\rangle (1 - T\gamma_{\min}) \qquad T \leq T_c \tag{3.68}$$

The disorder and thermal fluctuations take on similar forms, their ratio being $(1 - T\gamma_{\min})/T\gamma_{\min}$. The disorder fluctuations vanish at T_c. This result is reminiscent of the fact that at T_c the quenched and annealed free energies become identical.

Calculation of the thermal fluctuations

A $1/d$ expansion for the thermal transverse fluctuations on the d-dimensional hypercubic lattice defined earlier can be obtained by adding a chemical potential, μ, to count the number of steps taken in direction 1, i.e.

$$Z_L(\mathbf{r}) = \sum_w e^{-E_w/T+\mu(R_1(w)+L/d)} \tag{3.69}$$

where the sum runs over all walks of length L emanating from the point $\mathbf{r}$ and $(R_1(w) + L/d)$ is the number of steps taken by walk w in direction 1.

The average number of steps taken in the direction marked by μ, direction 1, is then given by

$$\left\langle \overline{R_1} \right\rangle + \frac{L}{d} = \frac{d}{d\mu} \langle \ln Z_L \rangle \Big|_{\mu=0} \tag{3.70}$$

and the thermal fluctuation of R_1 is given by the second derivative of $\langle \ln Z_L \rangle$,

$$\left\langle \overline{R_1^2} \right\rangle - \left\langle \overline{R_1}^2 \right\rangle = \frac{d^2}{d\mu^2} \langle \ln Z_L \rangle \Big|_{\mu=0} . \tag{3.71}$$

The method of n-tree approximations and the resulting $1/d$ expansion can be used, as in section 3.2.2, to calculate the free energy of the problem of eq.(3.69), providing that care is taken to include an extra factor, $e^{\mu\gamma T}$, for each step taken in the marked direction. For example, the free energy per unit length of the 1-tree approximation, $F_1(T,\mu)$, can be obtained, using eq.(3.55), from $G_1(\gamma)$:

$$G_1(\gamma) = \frac{1}{\gamma} \ln \left[\left(\frac{d - 1 + e^{\mu\gamma T}}{\gamma + 1} \right) \right] \tag{3.72}$$

where the exponential distribution, eq.(3.36), has again been used. The inclusion of the chemical potential has changed the embedding count of diagram a (fig. 3.4) from d^n to $\left(d - 1 + e^{\mu\gamma T}\right)^n$. The embedding counts for the diagrams of fig. 3.4, obtained using the chemical potential, are given in table 3.3. Combining the new embedding counts (table 3.3) with the energy factors (table 3.1), as in eq.(3.54), it is then possible to find $G_n(\gamma)$ and hence the $1/d$ expansion for the free energy, $F_n(T,\mu)$.

From $F_n(T,\mu)$ one can calculate the thermal fluctuations on the n-tree, eq.(3.71), by

$$\left\langle \overline{R_1^2} \right\rangle - \left\langle \overline{R_1}^2 \right\rangle = -\frac{L}{T} \frac{d^2}{d\mu^2} F_n(T,\mu) \Big|_{\mu=0} \tag{3.73}$$

Diagram	Embedding Count
a	$(d-1+e^{\mu\gamma T})^n$
b	$\frac{1}{2}(n-1)(d-1)\left(d-1+e^{\mu\gamma T}\right)^{n-2}(d-2+2e^{\mu\gamma T})$
c	$\frac{1}{2}(n-2)(d-1)\left(d-1+e^{\mu\gamma T}\right)^{n-3}(3d^2-13d+14$ $+(9d-16)e^{\mu\gamma T}+2e^{2\mu\gamma T})$
d	$(n-2)(d-1)\left(d-1+e^{\mu\gamma T}\right)^{n-3}(d^2-4d+4$ $+(3d-5)e^{\mu\gamma T}+e^{2\mu\gamma T})$
e	$\frac{1}{8}(n-2)(n-3)(d-1)^2\left(d-1+e^{\mu\gamma T}\right)^{n-4}(d-2+2e^{\mu\gamma T})^2$
f	$(n-3)(d-1)\left(d-1+e^{\mu\gamma T}\right)^{n-4}\left(\frac{13}{2}d^3-46d^2+109d-86\right.$ $\left.+(26d^2-105d+107)e^{\mu\gamma T}+\left(\frac{25}{2}d-22\right)e^{2\mu\gamma T}+e^{3\mu\gamma T}\right)$

Table 3.3: The embedding counts, A, for the diagrams of fig. 3.4 when a chemical potential, μ, is included to count the number of steps in a marked direction.

This formula is valid at all temperatures.

The disorder fluctuations in the low temperature phase

Combining the results just derived, eqs.(3.67),(3.68) and (3.73), one can obtain the disorder fluctuations.

$$\left\langle \overline{R_1}^2 \right\rangle = -\frac{(1-T\gamma_{\min})}{T^2\gamma_{\min}} L \left. \frac{d^2}{d\mu^2} F_n(T,\mu) \right|_{\mu=0} \tag{3.74}$$

Notice that eq.(3.74) is only valid for a tree problem, since eqs.(3.67) and (3.68) only apply to this case.

From eqs.(3.73) and (3.74), one can obtain the complete temperature dependence of both the thermal and disorder fluctuations. Here the results are only given at zero temperature. At $T = 0$ the thermal fluctuations vanish, whereas the disorder fluctuations are given by

$$\begin{aligned} \sum_{i=1}^{d} \left\langle \overline{R_i}^2 \right\rangle &= L\left[1 - \frac{1}{d} + \frac{6}{e^2 d^3}\left(\frac{n-1}{n}\right) + \frac{(136-6e)n - 276 + 6e}{n e^3 d^4}\right. \\ &+ \left. \frac{(3384-376e)n + 756e - 10454 + (108/n)}{n e^4 d^5} + O\left(d^{-6}\right)\right] . \end{aligned} \tag{3.75}$$

Taking the limit $n \to \infty$, one gets a $1/d$ expansion for the disorder transverse fluctuation at zero temperature for the hypercubic lattice. As with the free energy, each term in the expansion has a regular n-dependence when $n \to \infty$ and so it is reasonable to assume that the limits $d \to \infty$ and $n \to \infty$ can be exchanged.

One sees, from eq.(3.75), that the $1/d$ expansion does not change the value of ν which remains $1/2$. This would be consistent with ν remaining $1/2$ above a certain upper critical dimension, d_c, at which the coefficient of L (on the right-hand side of eq.(3.75) and for $n \to \infty$) would diverge. The series in eq.(3.75) is, however, too short to make any reliable prediction for d_c. Moreover, it could happen that the $1/d$ series, eq.(3.75) (for $n = \infty$), has a zero radius of convergence, as is the case in some $1/d$ expansions [56].

The transverse fluctuations have an interesting temperature dependence. From eqs.(3.72)–(3.74), one finds that the thermal fluctuations are given, to order $1/d$,

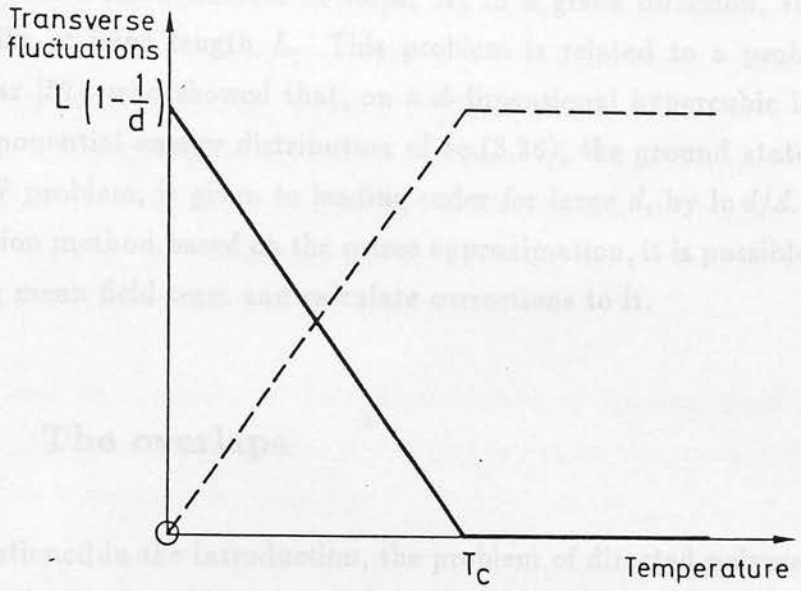

Figure 3.5: The temperature dependence of the disorder (—) and thermal (- - -) transverse fluctuations, eqs.(3.76) and (3.77).

by

$$\sum_{i=1}^{d} \left\langle \overline{R_i^2} \right\rangle - \left\langle \overline{R_i}^2 \right\rangle = L\left(1-\frac{1}{d}\right)\frac{T}{T_c} + O\left(\frac{1}{d^2}\right) \quad \text{for } T \le T_c$$
$$= L\left(1-\frac{1}{d}\right) \quad \text{for } T > T_c \qquad (3.76)$$

and the disorder fluctuations are given by

$$\sum_{i=1}^{d} \left\langle \overline{R_i}^2 \right\rangle = L\left(1-\frac{1}{d}\right)\left(1-\frac{T}{T_c}\right) + O\left(\frac{1}{d^2}\right) \quad \text{for } T \le T_c$$
$$= 0 \quad \text{for } T > T_c \qquad (3.77)$$

(see figure 3.5).

The fact that there are two kinds of transverse fluctuations in this problem is reminiscent of the susceptibility of spin glasses, for which one can define two susceptibilities (d.c. susceptibility and a.c. susceptibility, in the limit of zero frequency).

The inclusion of a chemical potential, as in eq.(3.69), also enables one to consider the problem of polymers in a random medium in different geometries. For example,

one can consider the problem in which the partition sum, eq.(1.2), runs over all walks with a fixed number of steps, N, in a given direction, rather than over all walks of fixed length L. This problem is related to a problem considered by Dhar [57], who showed that, on a d-dimensional hypercubic lattice and with the exponential energy distribution of eq.(3.36), the ground state energy of this fixed-N problem, is given to leading order for large d, by $\ln d/d$. Using the $1/d$ expansion method based on the n tree approximation, it is possible to recover this leading mean field term and calculate corrections to it.

3.2.4 The overlaps

As mentioned in the introduction, the problem of directed polymers in a random medium has a close analogy with spin glasses. The mean field spin glass [16,17] and the mean field polymer problem [14] both have low temperature phases characterised by broken replica symmetry. This is displayed in the polymer problem by the probability distribution of overlaps, $P(q)$, being the sum of two delta functions (see eq.(3.26)). The question of replica symmetry breaking in the finite-dimensional spin glass remains controversial and for this reason it is interesting to examine the overlaps for the polymer problem in finite dimension. Here, the overlaps on a d-dimensional hypercubic lattice are considered by extending the n-tree approach to obtain the probability distribution of the overlap between two walks (eqs.(3.83) and (3.84)).

The n-tree approximations to the directed polymer problem retain a general tree structure. Hence, if one performs the replica calculation of section 3.1.2 on the n-tree, one will see that, below T_c, $P(q)$ remains a sum of two delta functions with weights $T\gamma_{\min}$ and $1 - T\gamma_{\min}$. However, in the n-tree approximation, some of the branches of the tree structure are composed of two or more paths. Consider what can occur when two walks pass down such a branch. The walks can both take the same path, giving an overlap of 1 for this section, or they can take different routes, giving an overlap less than 1. So, instead of having one delta function at $q = 0$ and the other at $q = 1$, the latter will be shifted to a lower value of q.

To explain how one can calculate the position of the shifted delta function, let us

consider as an example a polymer of length L in the 2-tree approximation. Here one only has two kinds of branch (see fig. 3.2b): those which consist of only one path (type A), and so contribute $2/L$ to the overlap q and those which are made up of two paths (type B), which contribute between $1/L$ (at $T = \infty$) and $2/L$ (at $T = 0$) to q, depending on the temperature. To determine the distribution function of the overlaps, one therefore needs to know the fraction of each type of branch used by the walks and the contribution to the overlap from the type B branches, both as functions of temperature.

As is shown in appendix A, the typical fraction of branches used in the walk that are of type B and have energies $\epsilon_1 + \epsilon_2$ and $\epsilon_3 + \epsilon_4$ on the constituent links is given, in the low temperature phase, by

$$\frac{d(d-1)}{2}\left(e^{-(\epsilon_1+\epsilon_2)/T} + e^{-(\epsilon_3+\epsilon_4)/T}\right)^{T\gamma_{\min}} \rho(\epsilon_1)\rho(\epsilon_2)\rho(\epsilon_3)\rho(\epsilon_4) \exp\left[-2\gamma_{\min} G_2\left(\gamma_{\min}\right)\right] \tag{3.78}$$

where $G_2(\gamma)$ is given by eq.(3.50).

It now remains to calculate the contribution of such a branch to the overlap, q. This is simply given by

$$\frac{e^{-2(\epsilon_1+\epsilon_2)/T} + e^{-2(\epsilon_3+\epsilon_4)/T}}{\left(e^{-(\epsilon_1+\epsilon_2)/T} + e^{-(\epsilon_3+\epsilon_4)/T}\right)^2}, \tag{3.79}$$

as one has an overlap 1 if both walks go through the same path and zero overlap otherwise. Combining eqs.(3.78) and (3.79), one can conclude that $P(q)$ for the 2-tree consists of two delta functions, one at $q = 0$ with weight $T\gamma_{\min}$ and the other at

$$\begin{aligned} q &= \left[d\left\langle e^{-\epsilon\gamma_{\min}}\right\rangle^2\right. \\ &+ \left.\frac{d(d-1)}{2}\left\langle\left(e^{-(\epsilon_1+\epsilon_2)/T} + e^{-(\epsilon_3+\epsilon_4)/T}\right)^{T\gamma_{\min}-2}\left(e^{-2(\epsilon_1+\epsilon_2)/T} + e^{-2(\epsilon_3+\epsilon_4)/T}\right)\right\rangle\right] \\ &\times \exp\left[-2\gamma_{\min} G_2\left(\gamma_{\min}\right)\right]. \end{aligned} \tag{3.80}$$

Having seen how the calculation proceeds for the 2-tree, it is easy to generalise to the n-tree. The relative contribution to q from each branch like diagram a (fig. 3.4) is always 1. The relative contribution from branches like diagram b (fig. 3.4) will be

$$1 - \frac{2}{n} + \frac{2}{n}\frac{e^{-2(\epsilon_1+\epsilon_2)/T} + e^{-2(\epsilon_3+\epsilon_4)/T}}{\left(e^{-(\epsilon_1+\epsilon_2)/T} + e^{-(\epsilon_3+\epsilon_4)/T}\right)^2}. \tag{3.81}$$

This is just the direct generalisation of eq.(3.79): the walks have to be together for a fraction $1-\frac{2}{n}$ of the branch and can take two paths for a fraction $\frac{2}{n}$ of the branch. So for the n-tree, the average overlap $\langle q\rangle$ takes the form

$$\begin{aligned}\langle q\rangle &= \left[1-\left(\frac{n-1}{n}\right)\frac{(d-1)}{d}\left\langle e^{-\epsilon\gamma_{\min}}\right\rangle^{-2}\left\{\left\langle\left(e^{-(\epsilon_1+\epsilon_2)/T}+e^{-(\epsilon_3+\epsilon_4)/T}\right)^{T\gamma_{\min}}\right\rangle\right.\\ &- \left.\left\langle\left(e^{-(\epsilon_1+\epsilon_2)/T}+e^{-(\epsilon_3+\epsilon_4)/T}\right)^{T\gamma_{\min}-2}\left(e^{-2(\epsilon_1+\epsilon_2)/T}+e^{-2(\epsilon_3+\epsilon_4)/T}\right)\right\rangle\right\}\\ &+ O\left(d^{-3}\right)\ \Big]\times(1-T\gamma_{\min})\end{aligned} \tag{3.82}$$

where $\gamma_{\min}$ is given by eqs.(3.54) and (3.56).

Evaluating the averages, using eq.(3.36), and taking the limit $n\to\infty$ (again assuming the commutativity of limits), yields that the delta function in $P(q)$ at non-zero overlap is shifted from $q=1$ to $q=q_2$, where

$$q_2 = 1-\frac{4Ted}{(ed)^2}\int_0^\infty du\,(2+Tedu)\left(1+e^{-u}\right)^{Ted}\frac{e^{-u}}{(1+e^{-u})^2}+O(d^{-3}). \tag{3.83}$$

The distribution function, $P(q)$, remains non-trivial in finite dimension in the low temperature phase,

$$P(q) = T\gamma_{\min}\delta(q)+(1-T\gamma_{\min})\,\delta(q-q_2) \tag{3.84}$$

where q_2 is given by eq.(3.83) and $\gamma_{\min}$ is

$$\gamma_{\min} = ed-2+\frac{1}{ed}\left[-\frac{19}{2}+3\,g(Ted)-Ted\,g'(Ted)\right]+O\left(d^{-2}\right) \tag{3.85}$$

with $g(t)$ given by eq.(3.57).

So, the $1/d$ expansion predicts broken replica symmetry in the low temperature phase in the finite-dimensional directed polymer problem.

3.2.5 Generalisation to other distributions

In sections 3.2.2–3.2.4 the high dimension expansions were derived using the energy distribution eq.(3.36), $\rho(\epsilon)=\exp[-\epsilon]$. This choice facilitated the calculation of the averages in table 3.1 (see table 3.2). It is possible to perform the same calculations using other distributions, $\rho(\epsilon)$, for the disorder. However, for most

choices of $\rho(\epsilon)$, it is not possible to express the mean field results, eqs.(3.32)–(3.34), in a simple way in powers of d and it is difficult to calculate the energy factors required for the diagrammatic expansion (table 3.1). To examine the effect of using different energy distributions let us therefore limit ourselves to:

$$\rho(\epsilon) = \frac{\epsilon^{\alpha-1}\exp[-\epsilon]}{\Gamma(\alpha)} \qquad \alpha > 0, \epsilon \geq 0. \tag{3.86}$$

This choice allows one to study changes produced by varying the parameter α, whilst still keeping the calculations relatively simple.

Let us first consider how the value of α affects the mean field results. Using $\rho(\epsilon)$ given by eq.(3.86) with eqs.(3.32)–(3.34), one can show that, for large d, the mean field energy in the low temperature phase and transition temperature are given by

$$F_1(T) = \frac{\alpha}{ed^{1/\alpha}} + \frac{\alpha}{(ed^{1/\alpha})^2} + O\left(d^{-3/\alpha}\right) \qquad T \leq T_c \tag{3.87}$$

and

$$T_c = \frac{1}{ed^{1/\alpha}} + \frac{2}{(ed^{1/\alpha})^2} + O\left(d^{-3/\alpha}\right). \tag{3.88}$$

One can see that, in general, one has an expansion in powers of $d^{1/\alpha}$ rather than d. However, when one moves away from the mean field, by evaluating the energy factors of table 3.1 for the diagrammatic expansion, one sees that these still behave as powers of d, not $d^{1/\alpha}$. For example, the energy factor corresponding to diagram b of figure 3.4 is given by

$$\left\langle \left(e^{-(\epsilon_1+\epsilon_2)/T} + e^{-(\epsilon_3+\epsilon_4)/T}\right)^{\gamma T}\right\rangle - 2\left\langle e^{-\gamma\epsilon}\right\rangle^2 = -\frac{\Gamma(4\alpha)}{\alpha\Gamma^2(2\alpha)\gamma^{4\alpha}} + 2\frac{g_\alpha(t)}{\gamma^{4\alpha}} + O\left(\frac{1}{\gamma^{4\alpha+1}}\right)$$

where

$$g_\alpha(t) = \frac{t}{\Gamma^2(2\alpha)}\int_0^\infty\int_0^\infty dxdy\; x^{2\alpha-1}e^{-x}(x+ty)^{2\alpha-1}\left[\left(1+e^{-y}\right)^t - 1\right]. \tag{3.89}$$

So it still behaves as d^{-4}. (When $\alpha = 1$, $g_\alpha(t) \equiv g(t)$, defined in eq.(3.57).) Hence, for general α, one has an expansion in terms of $\gamma^{-\alpha}$ and γ^{-1} (or d^{-1} and $d^{-1/\alpha}$) to deal with. This makes calculations rather complicated, so here only the leading behaviour of the specific heat will be considered.

The specific heat can still be found easily for arbitrary α. To do this in the low temperature phase the behaviour of the function $g_\alpha(t)$ must be known for small t.

This behaviour changes at $\alpha = 1/4$. In the range $0 < \alpha \leq 1/4$, $g_\alpha(t)$ behaves as $t^{4\alpha+1}$ for small t, whereas for $\alpha \geq \frac{1}{4}$ this changes to a t^2 dependence. This produces two possible behaviours for the low temperature specific heat of the n-tree :

$$\begin{aligned} C_n &= \frac{\pi^2}{6}\frac{\Gamma(4\alpha-1)}{\Gamma^2(2\alpha)}\left(\frac{n-1}{n}\right)\frac{T}{\left(ed^{1/\alpha}\right)^{2\alpha-1}} \qquad \alpha \geq \frac{1}{4} \\ &= 4\alpha(4\alpha+1)\frac{J(\alpha)}{\Gamma^2(2\alpha)}\left(\frac{n-1}{n}\right)\left(ed^{1/\alpha}\right)^{2\alpha} T^{4\alpha} \qquad 0 < \alpha \leq \frac{1}{4} \end{aligned} \tag{3.90}$$

where

$$J(\alpha) = \int_0^\infty \int_0^\infty dxdy\; x^{4\alpha-1}\left(y+y^2\right)^{2\alpha-1} \ln\left(1+e^{-x}\right). \tag{3.91}$$

Notice that for $\alpha \geq \frac{1}{4}$ one obtains a linear behaviour at low temperature, whilst for $0 < \alpha < \frac{1}{4}$ one has a $T^{4\alpha}$ behaviour. The low temperature behaviour of the specific heat clearly depends on the nature of the disorder.

One should not be surprised by this change of behaviour for small values of α because one expects, from eq.(3.86), that the density of excitations around the ground state will increase as α becomes small.

3.2.6 Tests of the validity of the n-tree approximation method

The basic premise of the high dimension expansion method, which has been presented in the preceding sections, is that results valid for the d-dimensional hypercubic lattice can be obtained by expanding the n-tree approximation for high dimension and then taking the limit $n \to \infty$. As was discussed in section 3.2.2, this procedure entails exchanging the limits $n \to \infty$ and $d \to \infty$. Although the quantities calculated so far have a finite limit for $n \to \infty$ when one uses this method, there is, as yet, no proof that these limits commute. This section, therefore, discusses a few problems for which the results can be tested (either against a solution obtained by a different approach or against the results of simulations).

The percolation threshold for large d

The first problem to be considered, that of directed bond percolation, is simply the directed polymer problem with the random energies, ϵ_{ij}, chosen according to the distribution

$$\rho(\epsilon) = p\delta(\epsilon) + (1-p)\delta(\epsilon - 1) \tag{3.92}$$

with $0 \leq p \leq 1$. Again let us look at the problem on a d-dimensional hypercubic lattice, directing the walks, which emanate from the origin, along the $(1, 1, \ldots, 1)$ direction. If the weight p exceeds the percolation threshold, p_c, the ground state energy per unit length is zero. The aim is to calculate this threshold, p_c, as a function of dimension, for d large.

Using the diagrammatic expansion method of section 3.2.2, one sees, from eqs.(3.54)–(3.56), that the ground state energy per unit length, E_{GS}, of the n-tree approximation is given by

$$E_{GS} = -G_n\left(\gamma_{\min}\right)|_{T=0} \tag{3.93}$$

where

$$G_n(\gamma)|_{T=0} = \frac{1}{n\gamma}\ln\left[d^n\left\langle e^{-\gamma\epsilon}\right\rangle^n + \frac{n-1}{2}d^{n-1}(d-1)\left\langle e^{-\gamma\epsilon}\right\rangle^{n-2}\left\{\left\langle \max\left(e^{-(\epsilon_1+\epsilon_2)\gamma}, e^{-(\epsilon_3+\epsilon_4)\gamma}\right)\right\rangle - 2\left\langle e^{-\gamma\epsilon}\right\rangle^2\right\} + \cdots\right] \tag{3.94}$$

and $\gamma_{\min}$ is defined, as usual, by eq.(3.56).

Using the percolation distribution of equation (3.92), the averages can be performed to yield

$$\begin{aligned} G_n(\gamma)|_{T=0} = \frac{1}{n\gamma}\ln\Big[&d^n\left(p+(1-p)e^{-\gamma}\right)^n \\ +\ &\left(\frac{n-1}{2}\right)d^{n-1}(d-1)\left(p+(1-p)e^{-\gamma}\right)^{n-2}\left\{2p^2-p^4\right. \\ +\ &\left. 4p(1-p)^2e^{-\gamma} + (1-p)^4e^{-2\gamma} - 2\left(p+(1-p)e^{-\gamma}\right)^2\right\} + \cdots\Big]. \end{aligned} \tag{3.95}$$

To obtain the percolation threshold, p_c, one requires that when $p \geq p_c$ the ground state energy is zero. So, when $p \geq p_c$, the value of γ that minimises $G_n(\gamma)$ is $\gamma = \gamma_{\min} = \infty$. It is possible to show that $\gamma_{\min} = \infty$ as long as the argument of the logarithm in eq.(3.95) is larger than 1 for $\gamma = \infty$. Therefore the percolation

Diagram	Percolation factor
a	$+p^n$
b	$-p^{n+2}$
c	$-p^{n+3}$
d	$+p^{n+4}$
e	$+p^{n+4}$
f	$-p^{n+4}$

Table 3.4: The energy factors, B, for the diagrams of fig. 3.4 for the percolation distribution, $\rho(\epsilon) = p\delta(\epsilon) + (1-p)\delta(\epsilon - 1)$, in the limit $\gamma = \infty$.

threshold is given by the condition that the argument of the logarithm be 1 when $\gamma = \infty$. This implies that

$$d^n p_c^n \left[1 - \left(\frac{n-1}{2}\right)\left(1 - \frac{1}{d}\right) p_c^2 + O\left(p_c^3\right)\right] = 1 \tag{3.96}$$

which becomes, when one includes higher order diagrams,

$$\sum_{\text{diagrams}} A(\text{diagram})B(\text{diagram}) = 1 \tag{3.97}$$

where the embedding counts, A, are the same as in table 3.1 and the energy factors, B, are given for the percolation distribution, eq.(3.92), by table 3.4. As one only needs $G_n(\gamma = \infty)$ for the distribution eq.(3.92), the energy factors B depend only on p and are related to the percolation probability of each diagram. The solution, p_c, of eqs.(3.96) and (3.97) can be expanded in $1/d$ and one gets

$$p_c = \frac{1}{d} + \left(\frac{n-1}{2n}\right)\frac{1}{d^3} + \left(\frac{2n-5}{2n}\right)\frac{1}{d^4} + \left(3 - \frac{99}{8n} + \frac{5}{8n^2}\right)\frac{1}{d^5} + O\left(d^{-6}\right). \tag{3.98}$$

Taking the limit $n \to \infty$, one recovers the result obtained by Blease [55]. So, in this case, the n-tree approximation method gives the correct $1/d$ expansion.

The percolation problem in dimension d = 2

To further test the validity of the n-tree approximation method, consider the ground state energy per unit length, $E(p)$, for the polymer problem with energy

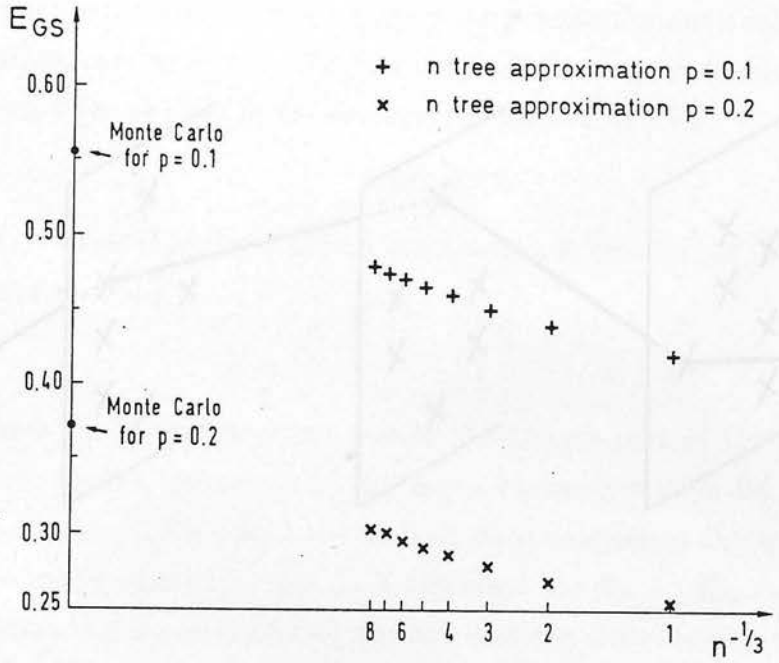

Figure 3.6: The n-tree approximation for the ground state energy of the percolation problem in dimension $1+1$.

distribution eq.(3.92), on a hypercubic lattice of dimension $1+1$, directed along the (1,1) direction. A direct Monte Carlo simulation, done on polymers of length 10^6, leads to $E(0.1) = 0.5537 \pm 0.0005$ and $E(0.2) = 0.3719 \pm 0.0005$.

By calculating the prediction, $E_n(p)$, of the n-tree approximation to this problem one obtains the results shown in fig. 3.6 for $1 \leq n \leq 8$. When plotted versus $n^{-1/3}$ the results seem to converge linearly to the results of the simulation. So here again, the n-tree approximation seems, in limit $n \to \infty$, to converge to the right answer. (There is probably a way of relating the convergence rate to the known exponents $\omega = 1/3$ and $\nu = 2/3$, in dimension $d = 1+1$, but it has proved elusive.)

The simplex problem

Another model that can be considered as a test of the n-tree approximation is a simplified model of directed polymers in a random medium, the simplex model (see fig. 3.7). In the transverse direction the lattice is a simplex and at each step

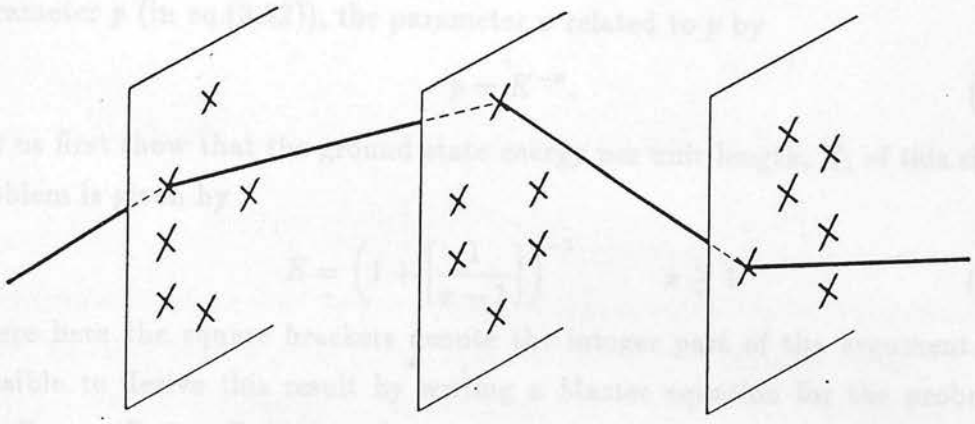

Figure 3.7: The geometry of the simplex model

along the preferred direction the polymer is allowed to jump from any corner of the simplex to any other corner.

So, in the simplex model, the lattice consists of L planes, with K points in each plane. Each point in a given plane is connected to all points in the previous and next planes. Therefore, there are K^2 links between two consecutive planes. As always, for each link between two planes one chooses a random energy, ϵ, according to a given distribution $\rho(\epsilon)$. A directed walk is one which visits a single site in each plane, so the energy, E_w, of a walk of L steps is the sum of the energies of the bonds visited by the walk.

For this problem one can write the following recursion for the partition function

$$Z_{L+1}(i) = \sum_{j=1}^{K} \mathrm{e}^{-\epsilon_{ij}(L)/T} Z_L(j) \tag{3.99}$$

where $Z_L(i)$ is the partition function of the walks that reach the i^{th} point on plane L. So, the calculation of the free energy is the same as finding the largest Lyapounov exponent of a product of $K \times K$ matrices, the elements of which are random, positive, independent and identically distributed. The answer to this problem is not known for a general distribution $\rho(\epsilon)$. However, in the particular

case of zero temperature, large K and the percolation distribution of eq.(3.92), the solution can be found. For large K it is convenient to use, instead of the parameter p (in eq.(3.92)), the parameter x related to p by

$$p = K^{-x}. \tag{3.100}$$

Let us first show that the ground state energy per unit length, E, of this simplex problem is given by

$$E = \left(1 + \left[\frac{1}{x-1}\right]\right)^{-1} \qquad x \geq 1 \tag{3.101}$$

where here the square brackets denote the integer part of the argument. It is possible to derive this result by writing a Master equation for the probability, $P_L(E_1, \ldots, E_i, \ldots, E_K)$, that the ground state energies of the walks of length L which reach the points $1, \ldots, i, \ldots, K$ of plane L are $E_1, \ldots, E_i, \ldots, E_K$. This Master equation can be solved using the fact that the differences in energy $|E_i - E_j|$ can only be zero or one, leading to eq.(3.101) for large K.

There is a simple argument which leads to eq.(3.101). It is easy to calculate the typical number of points in the plane $L = m$ that are connected by a path of zero energy to the plane $L = 0$. This typical number is $K^{1+m(1-x)}$. As long as $1 + m(1-x)$ is positive there is a path of zero energy from plane zero to plane m. So, if m is the largest integer such that

$$1 + m(1-x) > 0 \quad \text{and} \quad 1 + (m+1)(1-x) < 0 \tag{3.102}$$

the minimum energy to go from plane zero to plane $m+1$ is 1. Therefore, for large L, the ground state energy is $L/(m+1)$ where m satisfies eq.(3.102) and so one gets eq.(3.101).

Let us now consider the n-tree approximation for this simplex problem. As in section 3.2.2, the ground state energy E_n of the n-tree approximation will be given by

$$E_n = -\min_{\gamma} G_n(\gamma)|_{T=0}. \tag{3.103}$$

So one only needs to determine the large K behaviour of $G_n(\gamma)$. Clearly, from eq.(3.33),

$$\begin{aligned} G_1(\gamma) &= \frac{1}{\gamma} \ln \left[K \left(K^{-x} + \left(1 - K^{-x}\right) \mathrm{e}^{-\gamma}\right)\right] \\ &\simeq \frac{1}{\gamma} \ln \left[K^{1-x} + K\, \mathrm{e}^{-\gamma}\right] \end{aligned} \tag{3.104}$$

so one has, for large K,

$$\begin{aligned} E_1 &= (x-1)/x & x \geq 1 \\ &= 0 & x \leq 1. \end{aligned} \tag{3.105}$$

Going to the 2-tree approximation, one can show that for large K

$$G_2(\gamma) \simeq \frac{1}{2\gamma} \ln \left[K^{2-2x} + 2K^{2-x} e^{-\gamma} + K\, e^{-2\gamma} \right]. \tag{3.106}$$

This follows because the average number of points which can be reached after two steps, starting from a given point, behaves like: K^{2-2x} for zero energy, K^{2-x} for energy 1 and K for energy 2. Minimising over γ (eq.(3.103)), one finds that for large K

$$\begin{aligned} E_2 &= 0 & x \leq 1 \\ &= (x-1)/x & 1 \leq x \leq 2 \\ &= (2x-3)/2(x-1) & 2 \leq x. \end{aligned} \tag{3.107}$$

Already with this 2-tree approximation, one sees an improvement toward the true answer, eq.(3.101).

A simple way of solving the n-tree approximation for arbitrary x could not be found. However, for $x > 2$, one can generalise the reasoning which led to the expression of $G_2(\gamma)$ to arbitrary n. For example, for odd n, one gets for $x > 2$

$$G_n(\gamma) \simeq \frac{1}{n\gamma} \ln \left(\sum_{m=0}^{(n+1)/2} b_m K^{n-nx+mx} e^{-m\gamma} + \sum_{m=(n+3)/2}^{n} b_m K^{2n+1-2m-nx+mx} e^{-m\gamma} \right) \tag{3.108}$$

where b_m are constants, independent of K.

This leads to

$$\begin{aligned} E_n &= 1 - \frac{1}{n(x-2)} & \text{for} \quad x > 2n/(n-1) \\ &= (x-1)/x & \text{for} \quad 2n/(n-1) > x > 2 \end{aligned} \tag{3.109}$$

which converges to the exact result, $E = 1$ (see eq.(3.101)), in the limit $n \to \infty$.

Similarly, for even n and $x > 2$, one gets

$$E_n = 1 - \frac{1}{n(x-2)} \quad \text{for} \quad x > (2n-2)/(n-2)$$

$$= (2x-3)/2(x-1) \quad \text{for} \quad (2n-2)/(n-2) > x > 2. \quad (3.110)$$

So with this example one again sees that the limits $K \to \infty$ and $n \to \infty$ commute, at least for $x > 2$, and, since K plays a similar role to d for the hypercubic lattice, it supports the idea that these limits commute in general.

3.3 Summary of chapter 3

In sections 3.1.1 and 3.1.2, the mean field solution of the problem of directed polymers in a random medium has been presented. The mean field solution is obtained by formulating the problem on a tree. One finds two phases: a high temperature phase, in which the free energy is equal to the annealed free energy with probability 1, and a low temperature, frozen phase, characterised by broken replica symmetry.

Section 3.2.1 introduced the idea of n-tree approximations, as a method of systematically taking into account the correlations present in the system in any finite dimension. When the dimension is large, these n-tree approximations simplify, and one can use them to obtain $1/d$ expansions for the polymer problem on a d-dimensional lattice. In doing so, however, one has to exchange the limits $n \to \infty$ and $d \to \infty$ and although this presents no obvious difficulties and one can show that it is legitimate in certain cases (see section 3.2.6), there is no proof that these limits commute in general.

Sections 3.2.2–3.2.4 presented the high dimension expansions of the free energy (eq.(3.57)), transition temperature (eq.(3.60)), ground state energy (eq.(3.61)), disorder transverse fluctuations (eq.(3.75)) and the distribution of overlaps (eqs. (3.83)–(3.85)). In contrast to the mean field case, one finds that the low temperature phase is no longer frozen in finite dimension. However, within the $1/d$ expansions, the distribution of overlaps is found to remain non-trivial and the

exponent ν to remain 1/2. This would be consistent with the idea that there exists a finite upper critical dimension, above which the low temperature phase has broken replica symmetry and mean field exponents.

Chapter 4

Directed polymers on disordered hierarchical lattices

Real space renormalisation group techniques have often been used in the field of statistical mechanics, by considering models defined on hierarchical lattices (see, for example, [58-60]). The problems then reduce to the study of relatively simple renormalisation transformations. For disordered systems, when one is interested in the behaviour of some distribution under the renormalisation, one is still left with a formidable problem and one generally has to resort to numerical or perturbative methods of solution [61-63].

In this chapter, the problem of directed polymers in a random medium is considered on a hierarchical lattice which is constructed by an iterative procedure. One obtains recursion relations for the polymer problem, in which random variables are combined in a nonlinear way. These can then be investigated numerically (see section 4.2.2) or by a perturbative technique (sections 4.3.1–4.3.3).

4.1 Construction of the hierarchical lattice and the recursion relations

The family of hierarchical lattices that will be considered here are constructed by an iterative rule. The rule consists of building the lattice at the $n+1^{\text{th}}$ generation

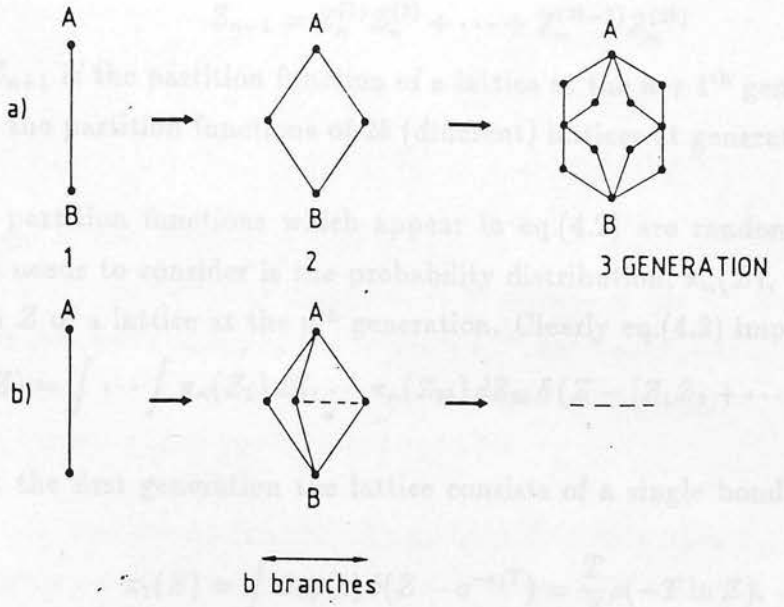

Figure 4.1: The iterative construction of (a) the diamond hierarchical lattice and (b) the generalised lattice.

by replacing each bond of the lattice at the n^{th} generation by a motif of $2b$ bonds, as shown in figure 4.1. The diamond lattice (which is the particular case $b = 2$) is shown in figure 4.1a and its generalisation to arbitrary b is shown in figure 4.1b.

Since at each new generation the number of bonds is multiplied by $2b$, the hierarchical lattice at the n^{th} generation consists of $(2b)^{n-1}$ bonds. As in the other lattice formulations of the polymer problem, one assigns a random energy, ϵ_{ij}, chosen according to a given probability distribution, $\rho(\epsilon_{ij})$, to each bond ij of the lattice. On this hierarchical lattice (fig. 4.1), one considers all the directed walks starting from point A and ending at point B. On a lattice at generation n, there are $b^{2^{n-1}-1}$ such walks and the length of each of these walks is $L = 2^{n-1}$. Although several of the results that will be presented here could be obtained for arbitrary distributions $\rho(\epsilon)$, this discussion will be limited to the Gaussian distribution

$$\rho(\epsilon) = (2\pi)^{-1/2} \exp\left(-\epsilon^2/2\right). \tag{4.1}$$

The lattice at generation $n+1$ can always be viewed as a combination of $2b$ lattices at generation n. Therefore, one can write the following recursion for the partition

function:

$$Z_{n+1} = Z_n^{(1)} Z_n^{(2)} + \cdots + Z_n^{(2b-1)} Z_n^{(2b)} \tag{4.2}$$

where Z_{n+1} is the partition function of a lattice at the $n+1^{\text{th}}$ generation and the $Z_n^{(i)}$ are the partition functions of $2b$ (different) lattices at generation n.

All the partition functions which appear in eq.(4.2) are random, so the quantity one needs to consider is the probability distribution, $\pi_n(Z)$, of the partition function Z of a lattice at the n^{th} generation. Clearly eq.(4.2) implies that

$$\pi_{n+1}(Z) = \int \cdots \int \pi_n(Z_1)\, dZ_1 \cdots \pi_n(Z_{2b})\, dZ_{2b}\, \delta\left(Z - [Z_1 Z_2 + \cdots + Z_{2b-1} Z_{2b}]\right). \tag{4.3}$$

Since at the first generation the lattice consists of a single bond, one can write that

$$\pi_1(Z) = \int d\epsilon\, \rho(\epsilon)\, \delta(Z - \mathrm{e}^{-\epsilon/T}) = \frac{T}{Z}\rho(-T \ln Z). \tag{4.4}$$

So, the problem of calculating the free energy is reduced to the study of the recursion, eq.(4.3), for the probability distribution, $\pi_n(Z)$, and the average free energy per unit length of the walk on a lattice at the n^{th} generation, $F_n(T)$, will be given by

$$F_n(T) = -T\frac{\langle \ln Z_n \rangle}{2^{n-1}} = -\frac{T}{2^{n-1}} \int dZ\, \pi_n(Z)\, \ln Z. \tag{4.5}$$

It is interesting to notice that this particular formulation of the directed polymer problem is closely related to a problem in probability theory: that of finding stable laws when one combines random variables in a nonlinear way. For example, if one takes eq.(4.2), one wants to know the shape of a distribution of Z which remains unchanged when one goes from the $Z_n^{(i)}$ to Z_{n+1}.

Apart from the thermal properties of the walk (i.e. the energy, specific heat etc.), which can be computed from the derivatives of $F_n(T)$ with respect to temperature, it is interesting to study other properties of the walk, such as the overlaps (see section 1.2 for their definition).

It is possible to obtain the average overlap $\langle q \rangle$ from a recursion relation. To do this, it is convenient to introduce the following generating function, $X_n(T, y)$, for a lattice at the n^{th} generation:

$$X_n(T, y) = \sum_{w_1} \sum_{w_2} \exp\left[-\frac{E_{w_1}}{T} - \frac{E_{w_2}}{T} + y 2^{n-1} q(w_1, w_2)\right]. \tag{4.6}$$

Then one can write the following recursion formula for X :

$$\begin{aligned} X_{n+1} &= X_n^{(1)} X_n^{(2)} + \cdots + X_n^{(2b-1)} X_n^{(2b)} \\ &+ \left(Z_n^{(1)} Z_n^{(2)} + \cdots + Z_n^{(2b-1)} Z_n^{(2b)} \right)^2 \\ &- \left[\left(Z_n^{(1)} Z_n^{(2)} \right)^2 + \cdots + \left(Z_n^{(2b-1)} Z_n^{(2b)} \right)^2 \right]. \end{aligned} \tag{4.7}$$

The origin of this relation is very similar to that of equation (4.2): the lattice at the $n+1^{\text{th}}$ generation is composed of $2b$ lattices at the n^{th} generation. If one considers two walks on the lattice at the $n+1^{\text{th}}$ generation, either they go through the same branch (first term of the right-hand side of eq.(4.7)) or they go through different branches (last two terms of eq.(4.7)).

In principle, one should consider the probability distribution $\tilde{\pi}_n(X, Z)$ of X and Z and write an iterative formula similar to eq.(4.3) with the following initial condition

$$\tilde{\pi}_1(X, Z) = \int d\epsilon \, \rho(\epsilon) \, \delta \left(X - \mathrm{e}^{y - 2\epsilon/T} \right) \delta \left(Z - \mathrm{e}^{-\epsilon/T} \right), \tag{4.8}$$

which expresses the fact that, at the first generation, the lattice consists of a single bond and that two walks on this lattice are identical and have the same energy. If one can calculate $\tilde{\pi}_n(X, Z)$, then the average $\langle X_n(T, y)/Z_n^2(T) \rangle$ can be obtained and one can deduce the average overlap, $\langle q \rangle$, from

$$\langle q \rangle = \frac{1}{2^{n-1}} \frac{d}{dy} \left\langle \frac{X_n(T, y)}{Z_n^2(T)} \right\rangle \Bigg|_{y=0}. \tag{4.9}$$

This procedure for the calculation of $\langle q \rangle$ can easily be extended to obtain other overlaps, such as $\langle q(m) \rangle$ (see eq.(1.12)). To calculate $\langle q(m) \rangle$ one would define a quantity $X_n(m; T, y)$ by

$$X_n(m; T, y) = \sum_{w_1} \sum_{w_2} \cdots \sum_{w_m} \exp \left[-\frac{E_{w_1}}{T} \cdots - \frac{E_{w_m}}{T} + y 2^{n-1} q_m(w_1, \ldots, w_m) \right]. \tag{4.10}$$

One can then write a recursion very similar to eq.(4.7)

$$\begin{aligned} X_{n+1} &= X_n^{(1)} X_n^{(2)} + \cdots + X_n^{(2b-1)} X_n^{(2b)} \\ &+ \left(Z_n^{(1)} Z_n^{(2)} + \cdots + Z_n^{(2b-1)} Z_n^{(2b)} \right)^m \\ &- \left[\left(Z_n^{(1)} Z_n^{(2)} \right)^m + \cdots + \left(Z_n^{(2b-1)} Z_n^{(2b)} \right)^m \right] \end{aligned} \tag{4.11}$$

with the initial condition

$$X_1^{(i)} = \mathrm{e}^y (Z_1^{(i)})^m. \tag{4.12}$$

One sees, from eqs.(4.2),(4.7) and (4.11), that the problem of a polymer on a random hierarchical lattice can be understood if one knows how to describe the probability distribution of variables such as X_{n+1} or Z_{n+1} which are obtained by combining other random variables (the $X_n^{(i)}$ and the $Z_n^{(i)}$) in a nonlinear way. Of course, if $b = 1$, $\ln Z_n$ is a sum of random variables and the solution is given by the central limit theorem. However, as soon as $b > 1$, the problem is much more complex and the shape of the limiting distribution of Z_n when $n \to \infty$ is not known.

At zero temperature, the recursion relation eq.(4.2) becomes a recursion relation for the ground state energy, E_n, of a lattice at the n^{th} generation

$$E_{n+1} = \min\left[E_n^{(1)} + E_n^{(2)}, \ldots, E_n^{(2b-1)} + E_n^{(2b)}\right]. \tag{4.13}$$

Then one can write the following recursion for the probability distribution of E_n, $P_n(E_n)$:

$$\begin{aligned} P_{n+1}(E) &= b\tilde{P}_n(E)\left[\int_E^\infty dE'\tilde{P}_n(E')\right]^{b-1} \\ \tilde{P}_n(E) &= \int dE' P_n(E')P_n(E-E'). \end{aligned} \tag{4.14}$$

This recursion was studied numerically and analytically by Derrida and Griffiths [47]. It was observed numerically that $P_n(E)$ takes the following form for large n,

$$P_n(E) = \frac{1}{\Delta_n} F_b\left(\frac{E-\gamma_n}{\Delta_n}\right) \tag{4.15}$$

where γ_n and Δ_n both depend on the initial distribution $P_1(E) = \rho(E)$ but F_b does not. Moreover, for $n \to \infty$, the ratio Δ_{n+1}/Δ_n was found to have a limit λ_b, independent of the initial distribution $P_1(E)$. This implies that the fluctuations of the ground state energy increase with the length, L, of the polymer as a power law

$$\left[\left\langle E_n^2\right\rangle - \langle E_n\rangle^2\right]^{1/2} \sim \Delta_n \sim (\lambda_b)^n \sim L^\omega \tag{4.16}$$

with

$$\omega = \ln\lambda_b / \ln 2 \tag{4.17}$$

see eq.(1.8). The ground state energy per unit length of the polymer, $\langle E_n\rangle / 2^{n-1}$, and the scaling factor λ_b were measured numerically for several values of b and it was shown that one could develop a perturbative approach for b close to 1,

which gives analytic expressions for these two quantities. In sections 4.3.1 and 4.3.3 these results will be recovered as the zero temperature limit of a study of recursion eq.(4.2).

4.2 Studies of the recursions for general b

First let us see what one can conclude about the system when the parameter b is arbitrary.

4.2.1 The integer moments and the overlaps

For most disordered systems, the calculation of the integer moments of the partition function is much easier than that of the average free energy. For the problem of directed polymers on these hierarchical lattices, it is easy to see that the calculation of the integer moments can be reduced to the study of simple iterations. From eq.(4.2), one can obtain the following recursion relations for the first moments of Z_n

$$\langle Z_{n+1} \rangle = b \langle Z_n \rangle^2 \tag{4.18}$$

$$\left\langle Z_{n+1}^2 \right\rangle = b \left\langle Z_n^2 \right\rangle^2 + b(b-1) \langle Z_n \rangle^4 \tag{4.19}$$

$$\begin{aligned} \left\langle Z_{n+1}^3 \right\rangle &= b \left\langle Z_n^3 \right\rangle^2 + 3b(b-1) \left\langle Z_n^2 \right\rangle^2 \langle Z_n \rangle^2 \\ &+ b(b-1)(b-2) \langle Z_n \rangle^6 \end{aligned} \tag{4.20}$$

$$\begin{aligned} \left\langle Z_{n+1}^4 \right\rangle &= b \left\langle Z_n^4 \right\rangle^2 + 4b(b-1) \left\langle Z_n^3 \right\rangle^2 \langle Z_n \rangle^2 + 3b(b-1) \left\langle Z_n^2 \right\rangle^4 \\ &+ 6b(b-1)(b-2) \left\langle Z_n^2 \right\rangle^2 \langle Z_n \rangle^4 + b(b-1)(b-2)(b-3) \langle Z_n \rangle^8 \end{aligned} \tag{4.21}$$

with the initial condition

$$\langle Z_1^p \rangle = \int \rho(\epsilon) \mathrm{e}^{-p\epsilon/T} d\epsilon. \tag{4.22}$$

To calculate the p^{th} moment of Z_n, one needs to study a simple dynamical system in a p-dimensional space, since the calculation of the p^{th} moment at the $n+1^{\text{th}}$ generation only requires the knowledge of the first p moments at the n^{th} generation. This dynamical system can be simplified further by considering the following ratios

$$z_p(n) = \langle Z_n \rangle^p \,/\, \langle Z_n^p \rangle \tag{4.23}$$

so that the recursions, eqs.(4.19)–(4.21), become

$$z_2(n+1) = b\,[z_2(n)]^2 \left[1 + (b-1)(z_2(n))^2\right]^{-1} \tag{4.24}$$

$$z_3(n+1) = b^2\,[z_3(n)]^2 \left[1 + 3(b-1)\left(\frac{z_3(n)}{z_2(n)}\right)^2 + (b-1)(b-2)(z_3(n))^2\right]^{-1} \tag{4.25}$$

$$\begin{aligned} z_4(n+1) = b^3\,[z_4(n)]^2 \Bigg[1 &+ 4(b-1)\left(\frac{z_4(n)}{z_3(n)}\right)^2 + 3(b-1)(z_4(n))^2(z_2(n))^4 \\ &+ 6(b-1)(b-2)\left(\frac{z_4(n)}{z_2(n)}\right)^2 + (b-1)(b-2)(b-3)(z_4(n))^2\Bigg]^{-1}. \end{aligned} \tag{4.26}$$

These recursions possess several attractive fixed points and each possible phase of $\langle Z^p \rangle$ corresponds to one of these attractive fixed points.

To describe the phase diagram of $\langle Z^2 \rangle$, it is sufficient to study the recursion eq.(4.24). Equation (4.24) has three fixed points: $z_2 = 1$, $z_2 = 0$ and $z_2 = 1/(b-1)$. For $b \leq 2$, $z_2 = 0$ is attractive and $z_2 = 1$ is unstable, whereas $z_2 = 1/(b-1)$ is unreachable if $0 < z_2(1) < 1$ (see eq.(4.23)). So, any initial $z_2(1) \neq 1$ converges to $z_2 = 0$. For $b > 2$, the two fixed points, $z_2 = 1$ and $z_2 = 0$, are attractive and the fixed point $z_2 = 1/(b-1)$ is unstable. Depending on the initial value $z_2(1)$, the point $z_2(n)$ converges to one of these two attractive fixed points: $z_2(n) \to 0$ if $z_2(1) < 1/(b-1)$ and $z_2(n) \to 1$ if $z_2(1) > 1/(b-1)$. So, one sees that in the plane (b, T), the line $T_2(b)$ given by

$$z_2(1) = \frac{\left[\int \rho(\epsilon)\exp(-\epsilon/T_2)\,d\epsilon\right]^2}{\int \rho(\epsilon)\exp(-2\epsilon/T_2)\,d\epsilon} = \frac{1}{b-1} \tag{4.27}$$

is a transition line for $\langle Z^2 \rangle$. For the Gaussian distribution, eq.(4.1), this line $T_2(b)$ is given by

$$T_2(b) = \left[\ln(b-1)\right]^{-1/2} \tag{4.28}$$

and is shown in figure 4.2. One sees that $T_2(b)$ diverges as $b \to 2$ and that for $b < 2$,

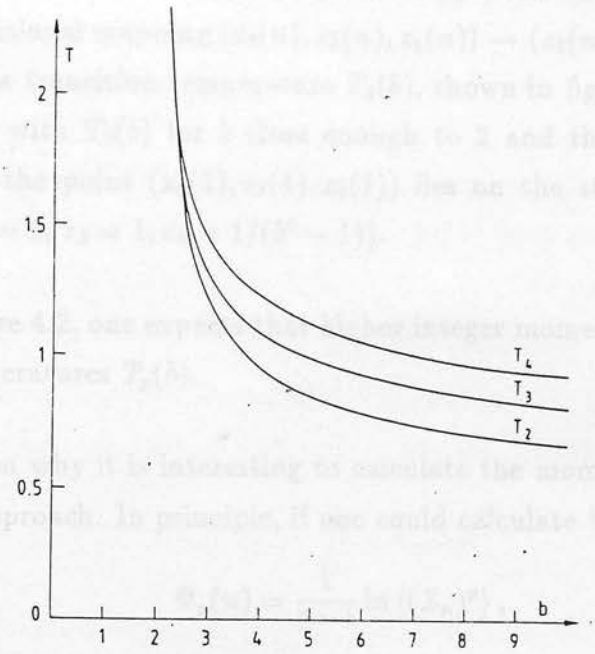

Figure 4.2: The transition temperatures $T_2(b)$, $T_3(b)$ and $T_4(b)$ of the moments $\langle Z^2 \rangle$, $\langle Z^3 \rangle$ and $\langle Z^4 \rangle$ versus b.

$\langle Z^2 \rangle$ is always in its low temperature phase. For $T > T_2(b)$, $z_2(n) \to 1$ as $n \to \infty$, and so one knows that $\langle Z_n^2 \rangle / \langle Z_n \rangle^2 \to 1$. This implies that the distribution of Z_n becomes very narrow around $\langle Z_n \rangle$. As a consequence, for $T > T_2(b)$, one has

$$\lim_{n\to\infty} \frac{1}{2^{n-1}} \ln Z_n = \lim_{n\to\infty} \frac{1}{2^{n-1}} \ln \langle Z_n \rangle \tag{4.29}$$

with probability 1. As in section 2.2, one can use this to determine bounds on the transition temperature of the free energy. One finds that the bounds are given by

$$(2 \ln b)^{-1/2} \leq T_c(b) \leq [\ln (b-1)]^{-1/2}. \tag{4.30}$$

Notice that the parameter b plays a role similar to the dimension of the hypercubic lattice, see eq.(2.19).

By looking at the two-dimensional mapping $(z_2(n), z_3(n)) \to (z_2(n+1), z_3(n+1))$, eq.(4.25), one can obtain the phase diagram of $\langle Z_n^3 \rangle$. The analytic form of the transition line $T_3(b)$ is not as simple as eq.(4.28): one can show that for $b < 2.303..., T_3(b) = T_2(b)$, whereas for $b > 2.303$, $T_3(b)$ is obtained by the condition that the point $(z_2(1), z_3(1))$ lies on the stable manifold of the fixed point $(z_2 = 1, z_3 = 1/(b^2-1))$. The transition line $T_3(b)$ versus b is shown in figure 4.2.

In a similar way, the transition temperature of $\langle Z^4 \rangle$ can be obtained by studying the three-dimensional mapping $(z_2(n), z_3(n), z_4(n)) \rightarrow (z_2(n+1), z_3(n+1), z_4(n+1))$. One finds a transition temperature $T_4(b)$, shown in figure 4.2. As for $T_3(b)$, $T_4(b)$ coincides with $T_2(b)$ for b close enough to 2 and then it is given by the condition that the point $(z_2(1), z_3(1), z_4(1))$ lies on the stable manifold of the fixed point $(z_2 = 1,\ z_3 = 1, z_4 = 1/(b^3 - 1))$.

Looking at figure 4.2, one expects that higher integer moments would have higher transition temperatures $T_p(b)$.

The main reason why it is interesting to calculate the moments $\langle Z_n^p \rangle$ is to try to use a replica approach. In principle, if one could calculate $\Psi_p(n)$, defined by

$$\Psi_p(n) = \frac{1}{2^{n-1}} \ln \langle (Z_n)^p \rangle , \tag{4.31}$$

for all p, the replica approach would give the average free energy, $F_n(T)$, by

$$F_n(T) = -\frac{T}{2^{n-1}} \langle \ln Z_n \rangle = -T \lim_{p \rightarrow 0} \frac{\Psi_p(n)}{p}. \tag{4.32}$$

From the previous relations, eqs.(4.18)–(4.26), one can get expressions for $\Psi_p(n)$ for $p = 1, 2, 3$ and 4. One finds that the results are given, for the Gaussian energy distribution eq.(4.1), by

$$\Psi_1(n) = \left(1 - \frac{1}{2^{n-1}}\right) \ln b + \frac{1}{2T^2} \tag{4.33}$$

$$\Psi_2(n) = \left(1 - \frac{1}{2^{n-1}}\right) \ln b + \frac{4}{2T^2} + \sum_{i=1}^{n-1} \frac{1}{2^{i-1}} \ln \left[1 + (b-1)(z_2(i))^2\right] \tag{4.34}$$

$$\begin{aligned} \Psi_3(n) &= \left(1 - \frac{1}{2^{n-1}}\right) \ln b + \frac{9}{2T^2} \\ &+ \sum_{i=1}^{n-1} \frac{1}{2^{i-1}} \ln \left[1 + 3(b-1)\left(\frac{z_3(i)}{z_2(i)}\right)^2 + (b-1)(b-2)(z_3(i))^2\right] \end{aligned} \tag{4.35}$$

$$\begin{aligned} \Psi_4(n) &= \left(1 - \frac{1}{2^{n-1}}\right) \ln b + \frac{16}{2T^2} \\ &+ \sum_{i=1}^{n-1} \frac{1}{2^{i-1}} \ln \left[1 + 4(b-1)\left(\frac{z_4(i)}{z_3(i)}\right)^2 + 3(b-1)\frac{(z_4(i))^2}{(z_2(i))^4}\right. \\ &+ \left. 6(b-1)(b-2)\left(\frac{z_4(i)}{z_2(i)}\right)^2 + (b-1)(b-2)(b-3)(z_4(i))^2\right]. \end{aligned} \tag{4.36}$$

Looking at these expressions, it is easy to guess an extrapolation to arbitrary p of the first two terms of the right-hand sides of eqs.(4.33)–(4.36). However, the extrapolation of the last term is not clear.

Exactly as it was possible to deduce the recursions, eqs.(4.18)–(4.21), from equation (4.2), one can also write a recursion for $\Phi_n(p)$ (p is an integer ≥ 2), which is defined by

$$\Phi_n(p) = \left\langle X_n (Z_n)^{p-2} \right\rangle \tag{4.37}$$

and X_n is given by eq.(4.6). For arbitrary p, the knowledge of $\Phi_n(p)$ would give the average overlap, $\langle Q_n(p) \rangle$, of two walks amongst p walks, from the formula

$$\langle Q_n(p) \rangle = \frac{d}{dy} \ln \left[\Phi_n(p) \right] \Big|_{y=0} \tag{4.38}$$

and the overlap $\langle q \rangle$, of equation (4.9), could be calculated by

$$\langle q \rangle = \lim_{p \to 0} \langle Q_n(p) \rangle. \tag{4.39}$$

For $p = 2, 3, 4$ one finds that the overlap between two configurations satisfies

$$\langle Q_n(2) \rangle = \prod_{i=1}^{n-1} \frac{1}{1 + (b-1)(z_2)^2} \tag{4.40}$$

$$\langle Q_n(3) \rangle = \prod_{i=1}^{n-1} \frac{1 + (b-1)(z_3/z_2)^2}{1 + 3(b-1)(z_3/z_2)^2 + (b-1)(b-2)(z_3)^2} \tag{4.41}$$

$$\begin{aligned} \langle Q_n(4) \rangle = & \prod_{i=1}^{n-1} \left[1 + 2(b-1) \left(\frac{z_4}{z_3} \right)^2 + (b-1) \frac{(z_4)^2}{(z_2)^4} + (b-1)(b-2) \left(\frac{z_4}{z_2} \right)^2 \right] \\ & \times \left[1 + 4(b-1) \left(\frac{z_4}{z_3} \right)^2 + 3(b-1) \frac{(z_4)^2}{(z_2)^4} \right. \\ & + \left. 6(b-1)(b-2) \left(\frac{z_4}{z_2} \right)^2 + (b-1)(b-2)(b-3)(z_4)^2 \right]^{-1} \end{aligned} \tag{4.42}$$

where, in eqs.(4.40)–(4.42), $z_2 = z_2(i), z_3 = z_3(i)$ and $z_4 = z_4(i)$. As was the case for eqs.(4.33)–(4.36), it is not obvious what the generalisation of these expressions for arbitrary p should be.

It is clear that expressions similar to eqs.(4.40)–(4.42) could be found for overlaps of more than two walks. Again looking at the expressions for the overlaps of m walks amongst $p = m, m+1, \ldots$ walks, it is hard to guess an expression valid for arbitrary p.

So, several properties concerning the integer moments of Z can be calculated on the hierarchical lattice. The calculation of the second moment allows one to obtain the exact expression, eq.(4.29), for the free energy above the temperature $T_2(b)$, given by eq.(4.28). The exact expressions for the first moments, eqs.(4.33)–(4.36), or for the overlaps associated with these first moments, eqs.(4.40)–(4.42), are, however, too complicated to permit one to guess their generalisation to non-integer moments. In sections 4.3.1–4.3.3, it will be shown that one can obtain such generalisations, at least in a perturbative way, when b is close to 1.

4.2.2 Monte Carlo simulation of the specific heat and of the overlaps

Despite the simplicity of the recursion eq.(4.2), it was not possible to find an analytic way of calculating $\pi_n(Z)$ (defined by eq.(4.3)) for arbitrary n and b to obtain the free energy, $\langle \ln Z_n \rangle$, as a function of temperature. As will be discussed in section 4.3.1, one can only get an analytic expression when b is close to 1.

For arbitrary b, however, it is possible to estimate the quantities of interest rather accurately by numerical methods. The method that has been used is a Monte Carlo sampling which has the advantage of being easy to program [44]. The idea is the following: although one cannot calculate $\pi_n(Z)$ analytically, one can sample it. So one can represent $\pi_n(Z)$ by N ($N = 5.10^4$ or 2.10^5 in these simulations) different values of Z : $Z_n^{(1)}, \ldots, Z_n^{(N)}$. For example, to represent $\pi_1(Z)$, N random Gaussian numbers, ϵ_i, are chosen and one obtains N values $Z_1^{(i)}$ by

$$Z_1^{(i)} = \exp(-\epsilon_i/T). \tag{4.43}$$

Then, to represent $\pi_2(Z)$ by N values $Z_2^{(i)}$, one chooses, for each i, $2b$ random indices $j_1(i), \ldots, j_{2b}(i)$ between 1 and N and one calculates the $Z_2^{(i)}$ using

$$Z_{n+1}^{(i)} = Z_n^{(j_1)} Z_n^{(j_2)} + \cdots + Z_n^{(j_{2b-1})} Z_n^{(j_{2b})} \tag{4.44}$$

for $n = 1$. Once the N values $Z_2^{(i)}$ have been calculated in this way, one can calculate N values of $Z_3^{(i)}$ to represent $\pi_3(Z)$. Again one chooses, for each i, $2b$ new random indices $j_1(i), \ldots, j_{2b}(i)$ and one calculates each $Z_3^{(i)}$ using eq.(4.44).

One can iterate this procedure many times and at the n^{th} step one gets N values, $Z_n^{(i)} (1 \leq i \leq N)$, which represent the distribution $\pi_n(Z)$.

If one then needs to estimate the average of a function of Z over the distribution $\pi_n(Z)$ (e.g. $\ln Z$), one replaces it by the average over the $Z_n^{(i)}$:

$$\int \ln Z \, \pi_n(Z) \, dZ \simeq \frac{1}{N} \sum_{i=1}^{N} \ln \left(Z_n^{(i)} \right). \tag{4.45}$$

It is often interesting to know the first or second derivative of Z with respect to temperature, so that one can obtain the energy or the specific heat. Using eq.(4.44), it is easy to write recursions for these derivatives and at each step one can represent the distribution by N triplets $(Z_n^{(i)}, dZ_n^{(i)}/dT, d^2Z_n^{(i)}/dT^2)$ which are calculated by the same procedure.

The curves of the specific heat obtained for a lattice built up to the sixteenth generation for $b = 2$ and $b = 5$ (with $N = 5.10^4$ and 2.10^5) are shown in figures 4.3a and 4.3b. For $b = 2$, the specific heat is a smooth function of temperature, whereas for $b = 5$ there is a sharp maximum at a temperature $T_c = 0.75 \pm 0.05$, which is strictly smaller than $T_2 \simeq 0.849$ (see eq.(4.28)). Above T_c, the numerical data agree well with the prediction for the specific heat per unit length

$$C = 1/T^2 \tag{4.46}$$

which follows from eqs.(4.29) and (4.1). For $b = 2$ the specific heat can be seen to approach the form given by eq.(4.46). However, it is not clear whether the specific heat has the form of eq.(4.46) above a certain finite transition temperature, T_c, or whether T_c is infinite.

The same procedure can be used to obtain the overlaps. As discussed in section 4.1, one has to calculate Z_n and X_n, through eqs.(4.2) and (4.7), in order to obtain $\pi_n(X, Z)$. This can be done by representing $\pi_n(X, Z)$ by N pairs $(X_n^{(i)}, Z_n^{(i)})$. Thus, each pair $(X_{n+1}^{(i)}, Z_{n+1}^{(i)})$ is calculated by choosing, for each i, $2b$ ancestors $j_1, \ldots, j_{2b}$ and by using eq.(4.44) and

$$\begin{aligned} X_{n+1}^{(i)} &= X_n^{(j_1)} X_n^{(j_2)} + \cdots + X_n^{(j_{2b-1})} X_n^{(j_{2b})} \\ &+ \left(Z_n^{(j_1)} Z_n^{(j_2)} + \cdots + Z_n^{(j_{2b-1})} Z_n^{(j_{2b})} \right)^2 \\ &- \left[\left(Z_n^{(j_1)} Z_n^{(j_2)} \right)^2 + \cdots + \left(Z_n^{(j_{2b-1})} Z_n^{(j_{2b})} \right)^2 \right]. \end{aligned} \tag{4.47}$$

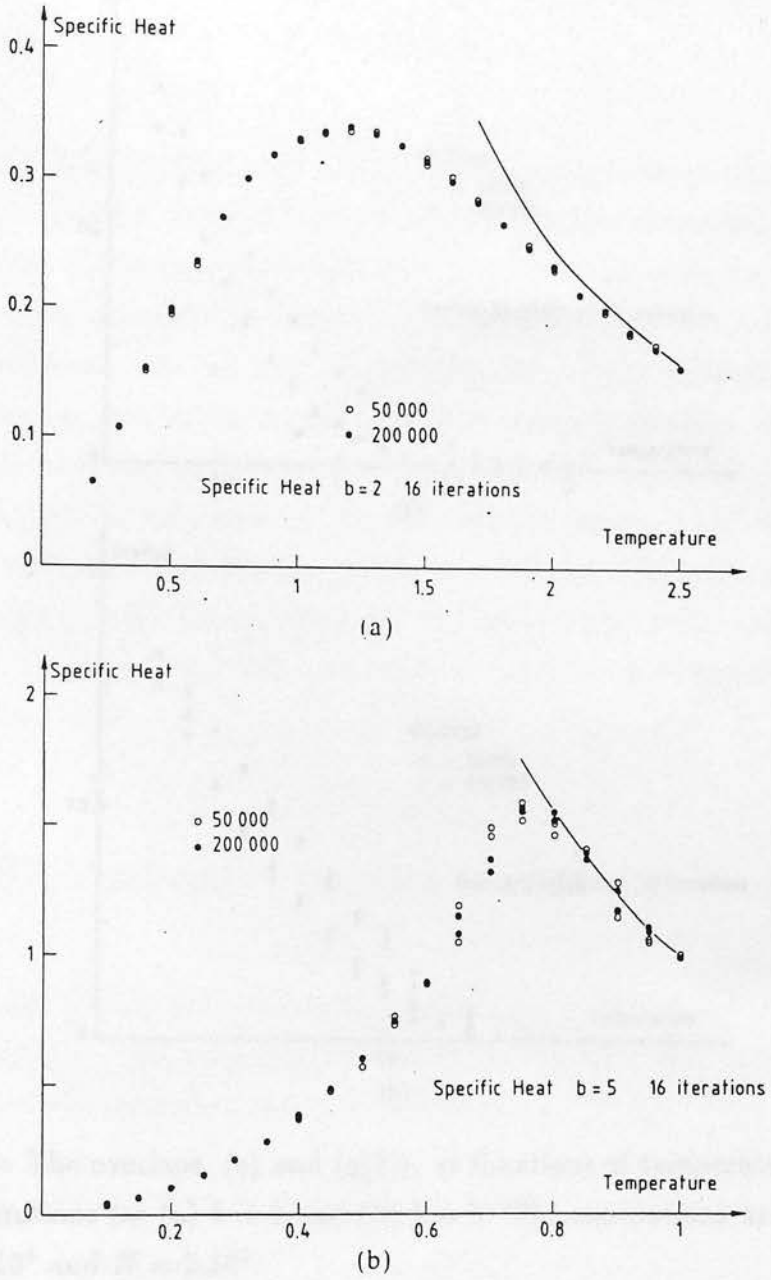

Figure 4.3: The specific heat of a lattice at the sixteenth generation as a function of temperature for (a) $b = 2$ and (b) $b = 5$. The simulations used sample sizes of $N = 5.10^4$ and $N = 2.10^5$. The solid line shows the specific heat (eq.(4.46)) of the high temperature phase.

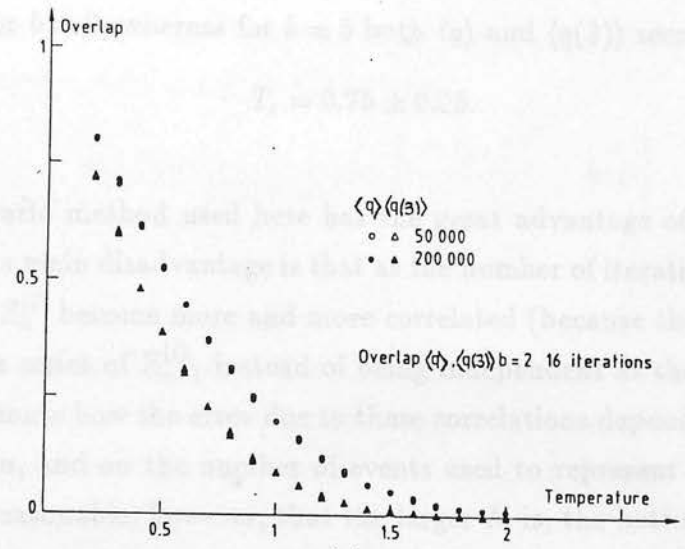

(a)

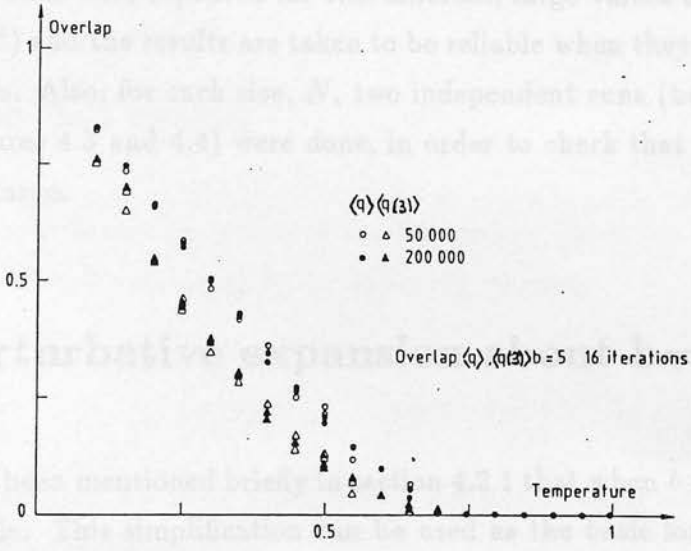

(b)

Figure 4.4: The overlaps, $\langle q \rangle$ and $\langle q(3) \rangle$, as functions of temperature for a lattice of 16 generations for (a) $b = 2$ and (b) $b = 5$. The simulations used sample sizes of $N = 5.10^4$ and $N = 2.10^5$.

Then the averages of functions of X and Z can be calculated as in eq.(4.45). When one only requires derivatives of X_n at $y = 0$ (see eq.(4.9)), it is easier to iterate Z and derivatives of X at $y = 0$ than to take the derivative numerically.

The overlaps, $\langle q \rangle$ and $\langle q(3) \rangle$, obtained using this Monte Carlo method are plotted in figures 4.4a and 4.4b for a hierarchical lattice of $n = 16$ generations using $N = 5.10^4$ and $N = 2.10^5$. As with the specific heat, one sees a smooth temperature

dependence for $b = 2$, whereas for $b = 5$ both $\langle q \rangle$ and $\langle q(3) \rangle$ seem to vanish at

$$T_c = 0.75 \pm 0.05. \tag{4.48}$$

The Monte Carlo method used here has the great advantage of being simple to implement. Its main disadvantage is that as the number of iterations, n, increases, the N values $Z_n^{(i)}$ become more and more correlated (because they are calculated from the same series of $Z_{n-1}^{(i)}$ instead of being independent as they should be). It is hard to estimate how the error due to these correlations depends on the number of iterations, n, and on the number of events used to represent the distribution, N. It seems reasonable, however, that the larger N is, the better the results are. So the simulations were repeated for two different, large values of N ($N = 5.10^4$ and $N = 2.10^5$) and the results are taken to be reliable when they are identical for these two sizes. Also, for each size, N, two independent runs (both of which are plotted in figures 4.3 and 4.4) were done, in order to check that the fluctuations were not too large.

4.3 Perturbative expansion about b=1

It has already been mentioned briefly in section 4.2.1 that when $b = 1$ the problem becomes simple. This simplification can be used as the basis for a perturbative treatment of the recursions obtained in section 4.1.

When $b = 1$ the recursion, eq.(4.2), for the partition function reduces to

$$Z_{n+1} = Z_n^{(1)} Z_n^{(2)} \tag{4.49}$$

and so the disorder average of $\ln Z_n$ obeys the simple relation

$$\langle \ln Z_{n+1} \rangle = 2 \langle \ln Z_n \rangle . \tag{4.50}$$

Suppose that the probability distribution of the energies, $\rho(\epsilon_{ij})$, is given by eq.(4.1). From eq.(4.4), the probability distribution of Z_1 for the first generation of the lattice, $\pi_1(Z)$, is given by

$$\pi_1(Z) = \frac{T}{(2\pi)^{1/2}} \exp\left[-\frac{T^2}{2} (\ln Z)^2 - \ln Z \right]. \tag{4.51}$$

Hence it is easy to show that the probability distribution of Z_n at the n^{th} generation of the lattice, $\pi_n(Z)$, will be of the form

$$\pi_n(Z) = \frac{1}{(2\pi)^{1/2}\delta_n} \exp\left[-\frac{1}{2}\frac{(\ln Z)^2}{\delta_n^2} - \ln Z\right] \tag{4.52}$$

where

$$\delta_n = \sqrt{2^{n-1}}/T. \tag{4.53}$$

So, for $b = 1$, the stable law of the recursion eq.(4.2) is a Gaussian in $\ln Z$, as given by the central limit theorem. Returning to the case of $b > 1$, one can now proceed to seek an expansion around $b = 1$ in terms of the parameter ε, where

$$\varepsilon = b - 1. \tag{4.54}$$

4.3.1 The free energy

To obtain a perturbative expansion of the free energy about $b = 1$ it is helpful to write the recursion for $\langle \ln Z_{n+1} \rangle$ in the following manner:

$$\begin{aligned} \langle \ln Z_{n+1} \rangle &= \left\langle \ln\left(Z_n^{(1)} Z_n^{(2)}\right)\right\rangle \\ &+ \left\langle \ln\left(Z_n^{(1)} Z_n^{(2)} + \cdots + Z_n^{(2b-1)} Z_n^{(2b)}\right) - \ln\left(Z_n^{(1)} Z_n^{(2)}\right)\right\rangle \end{aligned} \tag{4.55}$$

where the expression occuring when $b = 1$ has simply been added to and subtracted from the right-hand side.

Using the integral representation of the logarithm

$$\ln x = \int_0^\infty \frac{\mathrm{e}^{-t} - \mathrm{e}^{-tx}}{t} dt \tag{4.56}$$

one can rewrite the above as

$$\begin{aligned} \langle \ln Z_{n+1} \rangle &= 2\langle \ln Z_n \rangle + \int_0^\infty \frac{dt}{t} \left\langle \left\{ \exp(-tZ_n^{(1)} Z_n^{(2)}) \right.\right. \\ &- \left.\left. \exp\left[-t\left(Z_n^{(1)} Z_n^{(2)} + \cdots + Z_n^{(2b-1)} Z_n^{(2b)}\right)\right]\right\}\right\rangle \\ &= 2\langle \ln Z_n \rangle + \int_0^\infty \frac{dt}{t} \left[\left\langle \exp\left(-tZ_n^{(1)} Z_n^{(2)}\right)\right\rangle \right. \\ &- \left. \left\langle \exp\left(-tZ_n^{(1)} Z_n^{(2)}\right)\right\rangle^b\right], \end{aligned} \tag{4.57}$$

using the fact that the $Z_n^{(i)}$ are independent random variables.

It is useful to define a function, $\tilde{f}_n(t)$, such that

$$\tilde{f}_n(t) = \left\langle \exp(-tZ_n^{(1)}Z_n^{(2)}) \right\rangle . \tag{4.58}$$

Then the recursion, valid for all b, can be written as

$$\langle \ln Z_{n+1} \rangle = 2 \langle \ln Z_n \rangle + \int_0^\infty \frac{dt}{t} \left(\tilde{f}_n(t) - (\tilde{f}_n(t))^b \right) . \tag{4.59}$$

This clearly reduces to the correct recursion when $b = 1$. Equation (4.59) can now be expanded about $b = 1$, in powers of ε, where $\varepsilon = b - 1$.

$$\begin{aligned} \langle \ln Z_{n+1} \rangle &= 2 \langle \ln Z_n \rangle - \varepsilon \int_0^\infty \frac{dt}{t} \tilde{f}_n(t) \ln \tilde{f}_n(t) \\ &\quad - \frac{\varepsilon^2}{2} \int_0^\infty \frac{dt}{t} \tilde{f}_n(t) \ln^2 \tilde{f}_n(t) + \cdots \end{aligned} \tag{4.60}$$

The free energy to first order in ε

To obtain the recursion to first order in ε, it is only necessary to determine $\tilde{f}_n(t)$ to leading order, i.e. zeroth order in ε, or when $b = 1$.

$$\begin{aligned} \tilde{f}_n(t) &= \left\langle e^{-tZ_n^{(1)}Z_n^{(2)}} \right\rangle = \left\langle e^{-tZ_{n+1}} \right\rangle + O(\varepsilon) \\ &= \frac{1}{T} \int_{-\infty}^{\infty} \pi_{n+1} \left(e^{x/T} \right) \exp \left[\frac{x}{T} - te^{x/T} \right] dx + O(\varepsilon) \\ &= f\left(t, \sqrt{2}\delta_n\right) + O(\varepsilon) \end{aligned} \tag{4.61}$$

where

$$f(t,\lambda) = \frac{1}{(2\pi)^{1/2}} \int_{-\infty}^{+\infty} e^{-x^2/2} \exp \left[-te^{\lambda x} \right] dx. \tag{4.62}$$

Hence, to first order in ε,

$$\langle \ln Z_{n+1} \rangle = 2 \langle \ln Z_n \rangle - \varepsilon \int_0^\infty \frac{dt}{t} f\left(t, \sqrt{2}\delta_n\right) \ln f\left(t, \sqrt{2}\delta_n\right) + O(\varepsilon^2). \tag{4.63}$$

Using this recursion it is then easy to show that, to first order in ε, the average free energy per unit length of the system at the n^{th} generation is given by

$$F_n = -\frac{T}{2^{n-1}} \langle \ln Z_n \rangle = T\varepsilon \sum_{i=1}^{n-1} \frac{1}{2^i} \int_0^\infty \frac{dt}{t} f\left(t, \frac{\sqrt{2^i}}{T}\right) \ln f\left(t, \frac{\sqrt{2^i}}{T}\right) . \tag{4.64}$$

It will be shown in sections 4.3.2 and 4.3.3 that the overlaps and moments of the partition function can also be obtained to order ε by the same approach and that they can also be expressed in terms of the function $f(t,\lambda)$ only.

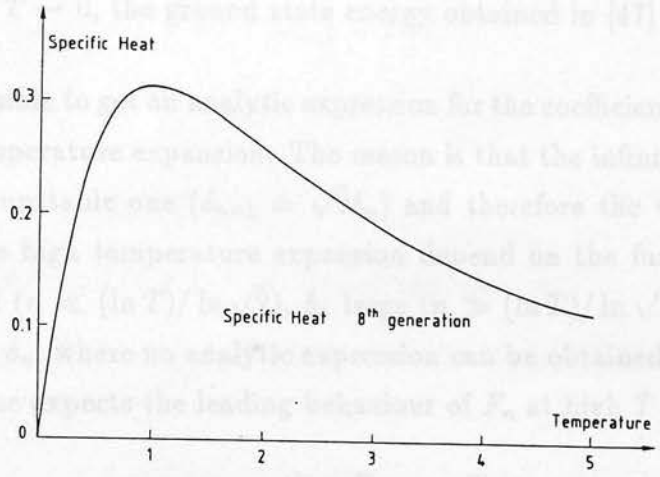

Figure 4.5: The specific heat of a lattice of eight generations calculated from the perturbative expansion, eq.(4.64). It looks rather similar to the results of the Monte Carlo simulation for $b = 2$, see fig. 4.3a.

Having obtained the expression for the free energy, F_n, to first order in ε, the energy, E_n, and specific heat, C_n, of the system at the n^{th} generation, can be obtained to the same order by differentiating F_n with respect to the temperature, T. The specific heat obtained in this manner is shown, as a function of temperature, in figure 4.5 for a lattice of $n = 8$ generations. One sees that the shape (linear at low temperature and the maximum at $T \simeq 1.0$) is rather similar to the results of the Monte Carlo simulation for $b = 2$.

At low temperature, using the asymptotic forms of $f(t, \lambda)$ for $\lambda \to \infty$, it is possible (see appendix B, eq.(B16)) to simplify the expression for the free energy to obtain

$$F_n = \varepsilon \left\{ -K_1 \sum_{i=1}^{n-1} \frac{1}{2^{i/2}} + \frac{1}{2} \left[(\Gamma^{(1)}(1))^2 - \Gamma^{(2)}(1) \right] K_1 T^2 \sum_{i=1}^{n-1} \frac{1}{2^{3i/2}} \right.$$
$$\left. + \quad K_2 T^3 \left[\Gamma^{(1)}(1)\Gamma^{(2)}(1) - \frac{2}{3} \left(\Gamma^{(1)}(1) \right)^3 - \frac{\Gamma^{(3)}(1)}{3} \right] \sum_{i=1}^{n-1} \frac{1}{4^i} + O(T^4) \right\} \quad (4.65)$$

where

$$K_1 \;=\; -\int_{-\infty}^{\infty} \frac{t e^{-t^2/2}}{(2\pi)^{1/2}} \ln \left[\int_t^{\infty} e^{-u^2/2} \frac{du}{(2\pi)^{1/2}} \right] dt = 0.90320 \quad (4.66)$$

$$K_2 = \int_{-\infty}^{\infty} \left(\frac{1-t^2}{2}\right) \frac{e^{-t^2/2}}{(2\pi)^{1/2}} \ln \left[\int_t^{\infty} e^{-u^2/2} \frac{du}{(2\pi)^{1/2}}\right] dt = 0.29782 . \quad (4.67)$$

In the limit $T \to 0$, the ground state energy obtained in [47] is recovered.

It is not possible to get an analytic expression for the coefficients of the corresponding high temperature expansion. The reason is that the infinite temperature fixed point is an unstable one ($\delta_{n+1} = \sqrt{2}\delta_n$) and therefore the value of some coefficients of the high temperature expansion depend on the functions at all points δ_n: δ_n small ($n \ll (\ln T)/\ln\sqrt{2}$), δ_n large ($n \gg (\ln T)/\ln\sqrt{2}$) and also intermediate values δ_n, where no analytic expression can be obtained. Nevertheless, from eq.(4.64), one expects the leading behaviour of F_n at high T to be

$$\lim_{n\to\infty} F_n \sim -\varepsilon T. \quad (4.68)$$

The free energy to second order in ε

The remainder of this section shows how the perturbative approach can be extended to higher order in ε. To do this, it is necessary to determine the function, $\tilde{f}_n(t)$, defined by eq.(4.58), to higher order in ε. Below, the first correction to $\tilde{f}_n(t)$ is obtained.

Let us define a new function $\tilde{F}_n(t)$ by

$$\tilde{F}_n(t) = \left\langle e^{-tZ_n} \right\rangle . \quad (4.69)$$

Then from eqs.(4.58),(4.69) and (4.2) it is true, for all b, that

$$\tilde{F}_{n+1}(t) = \left[\tilde{f}_n(t)\right]^b . \quad (4.70)$$

Hence, $\tilde{F}_{n+1}(t)$ is related to $\tilde{f}_n(t)$. Now one needs to find another relation to obtain $\tilde{f}_n(t)$ from $\tilde{F}_n(t)$. If b is close to 1, one can consider the probability distribution, $R_n(Y)$, of the quantity $Y = \ln Z_n$ to be the sum of a Gaussian distribution and a small correction

$$R_n(Y) = \frac{1}{(2\pi)^{1/2}\delta_n} \exp\left(\frac{-Y^2}{2\delta_n^2}\right) + \varepsilon \frac{1}{\delta_n} \varphi_n\left(\frac{Y}{\delta_n}\right) . \quad (4.71)$$

It is then clear that the probability distribution, $r_n(y)$, of the quantity $y = \ln\left(Z_n^{(1)} Z_n^{(2)}\right)$ is given by

$$\begin{aligned} r_n(y) &= \int R_n(Y) R_n(y-Y) dY \\ &= \frac{1}{(2\pi)^{1/2} 2^{1/2} \delta_n} \exp\left(-\frac{y^2}{4\delta_n^2}\right) \\ &+ \frac{2\varepsilon}{(2\pi)^{1/2}\delta_n^2} \int \varphi_n\left(\frac{Y}{\delta_n}\right) \mathrm{e}^{-(Y-y)^2/2\delta_n^2} dY + O(\varepsilon^2). \end{aligned} \tag{4.72}$$

From eqs.(4.69) and (4.71), $\tilde{F}_n(t)$ can be expressed as

$$\tilde{F}_n(t) = \int R_n(Y) \exp\left[-t\mathrm{e}^Y\right] dY = f(t, \delta_n) + \varepsilon s_n(t) \tag{4.73}$$

where

$$s_n(t) = \int \varphi_n(Y) \exp\left[-t\mathrm{e}^{\delta_n Y}\right] dY\,. \tag{4.74}$$

Similarly, from eqs.(4.58) and (4.72), one sees that $\tilde{f}_n(t)$ is given, for b close to 1, by

$$\begin{aligned} \tilde{f}_n(t) &= \int r_n(y) \exp\left(-t\mathrm{e}^y\right) dy \\ &= f(t, \sqrt{2}\delta_n) + 2\varepsilon \int \frac{\mathrm{e}^{-y^2/2}}{(2\pi)^{1/2}} s_n(t\mathrm{e}^{\delta_n y}) dy. \end{aligned} \tag{4.75}$$

Now, using the relation between $\tilde{f}_n(t)$ and $\tilde{F}_{n+1}(t)$, eq.(4.70), and expanding it for $b = 1 + \varepsilon$, a recursion can be obtained for $s_n(t)$, which reads

$$s_{n+1}(t) = f(t, \sqrt{2}\delta_n) \ln f(t, \sqrt{2}\delta_n) + 2 \int \frac{\mathrm{e}^{-y^2/2}}{(2\pi)^{1/2}} s_n(t\mathrm{e}^{\delta_n y}) dy. \tag{4.76}$$

Carrying out this recursion, with the initial condition that $\varphi_1(Y) = 0$, $s_n(t)$ can be computed explicitly and from eq.(4.75) one finds that

$$\begin{aligned} \tilde{f}_n(t) &= f(t, \sqrt{2}\delta_n) + \varepsilon \int_{-\infty}^{\infty} \sum_{i=1}^{n-1} 2^{n-i} f\left(t \exp\left[\frac{(2^n - 2^i)^{1/2} y}{T}\right], \frac{2^{i/2}}{T}\right) \\ &\times \ln f\left(t \exp\left[\frac{(2^n - 2^i)^{1/2} y}{T}\right], \frac{2^{i/2}}{T}\right) \frac{\mathrm{e}^{-y^2/2}}{(2\pi)^{1/2}} dy + O(\varepsilon^2). \end{aligned} \tag{4.77}$$

Having determined $\tilde{f}_n(t)$ to first order in ε, it is now possible, using eq.(4.60), to calculate the free energy, and indeed the overlaps and moments to be discussed in the next sections, to second order in ε. For example, the free energy now becomes

$$F_n(T) = \varepsilon T \sum_{i=1}^{n-1} \frac{1}{2^i} \left[\int_0^{\infty} \frac{dt}{t} f\left(t, \frac{2^{i/2}}{T}\right) \ln f\left(t, \frac{2^{i/2}}{T}\right) \right.$$

$$
\begin{aligned}
&+ \frac{\varepsilon}{2}\int_0^\infty \frac{dt}{t} f\left(t,\frac{2^{i/2}}{T}\right)\ln^2 f\left(t,\frac{2^{i/2}}{T}\right)\\
&+ \varepsilon\int_0^\infty \frac{dt}{t}\left[1+\ln f\left(t,\frac{2^{i/2}}{T}\right)\right]\sum_{j=1}^{i-1}2^{i-j}\\
&\times \int_0^\infty f\left(t\exp\left[\frac{(2^i-2^j)^{1/2}y}{T}\right],\frac{2^{j/2}}{T}\right)\\
&\times \ln f\left(t\exp\left[\frac{(2^i-2^j)^{1/2}y}{T}\right],\frac{2^{j/2}}{T}\right)\frac{e^{-y^2/2}dt}{(2\pi)^{1/2}}\Bigg] + O(\varepsilon^3). \quad (4.78)
\end{aligned}
$$

4.3.2 Perturbative treatment of the overlaps

Following the same approach as in the previous section, expressions for the overlaps will now be obtained to first order in ε, eqs.(4.91)–(4.93). The low temperature behaviour of these quantities will then be investigated. This section closes with the calculation, to first order in ε, of the probability distribution of the overlaps, $P(q)$.

The overlaps to first order in ε

Let us consider the average overlap between two walks, $\langle q\rangle$. As discussed in section 4.1, it is convenient when dealing with this problem to use the generating function, $X_n(T,y)$, defined in eq.(4.6). These generating functions (see section 4.1) obey the recursion given in eq.(4.7). When $b=1$ this recursion reduces to a simple expression:

$$X_{n+1}(T,y) = X_n^{(1)}(T,y)X_n^{(2)}(T,y). \quad (4.79)$$

Using the same procedure as in section 4.3.1, consider the quantity $\Phi_n(\mu+2) = \langle X_n(T,y)Z_n^\mu\rangle$. For an arbitrary power μ, the recursion of eq.(4.7) can be written as

$$
\begin{aligned}
\langle X_{n+1}Z_{n+1}^\mu\rangle &= \left\langle X_n^{(1)}X_n^{(2)}\left(Z_n^{(1)}Z_n^{(2)}\right)^\mu\right\rangle\\
&+ \left\langle\left(X_n^{(1)}X_n^{(2)}+\cdots+X_n^{(2b-1)}X_n^{(2b)}\right)\right.\\
&\times \left.\left(Z_n^{(1)}Z_n^{(2)}+\cdots+Z_n^{(2b-1)}Z_n^{(2b)}\right)^\mu\right\rangle - \left\langle X_n^{(1)}X_n^{(2)}\left(Z_n^{(1)}Z_n^{(2)}\right)^\mu\right\rangle\\
&+ \left\langle\left(Z_n^{(1)}Z_n^{(2)}+\cdots+Z_n^{(2b-1)}Z_n^{(2b)}\right)^{\mu+2}\right\rangle - \left\langle\left(Z_n^{(1)}Z_n^{(2)}\right)^{\mu+2}\right\rangle
\end{aligned}
$$

$$- \left\langle \left[\left(Z_n^{(1)} Z_n^{(2)} \right)^2 + \cdots + \left(Z_n^{(2b-1)} Z_n^{(2b)} \right)^2 \right] \right.$$
$$\left. \times \left(Z_n^{(1)} Z_n^{(2)} + \cdots + Z_n^{(2b-1)} Z_n^{(2b)} \right)^{\mu} \right\rangle + \left\langle \left(Z_n^{(1)} Z_n^{(2)} \right)^{\mu+2} \right\rangle . \qquad (4.80)$$

Following the spirit of the previous calculation, one can introduce the function $\tilde{g}_{y,n}(t,t')$, defined as

$$\tilde{g}_{y,n}(t,t') = \left\langle \exp(-tZ_n^{(1)} Z_n^{(2)}) \exp[-t' X_n^{(1)}(T,y) X_n^{(2)}(T,y)] \right\rangle \qquad (4.81)$$

and use the following integral representations of Z^{μ} to help to linearise the problem:

$$Z^{\mu} = \int_0^{\infty} dt \frac{t^{-\mu-1}}{\Gamma(-\mu)} \mathrm{e}^{-tZ} \qquad \mu < 0 \qquad (4.82)$$

$$Z^{\mu} = \int_0^{\infty} dt \frac{t^{p-\mu-1}}{\Gamma(p-\mu)} (-1)^p \frac{d^p}{dt^p} \left[\mathrm{e}^{-tZ} \right] \quad \mu > 0 \text{ and } p > \mu, p \text{ integer.} \qquad (4.83)$$

(For clarity, the case $\mu < -2$ will be considered first and the results for $\mu > 0$, which follow in exactly the same manner, will be given at the end. $-2 < \mu < 0$ can be considered in the same way.) Equation (4.80) can then be rewritten in the form

$$\langle X_{n+1} Z_{n+1}^{\mu} \rangle = \langle X_n Z_n^{\mu} \rangle^2 - \int_0^{\infty} dt \frac{t^{-\mu-1}}{\Gamma(-\mu)} \frac{d}{dt'} \left[(\tilde{g}_{y,n}(t,t'))^b - \tilde{g}_{y,n}(t,t') \right]_{t'=0}$$
$$+ \int_0^{\infty} dt \frac{t^{-\mu-3}}{\Gamma(-\mu-2)} \left[\left(\tilde{f}_n(t) \right)^b - \tilde{f}_n(t) \right]$$
$$+ \int_0^{\infty} dt \frac{t^{-\mu-1}}{\Gamma(-\mu)} \frac{d}{dt'} \left[(\tilde{g}_{0,n}(t,t'))^b - \tilde{g}_{0,n}(t,t') \right]_{t'=0} \qquad (4.84)$$

where $\tilde{f}_n(t)$ is defined in eq.(4.58), and it has been noted that $X_n(T,0) = Z_n^2$. It is now simple to expand about $b = 1$. Again, to obtain an expression correct to first order in ε, the functions $\tilde{f}_n(t)$ and $\tilde{g}_{y,n}(t,t')$ will only be required at $b = 1$. To this order $\tilde{f}_n(t) = f\left(t, 2^{n/2}/T\right)$, as shown earlier (eq.(4.61)) and

$$\left. \frac{d}{dt'} \tilde{g}_{y,n}(t,t') \right|_{t'=0} = -\exp(2^n y) \frac{d^2 f}{dt^2} \left(t, \frac{2^{n/2}}{T} \right), \qquad (4.85)$$

since, when $b = 1$,

$$\left. \frac{d}{dt'} \tilde{g}_{y,n}(t,t') \right|_{t'=0} = -\left\langle X_n^{(1)}(T,y) X_n^{(2)}(T,y) \exp(-tZ_n^{(1)} Z_n^{(2)}) \right\rangle$$
$$= -\left\langle [\exp(2^n y)] \left(Z_n^{(1)} Z_n^{(2)} \right)^2 \exp(-tZ_n^{(1)} Z_n^{(2)}) \right\rangle . \qquad (4.86)$$

Hence eq.(4.84) reduces to

$$\begin{aligned}\langle X_{n+1}Z_{n+1}^{\mu}\rangle &= \langle X_nZ_n^{\mu}\rangle^2 - \varepsilon(1-\mathrm{e}^{2^n y})\int_0^{\infty} dt\frac{t^{-\mu-1}}{\Gamma(-\mu)} \\ &\times \frac{d^2f}{dt^2}\left(t,\frac{2^{n/2}}{T}\right)\left[1+\ln f\left(t,\frac{2^{n/2}}{T}\right)\right] \\ &+ \varepsilon\int_0^{\infty} dt\frac{t^{-\mu-3}}{\Gamma(-\mu-2)}f\left(t,\frac{2^{n/2}}{T}\right)\ln f\left(t,\frac{2^{n/2}}{T}\right). \qquad (4.87)\end{aligned}$$

Carrying out this recursion to first order in ε, an expression for $\langle X_nZ_n^{\mu}\rangle$ can be obtained in terms of the initial condition

$$\langle X_1Z_1^{\mu}\rangle = \mathrm{e}^{y}\left\langle Z_1^{\mu+2}\right\rangle = \exp\left[y+\frac{(\mu+2)^2}{2T^2}\right] \qquad (4.88)$$

which reads

$$\begin{aligned}\frac{1}{2^{n-1}}\ln\langle X_nZ_n^{\mu}\rangle &= y+\frac{(\mu+2)^2}{2T^2} - \varepsilon\sum_{i=1}^{n-1}\frac{1}{2^i}\exp\left[\frac{-(\mu+2)^2}{2}\delta_{i+1}^2\right] \\ \times &\left\{\left[\exp(-2^iy)-1\right]\int dt\frac{t^{-\mu-1}}{\Gamma(-\mu)}\right. \\ \times &\frac{d^2f(t,\delta_{i+1})}{dt^2}\left[1+\ln f(t,\delta_{i+1})\right] \\ - &\left.\left[\exp(-2^iy)\right]\int dt\frac{t^{-\mu-3}}{\Gamma(-\mu-2)}f(t,\delta_{i+1})\ln f(t,\delta_{i+1})\right\}. \qquad (4.89)\end{aligned}$$

For $\mu > 0$ and $p > \mu$, it can be shown that a similar relation holds:

$$\begin{aligned}\frac{1}{2^{n-1}}\ln\langle X_nZ_n^{\mu}\rangle &= y+\frac{(\mu+2)^2}{2T^2} - \varepsilon\sum_{i=1}^{n-1}\frac{1}{2^i}\exp\left[\frac{-(\mu+2)^2}{2}\delta_{i+1}^2\right] \\ \times &\left\{\left[\exp(-2^iy)-1\right]\int dt\frac{t^{p-\mu-1}}{\Gamma(p-\mu)}(-1)^p\right. \\ \times &\frac{d^p}{dt^p}\left[\frac{d^2f(t,\delta_{i+1})}{dt^2}\left[1+\ln f(t,\delta_{i+1})\right]\right] \\ - &\left.\left[\exp(-2^iy)\right]\int dt\frac{t^{p-\mu-1}}{\Gamma(p-\mu)}(-1)^p\frac{d^{p+2}}{dt^{p+2}}\left[f(t,\delta_{i+1})\ln f(t,\delta_{i+1})\right]\right\}. \qquad (4.90)\end{aligned}$$

The overlap $\langle q\rangle$ can now be obtained by setting $\mu = -2$ in eq.(4.89) and differentiating with respect to y, to yield

$$\langle q\rangle = 1+\varepsilon\sum_{i=1}^{n-1}\int_0^{\infty} dt\,t\left[1+\ln f\left(t,\frac{2^{i/2}}{T}\right)\right]\frac{d^2f}{dt^2}\left(t,\frac{2^{i/2}}{T}\right) \qquad (4.91)$$

and the overlap of two walks calculated with $p+2$ replicas ($p > 0$) follows from eq.(4.90), giving

$$\begin{aligned}\langle Q_n(p+2)\rangle &= 1+\varepsilon\sum_{i=1}^{n-1}\exp\left[-(p+2)^2\frac{2^{i-1}}{T^2}\right](-1)^p \\ &\times \frac{d^p}{dt^p}\left\{\frac{d^2f}{dt^2}\left(t,\frac{2^{i/2}}{T}\right)\left[1+\ln f\left(t,\frac{2^{i/2}}{T}\right)\right]\right. \\ &- \left.\frac{d^2}{dt^2}\left[f\left(t,\frac{2^{i/2}}{T}\right)\ln f\left(t,\frac{2^{i/2}}{T}\right)\right]\right\}\Bigg|_{t=0}. \qquad (4.92)\end{aligned}$$

As mentioned in section 4.1, it is possible, using eqs.(4.11), (4.13) and (4.82), to compute the average overlap between m walks, $\langle q(m)\rangle$, in the same way, giving

$$\langle q(m)\rangle = 1+\varepsilon(-1)^m\sum_{i=1}^{n-1}\int dt\frac{t^{m-1}}{\Gamma(m)}\left[1+\ln f\left(t,\frac{2^{i/2}}{T}\right)\right]\frac{d^m}{dt^m}f\left(t,2^{i/2}/T\right). \quad (4.93)$$

Low temperature expansion of the overlaps

It is possible to obtain the low temperature expansions of these three overlaps, eqs.(4.91)–(4.93). Using the appropriate expansion of $f(t,\lambda)$, as explained in appendix B, it can be shown that the first correction to $\langle q\rangle$ is linear in temperature

$$\langle q\rangle = 1-\varepsilon K_1 T\sum_{i=1}^{n-1}\frac{1}{2^{i/2}}+O(T^3) \qquad (4.94)$$

where K_1 is defined in eq.(4.66). A similar expression can be obtained for $\langle q(m)\rangle$,

$$\begin{aligned}\langle q(m)\rangle &= 1-\varepsilon K_1 T\left(\frac{\Gamma^{(1)}(m)}{\Gamma(m)}-\Gamma^{(1)}(1)\right)\sum_{i=1}^{n-1}\frac{1}{2^{i/2}} \\ &- \varepsilon K_2 T^2\left[\frac{\Gamma^{(2)}(m)}{\Gamma(m)}-\frac{2\Gamma^{(1)}(1)\Gamma^{(1)}(m)}{\Gamma(m)}+2\left(\Gamma^{(1)}(1)\right)^2-\Gamma^{(2)}(1)\right]\sum_{i=1}^{n-1}\frac{1}{2^i}+O(T^3).\end{aligned} \qquad (4.95)$$

It is interesting to compare these results with the expressions for the overlaps $\langle q(m)\rangle$ on the tree [14]. For the tree, one can show that the overlap $\langle q(m)\rangle$ is given by $\langle q(m)\rangle = \Gamma(m-T/T_c)/\Gamma(m)\Gamma(1-T/T_c)$. At low temperature, this gives the same expression as eq.(4.95), with $\varepsilon K_1\sum 1/\sqrt{2^i}$ replaced by $1/T_c$ and $\varepsilon K_2\sum 1/2^i$ by $-1/2T_c^2$.

To calculate $\langle Q_n(p+2)\rangle$, it is necessary to know the first $p+1$ derivatives of $f\left(t,\sqrt{2^i}/T\right)$ with respect to t at $t=0$. However, as these derivatives have the simple form

$$f^{(p)}\left(0,\frac{2^{i/2}}{T}\right)=(-1)^p\exp\left[\frac{2^{i-1}p^2}{T^2}\right] \tag{4.96}$$

the leading term at low temperature can be seen to result from taking $i=1$ and the term with the highest possible derivative of $f\left(t,\sqrt{2}/T\right)$. Hence, it follows that

$$\langle Q_n(2)\rangle = 1-\varepsilon e^{-2/T^2}+\cdots \tag{4.97}$$

$$\langle Q_n(p+2)\rangle = 1-2\varepsilon e^{-2(p+1)/T^2}+\cdots \qquad p\geq 1. \tag{4.98}$$

It can be seen that $\langle Q_n(p+2)\rangle$ obtained in this manner agrees with that resulting from eqs.(4.40)–(4.42) expanded for $b=1+\varepsilon$, as expected. The first corrections to $\langle Q_n(p+2)\rangle$ are all exponentially small in temperature. One sees, from eqs.(4.94),(4.97) and (4.98), that the first order correction to the overlap $\langle Q_n(2+\mu)\rangle$ is exponentially small in the temperature except for $\mu=-2$, when it vanishes linearly with temperature. Similar behaviour will be seen in the next section when the moments of the partition function are considered.

The probability distibution of the overlap, q

As the polymer problem has many analogies with spin glasses, it is interesting to consider the distribution of the overlaps, $P(q)$. To determine the shape of the distribution $P(q)$, let us define y_n by

$$e^{y_n}=\left\langle X_n(T,y)Z_n^{-2}\right\rangle. \tag{4.99}$$

Then, from recursion eq.(4.89), the following recursion for y_n can be obtained:

$$y_{n+1}=2^n y+\varepsilon\sum_{i=1}^{n}2^{n-i}A_i(1-\exp[-2^i y]) \tag{4.100}$$

where

$$A_i=\int_0^\infty dt\,t\left[1+\ln f\left(t,\frac{2^{i/2}}{T}\right)\right]\frac{d^2}{dt^2}f\left(t,\frac{2^{i/2}}{T}\right). \tag{4.101}$$

Using a renormalised variable $\tilde{y}$ given by

$$\tilde{y}=2^n y \tag{4.102}$$

this can be recast as

$$\begin{aligned} y_{n+1} &= \tilde{y} + \varepsilon \sum_{i=1}^{n} 2^{n-i} \left[1 - \exp\left(-2^{i-n} \tilde{y} \right) \right] A_i \\ &\rightarrow \tilde{y} \left(1 + \varepsilon \sum_{i=1}^{\infty} A_i \right) \qquad \text{as } n \rightarrow \infty \end{aligned} \tag{4.103}$$

where the limit $n \rightarrow \infty$ has been taken and as $A_i \rightarrow 0$ when $i \rightarrow \infty$, only terms with $n - i \gg 0$ will contribute to the sum.

Hence one sees that

$$\left\langle X_n(T,y) Z_n^{-2} \right\rangle = \exp\left[\tilde{y} \left(1 + \varepsilon \sum_{i=1}^{n-1} A_i \right) \right]. \tag{4.104}$$

This shows that, at least to first order in ε, $P(q)$ is a delta function at $q = \langle q \rangle$.

4.3.3 Non-integer moments and the replica method

Let us now turn to a consideration of the moments of the partition function. First, an expression will be obtained for an arbitrary moment $\langle Z_n^{\mu} \rangle$, to first order in ε, (eqs.(4.108) and (4.109)), then the low temperature limit will be considered. From the expansion of the moments of the partition function it is possible to find the expansion of the ground state energy fluctuation exponent ω, see eq.(1.8). This is given in eq.(4.120).

The moments of the partition function to first order in ε

Consider the average of the μ^{th} power of the partition function at the n^{th} generation of the lattice, $\langle Z_n^{\mu} \rangle$ (take $\mu < 0$ to begin with). Following the perturbative approach of eqs.(4.55) and (4.80), the recursion for this quantity can be written as

$$\begin{aligned} \langle Z_{n+1}^{\mu} \rangle &= \langle Z_n^{\mu} \rangle^2 + \left[\left\langle \left(Z_n^{(1)} Z_n^{(2)} + \cdots + Z_n^{(2b-1)} Z_n^{(2b)} \right)^{\mu} \right\rangle - \left\langle \left(Z_n^{(1)} Z_n^{(2)} \right)^{\mu} \right\rangle \right] \\ &= \langle Z_n^{\mu} \rangle^2 + \int_0^{\infty} dt \frac{t^{-\mu-1}}{\Gamma(-\mu)} \left[\left(\tilde{f}_n(t) \right)^b - \tilde{f}_n(t) \right] \end{aligned} \tag{4.105}$$

where the integral representation of eq.(4.82) and the usual function $\tilde{f}_n(t)$, defined in eq.(4.58), have been used.

Expanding to first order in ε, one obtains

$$\langle Z_{n+1}^{\mu} \rangle = \langle Z_n^{\mu} \rangle^2 + \frac{\varepsilon}{\Gamma(-\mu)} \int_0^{\infty} dt\, t^{-\mu-1} f\left(t, \frac{2^{n/2}}{T}\right) \ln f\left(t, \frac{2^{n/2}}{T}\right) \tag{4.106}$$

and so, using the initial condition

$$\langle Z_1^{\mu} \rangle^2 = \exp\left[\mu^2/T^2\right], \tag{4.107}$$

it can be shown that for $\mu < 0$

$$\begin{aligned} \frac{1}{2^{n-1}} \ln \langle Z_n^{\mu} \rangle &= \frac{\mu^2}{2T^2} + \varepsilon \sum_{i=1}^{n-1} \frac{1}{2^i} \exp\left[\frac{-\mu^2 2^{i-1}}{T^2}\right] \\ &\times \int_0^{\infty} dt \frac{t^{-\mu-1}}{\Gamma(-\mu)} f\left(t, \frac{2^{i/2}}{T}\right) \ln f\left(t, \frac{2^{i/2}}{T}\right). \end{aligned} \tag{4.108}$$

For $\mu > 0$ one has to use the alternative integral representation, eq.(4.83), and this leads to a similar expression valid for $\mu > 0$ and $p > \mu$,

$$\begin{aligned} \frac{1}{2^{n-1}} \ln \langle Z_n^{\mu} \rangle &= \frac{\mu^2}{2T^2} + \varepsilon \sum_{i=1}^{n-1} \frac{1}{2^i} \exp\left[\frac{-\mu^2 2^{i-1}}{T^2}\right] \\ &\times \int_0^{\infty} dt \frac{t^{p-\mu-1}}{\Gamma(p-\mu)} (-1)^p \frac{d^p}{dt^p} \left[f\left(t, \frac{2^{i/2}}{T}\right) \ln f\left(t, \frac{2^{i/2}}{T}\right) \right]. \end{aligned} \tag{4.109}$$

It is interesting to note that once again the first correction depends only on the function $f(t, \lambda)$, as was the case for the overlaps and free energy.

For integer moments, the latter expression, eq.(4.109), reduces to

$$\begin{aligned} \frac{1}{2^{n-1}} \ln \langle Z_n^{p} \rangle &= \frac{p^2}{2T^2} + \varepsilon \sum_{i=1}^{n-1} \frac{1}{2^i} \\ &\times \exp\left[-p^2 \frac{2^{i-1}}{T^2}\right] (-1)^p \frac{d^p}{dt^p} \left[f\left(t, \frac{2^{i/2}}{T}\right) \ln f\left(t, \frac{2^{i/2}}{T}\right) \right] \Bigg|_{t=0}. \end{aligned} \tag{4.110}$$

The calculation of the derivatives of $f(t, \lambda) \ln f(t, \lambda)$ with respect to t at $t = 0$ can be done easily (see appendix B, eq.(B3)) and then the above equation gives answers in agreement with those obtained from an expansion about $b = 1$ of the recursions of the integer moments in eqs.(4.18)–(4.21). However, the perturbative expansion (ε small) has also given the interpolation between the integer moments.

It is interesting to consider whether a similar form of interpolation could be used in other problems where only the integer moments of the partition function can be determined. Consider a sequence of numbers $a(p)\,(p = 0, 1, 2, \ldots)$. The problem is how to extend them to a function $a(\mu)$ defined at all values of μ. By comparing equations (4.109) and (4.110), one sees that the interpolation formula valid here is to construct a function $J(t)$, which plays the role of $f(t,\lambda)\ln f(t,\lambda)$, via

$$J(t) = \sum_{p=0}^{\infty}(-1)^p \frac{t^p a(p)}{p!} \tag{4.111}$$

and then to decide that for non-integer μ with $\mu < p$, $a(\mu)$ is given by

$$a(\mu) = \int_0^{\infty} dt \frac{t^{p-\mu-1}}{\Gamma(p-\mu)}(-1)^p \frac{d^p}{dt^p}[J(t)]. \tag{4.112}$$

It is interesting to notice that this procedure will, in principle, only work if the function $J(t)$ has a finite radius of convergence and has an analytic extension to the real axis. In the case of eqs.(4.109) and (4.110), $f(t,\lambda)\ln f(t,\lambda)$ has a zero radius of convergence (see appendix B) and so the series expansion eq.(4.111) does not define a unique function $J(t)$. In the polymer problem the function to use is $f(t,\lambda)\ln f(t,\lambda)$, but there are other functions which have exactly the same series expansion, eq.(4.111), as this function and these would give an incorrect interpolation for the moments.

Low temperature expansion of the moments of the partition function

To learn more about the character of the interpolation, let us consider the low temperature expansion of eqs.(4.108)–(4.110). Details of these expansions are given in appendix B. For $\mu < 0$ the low temperature behaviour can be shown to be, eq.(B19),

$$\langle Z_{n+1}^{\mu}\rangle - \langle Z_n^{\mu}\rangle^2 = \varepsilon \exp\left(\mu^2 \frac{2^{n-1}}{T^2}\right)\left[-\frac{2^{n-1}\mu^2}{T^2} - \frac{1}{2}\right.$$
$$\left. - \ln\left(\frac{(2\pi)^{1/2}2^{n/2}}{T}\right) + \frac{\mu\Gamma^{(1)}(-\mu)}{\Gamma(-\mu)} + \ln\Gamma(-\mu) + \cdots\right]. \tag{4.113}$$

So, the dependence upon T is dominated by the exponential factor.

For $\mu > 0$ one can show that the leading behaviour is of the form

$$\langle Z_{n+1}^{\mu}\rangle - \langle Z_n^{\mu}\rangle^2 = \varepsilon \exp\left[\frac{2^{n-1}\mu^2}{T^2}\right]. \tag{4.114}$$

So, again the first correction is exponential in temperature.

One can see that the expressions for $\mu > 0$ and $\mu < 0$ are quite different. It is, however, possible to reconcile them by considering that as $T \to 0$, the ratio μ/T remains fixed. By making the substitution $t = \exp(\sqrt{2^n}u/T)$ in eq.(4.106) and using the correct asymptotic expansion for $f(t,\lambda)$, one sees that when μ is small

$$\begin{aligned} \langle Z_{n+1}^{\mu} \rangle - \langle Z_n^{\mu} \rangle^2 &= -\varepsilon\mu \frac{2^{n/2}}{T} \int_{-\infty}^{+\infty} du \, \exp\left(-\frac{2^{n/2}u\mu}{T}\right) \\ &\times \int_u^{\infty} dz \, \frac{e^{-z^2/2}}{(2\pi)^{1/2}} \ln\left(\int_u^{\infty} dx \, \frac{e^{-x^2/2}}{(2\pi)^{1/2}}\right). \end{aligned} \tag{4.115}$$

This expression shows that when μ and T are small, the result depends only on their ratio μ/T. For $(\mu/T) \to 0$, one recovers the free energy result eq.(4.65), whereas for $(\mu/T) \to \pm\infty$ it becomes consistent with eqs.(4.113) and (4.114). So, the limits $\mu \to 0$ and $T \to 0$ do not commute and it is only if one takes $\mu/T \to 0$ as $T \to 0$ that the replica approach leads to the correct free energy.

The ground state energy fluctuation exponent, ω

It is interesting to notice how the width, Δ_n, of the distribution of $\ln Z_n$ behaves. Expanding in powers of μ, it is easy to show that

$$\begin{aligned} \ln \langle Z_n^{\mu} \rangle &= \mu \langle \ln Z_n \rangle + \frac{\mu^2}{2} \left[\left\langle \ln^2 Z_n \right\rangle - \langle \ln Z_n \rangle^2 \right] + \cdots \\ &= \mu \langle \ln Z_n \rangle + \frac{\mu^2 \Delta_n^2}{2} + \cdots . \end{aligned} \tag{4.116}$$

Hence Δ_n^2 can be computed by expanding either eq.(4.108) or eq.(4.109) in powers of μ, to give

$$\begin{aligned} \Delta_n^2 &= \frac{L}{T^2} - 2L\varepsilon \sum_{i=1}^{n-1} \frac{\Gamma^{(1)}(1)}{2^i} \int \frac{dt}{t} f\left(t, \frac{2^{i/2}}{T}\right) \ln f\left(t, \frac{2^{i/2}}{T}\right) \\ &+ 2L\varepsilon \sum_{i=1}^{n-1} \frac{1}{2^i} \int \frac{dt}{t} (\ln t) f\left(t, \frac{2^{i/2}}{T}\right) \ln f\left(t, \frac{2^{i/2}}{T}\right) \end{aligned} \tag{4.117}$$

where $L = 2^{n-1}$ is the length of the polymer .

The first summation in eq.(4.117) is proportional to the free energy per unit length of the polymer, F_n, given by eq.(4.64). Hence, as $n \to \infty$, the second term on

the right-hand side of eq.(4.117) is proportional to L. The second summation does not tend to a finite limit as $n \to \infty$. Instead, as $n \to \infty$ (i.e. $\lambda \to \infty$), it can be shown, using the asymptotic expansion of $f(t, \lambda)$ given in appendix B, eq.(B8), that each term in the series tends to $-2\varepsilon K_2 L/T^2$ (where K_2 is defined in eq.(4.67)). Hence, this last term in eq.(4.117) is proportional, for large n, to $L \ln L$. Indeed, as n increases,

$$\Delta_n^2 \to \frac{L}{T^2}\left[1 - 2T\Gamma^{(1)}(1)F_n(T) - 2\varepsilon K_2\right] - \frac{2\varepsilon K_2}{T^2 \ln 2} L \ln L. \tag{4.118}$$

As L increases, the corrections increase faster than the leading order and so this expression can only be trusted for $\varepsilon \ln L \ll 1$. For $\varepsilon \ln L \gg 1$, one should "renormalise" the problem as was done in [47]. However, it is easy to show that eq.(4.118) is consistent with the results of [47], which claimed that in the limit $n \to \infty$, the width Δ_n behaves for large L as L^ω and that $\Delta_{n+1}/\Delta_n \to \lambda = 2^\omega$. If one calculates the ratio Δ_{n+1}/Δ_n from eq.(4.118) one finds that

$$\frac{\Delta_{n+1}}{\Delta_n} = 2^{1/2}(1 - \varepsilon K_2) \tag{4.119}$$

so that the ground state energy fluctuation exponent ω, see eq.(1.8), is given by

$$\omega = \frac{1}{2} - \frac{\varepsilon K_2}{\ln 2}. \tag{4.120}$$

4.4 Summary of chapter 4

This chapter has examined directed polymers on disordered hierarchical lattices. It has been shown that on these lattices the directed polymer problem reduces to the study of the stable distributions that occur when one combines random variables in a nonlinear way. One can easily obtain the average of the first few integer moments of the partition function, eqs.(4.33)–(4.36), but it is not clear how these should be generalised to non-integer moments. Using the second moment of the partition function, one can prove the existence of a phase transition on lattices with $b > 2$. Simulations of the system for $b = 5$ showed this transition clearly.

It was noticed that the problem becomes simple if $b = 1$, as then one just has a sum of random variables and the central limit theorem can be invoked. It is

possible to perform a perturbative expansion around this simple limit $b = 1$, and this expansion was the subject of sections 4.3.1–4.3.3. Expressions, to first order in $b-1$, were obtained for the free energy (eq.(4.64)), the overlap (eq.(4.91)), the non-integer moments of the partition function (eqs.(4.108) and (4.109)) and the ground state energy fluctuation exponent, ω (eq.(4.120)). It was also demonstrated that one could extend these expressions to higher order in $b - 1$.

The expansion is not able to shed light on the phase transition, as this only seems to exist for $b > 2$. However, it is able to show a linear specific heat at low temperature (for a Gaussian distribution of energies) and that the probability distribution of the overlaps, $P(q)$, is a single delta function, at least to first order in $b - 1$. Also, being able to calculate the non-integer moments of the partition function provides an interpolation between the integer moments, when b is close to 1, and this allowed a study of the replica formalism for this problem.

Chapter 5

Directed polymers with complex random weights

Recently, generalised models of directed polymers in random media have been introduced [26], in which one allows the walks to contribute either positive and negative or complex weights to the partition sum. The model with positive and negative real weights was briefly introduced, in the context of the NSS model of hopping conductivity [27,28], in section 1.3.

In this chapter the mean field solution of these models is considered. The discussion will be limited to the case of positive and negative weights, but the arguments can be extended to allow the weights to have more general discrete sets of phases. The model to be studied is defined in section 5.1. Then, the method of solution is discussed. So far, it has not been possible to solve the model directly, as the replica and travelling wave approaches to the standard mean field polymer problem are not amenable to extension to negative "Boltzmann weights". However, using a close analogy between the mean field directed polymer problem and two other disordered systems, the random energy model (REM) [64] and the generalised random energy model (GREM) [65,51], one can obtain the mean field solution indirectly. The solutions of the corresponding REM and GREM are given in sections 5.3 and 5.4. The main result of this chapter, the phase diagram of the mean field generalised directed polymer problem, is presented in section 5.5. Finally, the chapter closes with a discussion of the relationship between the mean field generalised polymer problem and the problem of finding the largest Lyapounov

exponent of a product of large, sparse random matrices.

5.1 Definition of the model

In the particular generalisation of directed polymers in a random medium that will be considered here, one allows the walks to make both positive and negative contibutions to the "partition sum". The model is defined as follows. As usual, one has a regular lattice and for each bond, ij, of the lattice one chooses a random energy, ϵ_{ij}, according to a given probability distribution, $\rho(\epsilon_{ij})$. However, one also places a random sign S_{ij} on each bond ij. The sign is taken to be positive with probability $1-p$ and negative with probability p. One then considers all directed walks, w, of length L, emanating from some origin. The energy of each walk is defined as before, eq.(1.1), i.e.

$$E_w = \sum_{ij \in w} \epsilon_{ij} \tag{5.1}$$

and the "partition function" is now taken to be

$$Z_L(\mathbf{r}) = \sum_w \left(\prod_{ij \in w} S_{ij} \right) \exp\left[-E_w/T\right] \tag{5.2}$$

where the sum runs over all directed walks of length L emanating from the point $\mathbf{r}$ and the product includes all the bonds visited by w.

Although it is convenient to call Z_L a partition function it can be positive or negative, due to the inclusion of the random signs into the problem. In calculating the "thermal properties" of the system one is therefore interested in evaluating the quantity $\langle \ln |Z_L| \rangle$. Notice that one recovers the standard directed polymer problem when $p = 0$ or 1.

In addition to the "free energy", one might also be interested in calculating the analogues of the ground state energy and disorder transverse fluctuation exponents, ω and ν, see eqs.(1.8) and (1.10). These are now defined as

$$\left(\left\langle (\ln |Z_L|)^2 \right\rangle - \langle \ln |Z_L| \rangle^2 \right)_{T=0} \sim L^{2\omega} \tag{5.3}$$

$$\left(\sum_{\mathbf{x}} |Z_L(\mathbf{0},\mathbf{x})|^2 \mathbf{R}^2(\mathbf{x}) \right) \left(\sum_{\mathbf{x}} |Z_L(\mathbf{0},\mathbf{x})|^2 \right)^{-1} \sim L^{2\nu} \tag{5.4}$$

where $Z_L(\mathbf{0},\mathbf{x})$ is the partial partition function for all directed walks of length L emanating from the origin $\mathbf{0}$ and terminating at $\mathbf{x}$ and $\mathbf{R}(\mathbf{x})$ is the transverse displacement of the point $\mathbf{x}$. These exponents have recently been the topic of some controversy. Certain simulations and general arguments have indicated that the exponents should keep their standard ($p = 0$ or 1) values [66]. However, Zhang [67-69] has predicted, on the basis of numerical studies and analytical arguments, that the exponents should change when $p \neq 0$ or 1.

The remainder of this chapter is concerned with the mean field limit of the model described above. It will again be helpful to take the mean field limit by formulating the problem on a tree (see fig. 3.1).

5.2 The relationship between directed polymers, the REM and the GREM

The solution of the mean field generalised directed polymer problem will be obtained by making use of the close relationship that exists between three problems in statistical mechanics: the mean field directed polymer problem, the REM and the GREM.

When the mean field solution of the standard directed polymer problem was first obtained [14], it was noticed that its free energy, eqs.(3.10)–(3.13), was identical to that of the corresponding REM and GREM at all temperatures. To see why one expects this to remain true when one adds random signs to the problem it is necessary to consider the structure of the REM and the GREM.

5.2.1 Definition of the REM

In the random energy model the partition function, Z, is defined as the sum of K^L independent terms

$$Z = \sum_{\mu=1}^{K^L} S_\mu \exp(-E_\mu/T) \tag{5.5}$$

where $S_\mu = \pm 1$ and $\exp(-E_\mu/T)$ are, respectively, the sign and amplitude of the μ^{th} term of the sum.

The number of terms in eq.(5.5), K^L, is chosen to be the number of directed polymers of length L on the tree, the random energy E_μ has the same distribution as the energy of a walk of L steps on the tree, i.e. its generating function is equal to

$$\langle \exp(-\Lambda E_\mu) \rangle = \langle \exp(-\Lambda \epsilon) \rangle^L = \left[\int \rho(\epsilon) \exp(-\Lambda \epsilon)\, d\epsilon \right]^L \tag{5.6}$$

where ϵ is the energy of a bond on the tree, and the sign S_μ has the same distribution as the sign of a path of L steps on the tree, i.e.

$$\begin{aligned} S_\mu = +1 \quad &\text{with probability} \quad \frac{1}{2}\left(1 + (1-2p)^L\right) \\ S_\mu = -1 \quad &\text{with probability} \quad \frac{1}{2}\left(1 - (1-2p)^L\right). \end{aligned} \tag{5.7}$$

In general, for large L, the distribution of E_μ, $\Pi(E)$, takes the form

$$\Pi(E) \simeq (2\pi L)^{-1/2} \left(-f''(E/L)\right)^{-1/2} \exp\left[L f(E/L)\right] \tag{5.8}$$

where the function $f(x)$ is related to $\rho(\epsilon)$ by a Legendre transform

$$\max_\epsilon (f(\epsilon) - \epsilon\Lambda) = \ln \left[\int \rho(\epsilon) \exp(-\Lambda\epsilon)\, d\epsilon \right]. \tag{5.9}$$

Using eqs.(5.6) and (5.8), one can show that the function f is necessarily convex ($f'' < 0$). For a Gaussian bond distribution $\rho(\epsilon)$, for example, one obtains a Gaussian $\Pi(E)$

$$\rho(\epsilon) = (2\pi)^{-1/2} \exp(-\epsilon^2/2) \Longrightarrow \Pi(E) = (2\pi L)^{-1/2} \exp(-E^2/2L) \tag{5.10}$$

One sees that when the REM is defined in this way it has the same number of terms in the partition sum and the same distribution of single energies, E, as the tree problem. However, as always in the REM approach [64], it neglects the correlations between the energies and signs of different paths.

5.2.2 Definition of the GREM

The generalised random energy model aims to restore some of the correlations between energy levels and signs that have been ignored in the REM. In a GREM

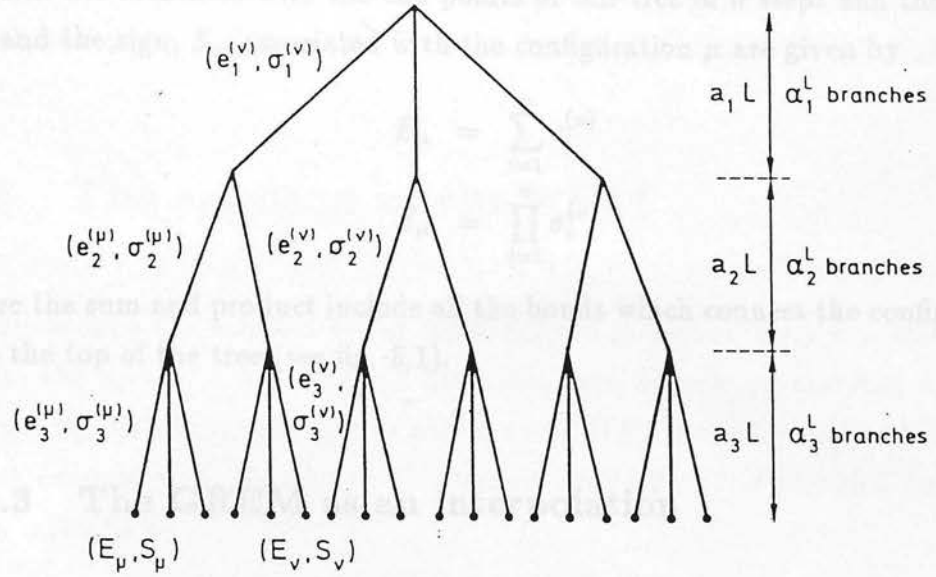

Figure 5.1: The structure of a three step ($n = 3$) generalised random energy model.

of n steps, the possible configurations of the system can be represented by the end points of a tree of n steps, see figure 5.1. The model is defined by two sets of numbers: α_i; $1 \leq i \leq n$ and a_i; $1 \leq i \leq n$ which satisfy

$$\prod_{i=1}^{n} \alpha_i = K\,; \qquad \alpha_i > 1 \tag{5.11}$$

$$\sum_{i=1}^{n} a_i = 1\,; \qquad a_i > 0. \tag{5.12}$$

For each branch of the tree of n steps one chooses a random sign $\sigma_i^{(\mu)}$, according to

$$\begin{aligned} \sigma_i^{(\mu)} = +1 \quad &\text{with probability} \quad \frac{1}{2}\left(1 + (1-2p)^{La_i}\right) \\ \sigma_i^{(\mu)} = -1 \quad &\text{with probability} \quad \frac{1}{2}\left(1 - (1-2p)^{La_i}\right), \end{aligned} \tag{5.13}$$

and a random energy, $e_i^{(\mu)}$, from a distribution $\Pi(e, a_i)$ which satisfies

$$\left\langle \exp\left(-\Lambda e_i^{(\mu)}\right)\right\rangle \;=\; \left[\int \rho(\epsilon)\exp(-\Lambda\epsilon)\,d\epsilon\right]^{La_i} \tag{5.14}$$

$$\Pi(e, a_i) \;\sim\; \exp\left[La_i f\left(\frac{e}{La_i}\right)\right]. \tag{5.15}$$

The total number of branches at level i is $(\alpha_1 \alpha_2 \ldots \alpha_i)^L$. By definition, the configurations are identified with the end points of this tree of n steps and the energy, E_μ, and the sign, S_μ, associated with the configuration μ are given by

$$E_\mu = \sum_{i=1}^{n} e_i^{(\mu)} \tag{5.16}$$

$$S_\mu = \prod_{i=1}^{n} \sigma_i^{(\mu)} \tag{5.17}$$

where the sum and product include all the bonds which connect the configuration μ to the top of the tree (see fig. 5.1).

5.2.3 The GREM as an interpolation

In the case $n = 1$, the GREM reduces to the REM. In the other limit ($n = L$; $a_i = 1/L$; $\alpha_i = K^{1/L}$) one recovers the mean field generalised directed polymer problem, defined in section 5.1. So, the GREM gives an interpolation between the REM and the tree with branching ratio K. As long as n is finite, one can solve the GREM, in the limit $L \to \infty$ [65], using the same ideas involved in the solution of the REM [64]. However, as n increases (if one chooses $a_i = 1/n$ and $\alpha_i = K^{1/n}$),the correlations between the energies, E_μ, and the signs, S_μ, of different configurations look more and more like those of the mean field generalised polymer problem.

It will be shown in sections 5.3 and 5.4 that, when L is large, the REM and the GREM of two steps have exactly the same expression for $\langle \ln |Z_L| \rangle / L$ over the whole phase diagram. The calculation of section 5.4 can, in fact, be extended to a GREM of an arbitrary (finite) number of steps and one still obtains the same result.

In the case $p = 0$ or 1, this common free energy of the REM and GREM is known to be the same as the free energy of the mean field directed polymer problem [14]. Although it has not proved possible to derive the solution of the mean field generalised directed polymer problem directly, it seems extremely likely that, as $\langle \ln |Z_L| \rangle / L$ is the same for both the REM and the GREM with an arbitrary finite number of steps (when one chooses the energy and sign distributions and the

branching ratios to mimic the polymer problem, eqs.(5.11)–(5.15)), this expression will remain valid for the mean field generalised polymer problem. The numerical simulations presented in section 5.5 seem to confirm that this is, in fact, the case.

5.3 The solution of the REM

In this section the solution of the REM defined in section 5.2.1 is presented. To recap, the system consists of K^L branches, each branch, μ, carrying a random energy, E_μ, chosen according to a distribution $\Pi(E)$, given by eqs.(5.6) and (5.8), and a random sign, S_μ, chosen according to eq.(5.7). The partition function is then taken to be

$$Z_L = \sum_{\mu=1}^{K^L} S_\mu \exp(-E_\mu/T). \tag{5.18}$$

To determine the phase diagram of the model one needs to calculate the equivalent of the free energy, $-T\langle \ln |Z_L| \rangle / L$.

One can divide Z_L into two parts: one part, Z_L^+, being the sum of the weights of all the branches with a positive sign, S_μ, and the other, Z_L^-, being the modulus of the sum of the weights of all the branches which have a negative sign.

$$Z_L = Z_L^+ - Z_L^- \tag{5.19}$$

Now one can solve the generalised problem provided that one knows enough about the problem with $p = 0$, as $Z_L^\pm$ are both $p = 0$ REM partition functions.

5.3.1 The case p=0

To determine the phase diagram of the model eq.(5.18) one needs to know the solution of the $p = 0$ REM and also something about its sample-to-sample fluctuations. Here, the REM will be solved by the most intuitive approach, using the microcanonical ensemble [64]. If $\mathcal{N}(E)$ is the density of levels at energy E, the average of $\mathcal{N}(E)$ is given by (see eq.(5.8))

$$\langle \mathcal{N}(E) \rangle = (2\pi L)^{-1/2} \left(-f''(E/L)\right)^{-1/2} K^L \exp\left[L f(E/L)\right]. \tag{5.20}$$

The function f is convex and therefore one expects that there are, in general, two energies E_{GS} and E'_{GS} ($E_{GS} < E'_{GS}$) for which $\langle \mathcal{N}(E) \rangle \simeq 1$. For energies such that $E/L < E_{GS}/L$ or $E/L > E'_{GS}/L$, the average $\langle \mathcal{N}(E) \rangle$ is exponentially small in L. Therefore

$$\mathcal{N}_{\text{typical}}(E) = 0. \tag{5.21}$$

For energies such that $E_{GS}/L < E/L < E'_{GS}/L$, the average $\langle \mathcal{N}(E) \rangle$ is exponentially large in L. Therefore, the typical value is the same as the average

$$\mathcal{N}_{\text{typical}}(E) = \langle \mathcal{N}(E) \rangle \pm \langle \mathcal{N}(E) \rangle^{1/2}. \tag{5.22}$$

Lastly, for energies E which, for large L, differ from E_{GS} or E'_{GS} by order 1, $\mathcal{N}_{\text{typical}}(E)$ is of order 1 and so eq.(5.22) still gives the magnitude of the typical value and typical fluctuations.

From eqs.(5.21) and (5.22) one can obtain the large L behaviour and fluctuations of the partition function, as

$$Z_L = \int \mathcal{N}_{\text{typical}}(E) \exp(-E/T)\, dE. \tag{5.23}$$

The ground state energy E_{GS}/L is given by the condition $\langle \mathcal{N}(E) \rangle = 1$, i.e. is the lower solution of

$$f(E_{GS}/L) = -\ln K \tag{5.24}$$

where the function f is defined by eqs.(5.6) and (5.8). The transition temperature, T_c, is given by

$$f'(E_{GS}/L) = \frac{1}{T_c}. \tag{5.25}$$

Above T_c, the integral in eq.(5.23) is dominated by energies, E, where $\langle \mathcal{N}(E) \rangle$ is very large, so the free energy, for $T > T_c$, is given by (see eq.(5.9))

$$\begin{aligned} \lim_{L\to\infty} \frac{\ln Z_L}{L} &= \max_{\epsilon} (f(\epsilon) - \epsilon/T) + \ln K \\ &= \ln \left[K \int \rho(\epsilon) \exp(-\epsilon/T)\, d\epsilon \right] \\ &= \lim_{L\to\infty} \frac{\ln \langle Z_L \rangle}{L}. \end{aligned} \tag{5.26}$$

For $T < T_c$, the integral in eq.(5.23) is dominated by energies close to E_{GS}, because when $E/L < E_{GS}/L$, one has $\mathcal{N}_{\text{typical}} = 0$. Therefore

$$\lim_{L\to\infty} \frac{\ln Z_L}{L} = \lim_{L\to\infty} -\frac{E_{GS}}{LT}. \tag{5.27}$$

This reasoning can easily be generalised to calculate the typical fluctuations of the partition function. Using the fact that the fluctuations of $\mathcal{N}(E)$ are given by eq.(5.22), one finds that the magnitude of the fluctuations changes at $2T_c$. Thus one obtains

for $T < T_c$

$$Z_L(T) = c(T) \exp\left(-\frac{E_{GS}}{T}\right) \tag{5.28}$$

for $T_c < T < 2T_c$

$$\begin{aligned} Z_L(T) &= \langle Z_L(T) \rangle \pm c(T) \exp\left(-\frac{E_{GS}}{T}\right) \\ &= K^L \langle \exp(-\epsilon/T) \rangle^L \pm c(T) \exp\left(-\frac{E_{GS}}{T}\right) \end{aligned} \tag{5.29}$$

for $T > 2T_c$

$$\begin{aligned} Z_L(T) &= \langle Z_L(T) \rangle \pm c(T) \langle Z_L(T/2) \rangle^{1/2} \\ &= K^L \langle \exp(-\epsilon/T) \rangle^L \pm c(T) K^{L/2} \langle \exp(-2\epsilon/T) \rangle^{L/2} \end{aligned} \tag{5.30}$$

where in eqs.(5.28)–(5.30), $c(T)$ is a quantity which has sample-to-sample fluctuations of order 1. The appearance of the temperature $2T_c$ is simply due to the fact that

$$\int_{E_{GS}}^{E'_{GS}} \langle \mathcal{N}(E) \rangle^{1/2} \exp(-E/T)\, dE \tag{5.31}$$

is dominated by energies where $\langle \mathcal{N}(E) \rangle$ is large when $T > 2T_c$, whereas it is dominated by the neighbourhood of $E = E_{GS}$ when $T < 2T_c$.

5.3.2 The case $p \neq 0$

It was observed in eq.(5.19) that one could write Z_L as the difference of two $p = 0$ REM partition functions, Z_L^+ and Z_L^-. Since the random signs are chosen according to eq.(5.7), one knows that Z_L^+ and Z_L^- are the sum of

$$\frac{K^L}{2}\left(1 \pm (1-2p)^L \pm bK^{-L/2}\right) \tag{5.32}$$

terms respectively, where b is a sample-dependent number of order 1.

Using the results of eqs.(5.28)–(5.32) for Z_L^+ and Z_L^-, one finds that

for $T < T_c$

$$Z_L = Z_L^+ - Z_L^- \sim c(T) \exp\left(-\frac{E_{GS}}{T}\right) \tag{5.33}$$

for $T_c < T < 2T_c$

$$Z_L = Z_L^+ - Z_L^- = K^L \langle \exp(-\epsilon/T) \rangle^L (1-2p)^L \pm c(T) \exp\left(-\frac{E_{GS}}{T}\right) \tag{5.34}$$

for $2T_c < T$

$$Z_L = Z_L^+ - Z_L^- = K^L \langle \exp(-\epsilon/T) \rangle^L (1-2p)^L \pm c(T) K^{L/2} \langle \exp(-2\epsilon/T) \rangle^{L/2}. \tag{5.35}$$

The main difference between eqs.(5.34) and (5.35) and the case $p = 0$, eqs.(5.29) and (5.30), is that in eqs.(5.29) and (5.30) the fluctuating part was negligible compared with the leading term $\langle Z_L(T) \rangle$. In eqs.(5.34) and (5.35), the effect of the signs has been to reduce the average $\langle Z_L(T) \rangle$ by a factor $(1-2p)^L$, whilst the magnitude of the fluctuations is not affected by the signs. Therefore, depending on the temperature T and the probability p, the term which dominates eqs.(5.34) and (5.35) is either the term coming from the average or the fluctuating term. This leads to the following three possible expressions for $\langle \ln |Z_L(T)| \rangle / L$:

Phase I:

$$\lim_{L \to \infty} \frac{\ln |Z_L|}{L} = \ln \left[K \langle \exp(-\epsilon/T) \rangle \, |1-2p| \, \right] \tag{5.36}$$

Phase II:

$$\lim_{L \to \infty} \frac{\ln |Z_L|}{L} = -\frac{E_{GS}}{T} \tag{5.37}$$

Phase III:

$$\lim_{L \to \infty} \frac{\ln |Z_L|}{L} = \frac{1}{2} \ln \left[K \langle \exp(-2\epsilon/T) \rangle \, \right] \tag{5.38}$$

and to the facts that

- for $T < T_c$, the system is always in phase II
- for $T_c < T < 2T_c$, the system is either in phase I or phase II, depending upon which has the lower free energy
- for $T > 2T_c$, the system is either in phase I or phase III, again depending upon which has the lower free energy.

As eqs.(5.36) and (5.38) are both expressed in terms of the energy distribution $\rho(\epsilon)$, it would be more consistent to express E_{GS} in terms of $\rho(\epsilon)$ as well. This

can be done as follows. One can rewrite the relation between the function f and the distribution $\rho(\epsilon)$, eq.(5.9), as

$$\max_{\epsilon}\left(f(\epsilon)-\epsilon\Lambda+\ln K\right)=\ln\left[K\int\rho(\epsilon)\exp(-\Lambda\epsilon)\,d\epsilon\right]. \tag{5.39}$$

One can see that, if ϵ_0 is the value of ϵ which maximises the left-hand side of eq.(5.39), one has

$$f(\epsilon_0)+\ln K=\left(1-\Lambda\frac{d}{d\Lambda}\right)\ln\left[K\int\rho(\epsilon)\exp(-\Lambda\epsilon)\,d\epsilon\right]. \tag{5.40}$$

Therefore, if $\Lambda_{\min}$ is the value of Λ which minimises

$$\frac{1}{\Lambda}\ln\left[K\int\rho(\epsilon)\exp(-\Lambda\epsilon)\,d\epsilon\right], \tag{5.41}$$

one can see that the right-hand side of eq.(5.40) vanishes for $\Lambda=\Lambda_{\min}$. So, the corresponding energy ϵ_0 is the ground state energy, i.e.

$$f(\epsilon_0)+\ln K=0 \tag{5.42}$$

and, from eq.(5.39), it then follows that

$$E_{GS}=-\min_{\Lambda}\frac{1}{\Lambda}\ln\left[K\int\rho(\epsilon)\exp(-\Lambda\epsilon)\,d\epsilon\right]. \tag{5.43}$$

Using this formula for the ground state energy, the free energy in phase II can be written as

$$\lim_{L\to\infty}\frac{-T\ln|Z_L|}{L}=-\min_{\Lambda}\frac{T}{\Lambda}\ln\left[K\langle\exp(-\Lambda\epsilon/T)\rangle\right]. \tag{5.44}$$

5.4 The solution of the GREM of two steps

The GREM of n steps was defined in section 5.2.2. Here the case $n=2$ will be considered. One has a two-step tree structure with branching ratios α_1^L and α_2^L at the first and second steps respectively and one can choose that $\alpha_1\alpha_2=K$ (see eq.(5.11)). On each branch of the GREM one places a random energy $e_i^{(\mu)}$, chosen from the probability distribution of eq.(5.15), and a random sign $\sigma_i^{(\mu)}$, chosen according to

$$\begin{aligned}\sigma_i^{(\mu)}&=+1 \quad \text{with probability} \quad \frac{1}{2}\left(1+\phi_i^L(e_i^{(\mu)})\right)\\ \sigma_i^{(\mu)}&=-1 \quad \text{with probability} \quad \frac{1}{2}\left(1-\phi_i^L(e_i^{(\mu)})\right).\end{aligned} \tag{5.45}$$

The sign distribution has now been generalised to depend on energy (this will be useful in section 5.6). The case of uncorrelated sign and energy distributions can be recovered by setting $\phi_i(e_i^{(\mu)}) = (1-2p)^{a_i}$. The sign, S_μ, and the energy, E_μ, of the configuration μ, associated with a particular end point of the two-step tree, are defined as in eqs.(5.16) and (5.17) and one then defines the partition function to be

$$Z = \sum_{\mu=1}^{K^L} S_\mu \exp\left[-\frac{E_\mu}{T}\right]. \tag{5.46}$$

This problem has already been solved when all the signs are chosen to be the same [65,51]. This solution will now be extended to the more general case of eq.(5.45).

The average number of first step branches with a sign σ_1 and an energy e_1, $\langle \mathcal{N}_1^{\sigma_1}(e_1)\rangle$, is given by

$$\langle \mathcal{N}_1^{\sigma_1}(e_1)\rangle \sim \left(1+\sigma_1\phi_1^L(e_1)\right)\exp\left[L\left(a_1 f\left(\frac{e_1}{La_1}\right)+\ln\alpha_1\right)\right] \tag{5.47}$$

where the energy distribution eq.(5.15) has been used. The function f is convex and so one expects there to be two energies, e_{GS} and e'_{GS} ($e_{GS} < e'_{GS}$), for which $\langle \mathcal{N}_1^{\sigma_1}(e_1)\rangle \sim 1$. For energies below e_{GS} or above e'_{GS}, the average, eq.(5.47), is exponentially small in L. Hence

$$\mathcal{N}_1^{\sigma_1}(e_1)_{\text{typical}} = 0. \tag{5.48}$$

For energies between e_{GS} and e'_{GS}, $\langle \mathcal{N}_1^{\sigma_1}\rangle$ is exponentially large in L and so

$$\mathcal{N}_1^{\sigma_1}(e_1)_{\text{typical}} = \langle \mathcal{N}_1^{\sigma_1}(e_1)\rangle + c^{\sigma_1}(e_1)\langle \mathcal{N}_1^{\sigma_1}(e_1)\rangle^{1/2} \tag{5.49}$$

where $c^{\sigma_1}(e_1)$ is a fluctuating quantity of order 1.

Knowing the typical values of $\mathcal{N}_1^{\sigma_1}(e_1)$, one can then calculate the average number of configurations with energy E and sign σ_1 on the first step and σ_2 on the second step, $\langle \mathcal{N}^{\sigma_1,\sigma_2}(E)\rangle$, given that $\mathcal{N}_1^{\sigma_1}(e_1)$ is given by its typical value, eqs.(5.48) and (5.49).

$$\langle \mathcal{N}^{\sigma_1,\sigma_2}(E)\rangle \sim \int de\, \mathcal{N}_1^{\sigma_1}(e)_{\text{typical}}\left(1+\sigma_2\phi_2^L(E-e)\right)\exp\left[L\left(\ln\alpha_2 + a_2 f\left(\frac{E-e}{La_2}\right)\right)\right] \tag{5.50}$$

So, using eqs.(5.48) and (5.49),

$$\langle \mathcal{N}^{\sigma_1,\sigma_2}(E)\rangle \sim \int_{e_{GS}}^{e'_{GS}} de\left\{\left(1+\sigma_1\phi_1^L(e)\right)\exp\left[L\left(\ln\alpha_1 + a_1 f\left(\frac{e}{La_1}\right)\right)\right]\right.$$

$$+ \quad c^{\sigma_1}(e) \exp\left[\frac{L}{2}\left(\ln \alpha_1 + a_1 f\left(\frac{e}{La_1}\right)\right)\right]\Big\}$$
$$\times \quad \left(1+\sigma_2 \phi_2^L(E-e)\right) \exp\left[L\left(\ln \alpha_2 + a_2 f\left(\frac{E-e}{La_2}\right)\right)\right]. \quad (5.51)$$

The integrals in eq.(5.51) can be done by a saddle method. One replaces each integral by the integrand evaluated either at its saddle point, if the saddle point lies within the range of integration, or at the boundary, if the saddle point is not in the allowed range. From its average, eq.(5.51), one can then determine the typical value of $\mathcal{N}^{\sigma_1,\sigma_2}(E)$, as was done for $\mathcal{N}_1^{\sigma_1}(e_1)$, i.e.

$$\begin{aligned} \mathcal{N}^{\sigma_1,\sigma_2}(E)_{\text{typical}} &= 0 && \text{if } \langle \mathcal{N}^{\sigma_1,\sigma_2}(E)\rangle \ll 1 \\ &= \langle \mathcal{N}^{\sigma_1,\sigma_2}(E)\rangle + d^{\sigma_1,\sigma_2}(E)\langle \mathcal{N}^{\sigma_1,\sigma_2}(E)\rangle^{1/2} && \text{if } \langle \mathcal{N}^{\sigma_1,\sigma_2}(E)\rangle \gg 1 \end{aligned} \quad (5.52)$$

where $d^{\sigma_1,\sigma_2}(E)$ is a fluctuating quantity of order 1. The total density of levels weighted by the signs, $\mathcal{N}(E)$, can then be evaluated by summing over the contributions from each $\mathcal{N}^{\sigma_1,\sigma_2}$:

$$\mathcal{N}(E)_{\text{typical}} = \sum_{\sigma_1,\sigma_2=\pm 1} \sigma_1\sigma_2 \mathcal{N}^{\sigma_1,\sigma_2}(E)_{\text{typical}}. \quad (5.53)$$

As expression eq.(5.51) is rather cumbersome, let us just consider the case

$$f(x) = -\frac{x^2}{2}; \quad \phi_i(e) = (1-2p)^{a_i}; \quad a_i = \frac{\ln \alpha_i}{\ln K}. \quad (5.54)$$

For this choice, one obtains

$$\begin{aligned} \mathcal{N}(E)_{\text{typical}} &= (1-2p)^L K^L \exp\left[-\frac{e^2}{2La_1} - \frac{(E-e)^2}{2La_2}\right] \\ &+ d(E) K^{L/2} \exp\left[-\frac{e^2}{4La_1} - \frac{(E-e)^2}{4La_2}\right] \end{aligned} \quad (5.55)$$

where

$$\begin{aligned} e &= a_1 E && \text{if } \left|\frac{E}{L}\right| < \left(\frac{2\ln \alpha_1}{a_1}\right)^{1/2} \\ &= L\sqrt{2a_1 \ln \alpha_1} && \text{otherwise} \end{aligned} \quad (5.56)$$

and $d(E)$ is a fluctuating quantity of order 1 and therefore such that

$$\lim_{L\to\infty} (\ln d(E))/L \to 0.$$

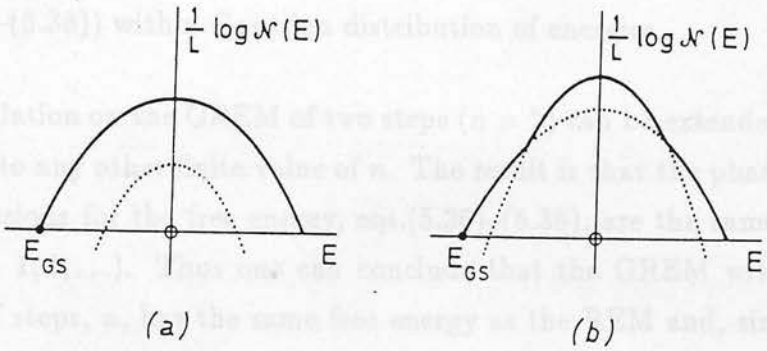

Figure 5.2: The solid line shows the shape of $(\ln \mathcal{N}(E)_{\text{typical}})/L$ for the two-step GREM of section 5.4 for two values of p, (a) if $\ln|1-2p| < -\frac{1}{2}\ln K$ and (b) if $-\frac{1}{2}\ln K < \ln|1-2p|$. In (a) $\mathcal{N}(E)_{\text{typical}}$ is dominated at all energies by fluctuations. In (b) there are three regions: the middle one where $\mathcal{N}(E)_{\text{typical}}$ is equal to $\langle\mathcal{N}(E)\rangle$ and the side ones where $\mathcal{N}(E)_{\text{typical}}$ is dominated by fluctuations.

Also, if eq.(5.55) gives an exponentially small value, one must take $\mathcal{N}(E)_{\text{typical}} = 0$.

For this particular choice of energy and sign distribution, eq.(5.54), chosen to mimic the mean field generalised polymer, one finds that eqs.(5.55) and (5.56) lead to $\mathcal{N}(E)_{\text{typical}}$ of the form shown in figure 5.2.

Knowing $\mathcal{N}(E)_{\text{typical}}$ one can calculate the typical value of the partition function using the relation

$$Z(T) = \int dE\, \mathcal{N}(E) \exp(-E/T). \tag{5.57}$$

Evaluating this integral by taking the saddle point corresponds to identifying $1/T$ with the slope of the curve $\ln \mathcal{N}(E)$. One can see that this leads to two phases, separated by a second order transition, when $\ln \mathcal{N}(E)$ has the form shown in figure 5.2a.

When $\ln \mathcal{N}(E)$ has the form of figure 5.2b, one can obtain three phases, with the

two high temperature phases separated by a first order transition. This corresponds geometrically to the existence of a straight line that is tangent to $\ln \mathcal{N}(E)$ at two points. Carrying out this procedure for all values of p, one sees that this two-step GREM has the same free energy as the corresponding REM, (see eqs.(5.36)–(5.38)) with a Gaussian distribution of energies.

This calculation on the GREM of two steps ($n = 2$) can be extended, without any difficulty, to any other finite value of n. The result is that the phase diagram and the expressions for the free energy, eqs.(5.36)–(5.38), are the same for all values of n ($n = 1, 2, \ldots$). Thus one can conclude that the GREM with an arbitrary number of steps, n, has the same free energy as the REM and, since for large n, the GREM looks increasingly like the mean field generalised polymer problem, it is reasonable to conjecture that the generalised directed polymer problem also has the same free energy in the mean field limit.

The reasoning of this section can be extended to functions f more general then that of eq.(5.54). Also, if instead of random signs on each branch of the GREM one took some complex phases, i.e. $\sigma = \exp(i\theta)$ with θ random, the reasoning of sections 5.3 and 5.4 would remain unchanged and one would conclude that the REM, the GREM and the corresponding mean field directed polymer problem would still have identical free energies.

Of course, if one makes a more general choice for the a_i and the α_i (which would not mimic the mean field polymer) then the final results would depend on n and on the particular choices of the a_i and the α_i, as has already been noticed for the GREM when $p = 0$ [65,51].

5.5 The mean field solution of the generalised directed polymer problem

Having solved the REM and GREM and found that they have identical free energies over the entire phase diagram, it has been concluded, see sections 5.2 and 5.4, that this free energy will also be that of the mean field limit of the generalised

directed polymer problem of section 5.1.

In contrast to the two phases that occur in the standard mean field directed polymer problem, in the generalised model there are three phases.

Phase I:

$$\lim_{L\to\infty} \frac{\langle \ln |Z_L| \rangle}{L} = \ln \left[K \int \rho(\epsilon) \exp(-\epsilon/T)\, d\epsilon \right] + \ln\left(|1-2p|\right) \tag{5.58}$$

Phase II:

$$\lim_{L\to\infty} \frac{\langle \ln |Z_L| \rangle}{L} = \min_{\Lambda} \frac{1}{\Lambda} \ln \left[K \int \rho(\epsilon) \exp(-\Lambda\epsilon/T)\, d\epsilon \right] \tag{5.59}$$

Phase III:

$$\lim_{L\to\infty} \frac{\langle \ln |Z_L| \rangle}{L} = \frac{1}{2} \ln \left[K \int \rho(\epsilon) \exp(-2\epsilon/T)\, d\epsilon \right] \tag{5.60}$$

Which phase the system finds itself in is determined by the value of Λ, $\Lambda_{\min}$, that minimises the right-hand side of eq.(5.59). If $\Lambda_{\min} < 1$, the system is always in phase II. If $1 < \Lambda_{\min} < 2$, $\langle \ln |Z_L| \rangle / L$ is given by the larger of the expressions in eqs.(5.58) and (5.59). If $\Lambda_{\min} > 2$, $\langle \ln |Z_L| \rangle / L$ is given by the larger of the expressions given in eqs.(5.58) and (5.60).

The phase diagram for the case when the energy distribution is chosen to be the Gaussian

$$\rho(\epsilon) = \frac{1}{\sqrt{2\pi}} \exp[-\epsilon^2/2] \tag{5.61}$$

and $K = 2$ is shown in figure 5.3. For this distribution the three possible expressions for $\langle \ln |Z_L| \rangle / L$ are

Phase I:

$$\lim_{L\to\infty} \frac{\langle \ln |Z_L| \rangle}{L} = \frac{1}{2T^2} + \ln K + \ln\left(|1-2p|\right) \tag{5.62}$$

Phase II:

$$\lim_{L\to\infty} \frac{\langle \ln |Z_L| \rangle}{L} = \frac{(2\ln K)^{1/2}}{T} \tag{5.63}$$

Phase III:

$$\lim_{L\to\infty} \frac{\langle \ln |Z_L| \rangle}{L} = \frac{1}{T^2} + \frac{1}{2} \ln K \tag{5.64}$$

and the transition lines are

$$\ln|1-2p| = -\frac{1}{2}\left(\frac{1}{T} - \frac{1}{T_0}\right)^2 \quad \text{for} \quad T \le 2T_0 \tag{5.65}$$

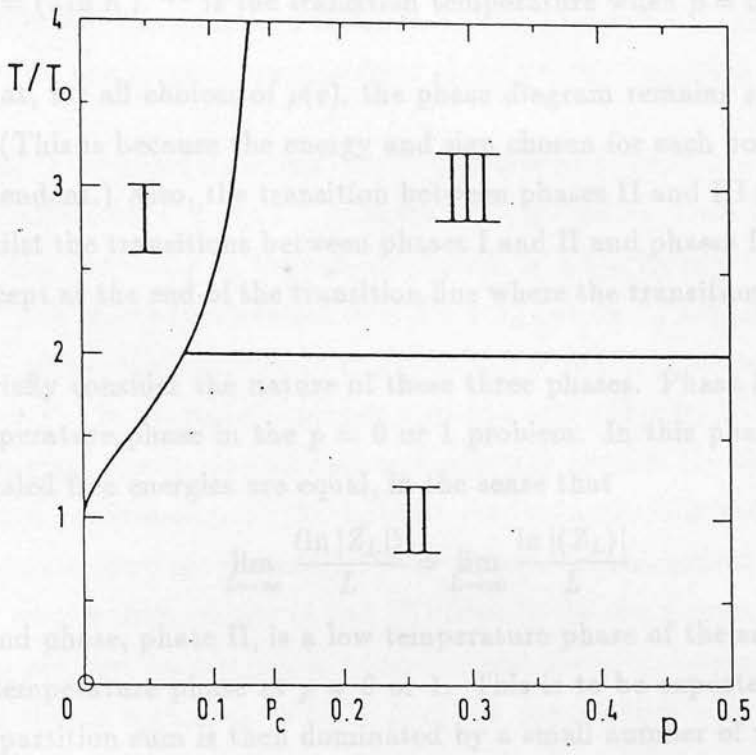

Figure 5.3: The phase diagram for the mean field directed polymer problem with $K = 2$ and Gaussian bonds (eq.(5.61)), showing the positions of the three phases, eqs.(5.62)–(5.64). p_c shows the asymptotic position of the boundary between phases I and II when $T \to \infty$. The temperature scale is in units of $T_0 = (2\ln 2)^{-1/2}$.

$$\ln|1-2p| = \frac{1}{2T^2} - \frac{1}{4T_0^2} \quad \text{for} \quad T \geq 2T_0 \tag{5.66}$$

$$\ln|1-2p| \leq -\frac{1}{8T_0^2} \quad \text{for} \quad T = 2T_0 \tag{5.67}$$

where $T_0 = (2\ln K)^{-1/2}$ is the transition temperature when $p = 0$ or 1.

Notice that, for all choices of $\rho(\epsilon)$, the phase diagram remains symmetric about $p = 1/2$. (This is because the energy and sign chosen for each bond of the lattice are independent.) Also, the transition between phases II and III is always second order, whilst the transitions between phases I and II and phases I and III are first order, except at the end of the transition line where the transition is second order.

Let us briefly consider the nature of these three phases. Phase I is very like the high temperature phase in the $p = 0$ or 1 problem. In this phase the quenched and annealed free energies are equal, in the sense that

$$\lim_{L\to\infty} \frac{\langle \ln|Z_L| \rangle}{L} = \lim_{L\to\infty} \frac{\ln|\langle Z_L \rangle|}{L}. \tag{5.68}$$

The second phase, phase II, is a low temperature phase of the same character as the low temperature phase at $p = 0$ or 1. This is to be expected, as one knows that the partition sum is then dominated by a small number of walks and so the addition of random signs is unlikely to lead to any dramatic interference effects. Phase III is a high temperature phase in which interference effects between walks with similar energies, but opposite signs, are very important.

Having presented the solution and briefly discussed the nature of the three phases, these theoretical predictions will now be compared with numerical simulations. The simulations were performed in the following manner. Instead of directly simulating a tree structure, which would be difficult due to the exponential growth of the number of bonds with the polymer length, the geometry of figure 3.7 was used. The lattice was taken to consist of L layers, each containing N points. Each site at layer l was connected to K randomly chosen sites in layer $l+1$, the bonds being assigned random energies, according to the distribution of eq.(5.61), and random signs ($-$ with probability p and $+$ with probability $1-p$). If one keeps K fixed, as one increases the number of sites in each layer, N, the structure will begin locally to resemble a tree with branching ratio K. This procedure of keeping K fixed and examining how the simulations converge as N becomes large allows one

to simulate much larger systems. The particular case chosen for the simulation was $K = 2$ and Gaussian bonds (see eq.(5.61)). (The phase diagram for this case is shown in figure 5.3.) Polymers of length $L = 5.10^5$ for $N = 1$, $L = 15.10^4$ for $N = 10$, $L = 5.10^4$ for $N = 100$, $L = 15.10^3$ for $N = 1000$ and $L = 5.10^3$ for $N = 10000$ were simulated. In order to explore the phase diagram of figure 5.3 three lines on the diagram were selected along which to perform the simulations.

The results of the simulations are shown, together with the theoretical predictions, see eqs.(5.62)–(5.64) and fig. 5.3, in figure 5.4. Figure 5.4a shows how $T\langle \ln |Z_L| \rangle / L$ varies as one changes p at the temperature $T = 1.5 \times T_0$ and figure 5.4b shows the same, but at the temperature $T = 2.5 \times T_0$ (where $T_0 = (2 \ln 2)^{-1/2}$). Lastly, figure 5.4c shows the dependence of $T\langle \ln |Z_L| \rangle / L$ on temperature, when one fixes p at $p = 0.05$. In all three cases one sees the first order transition as a cusp in the free energy. The numerical data converge well towards the theoretical results, giving good confirmation of the analytic expressions. It is noticeable that the numerical data converge markedly better towards the theoretical prediction in the two high temperature phases (I and III) than in the low temperature phase (II). It has, as yet, not been possible to understand these convergence rates. (There is only a simple argument to show that the convergence is always faster than $\ln(\ln N)/\ln N$.)

Unfortunately, the mean field solution presented above cannot settle the debate about the values of the exponents ω and ν for $p \neq 0$ or 1, that was mentioned in section 5.1. One can conclude from these results that a new phase (phase III) appears at the mean field level, which is not present when there are no random signs in the problem. However, one does not know whether this phase persists in low dimensions, and if it does, whether it would lead to changed values for the exponents.

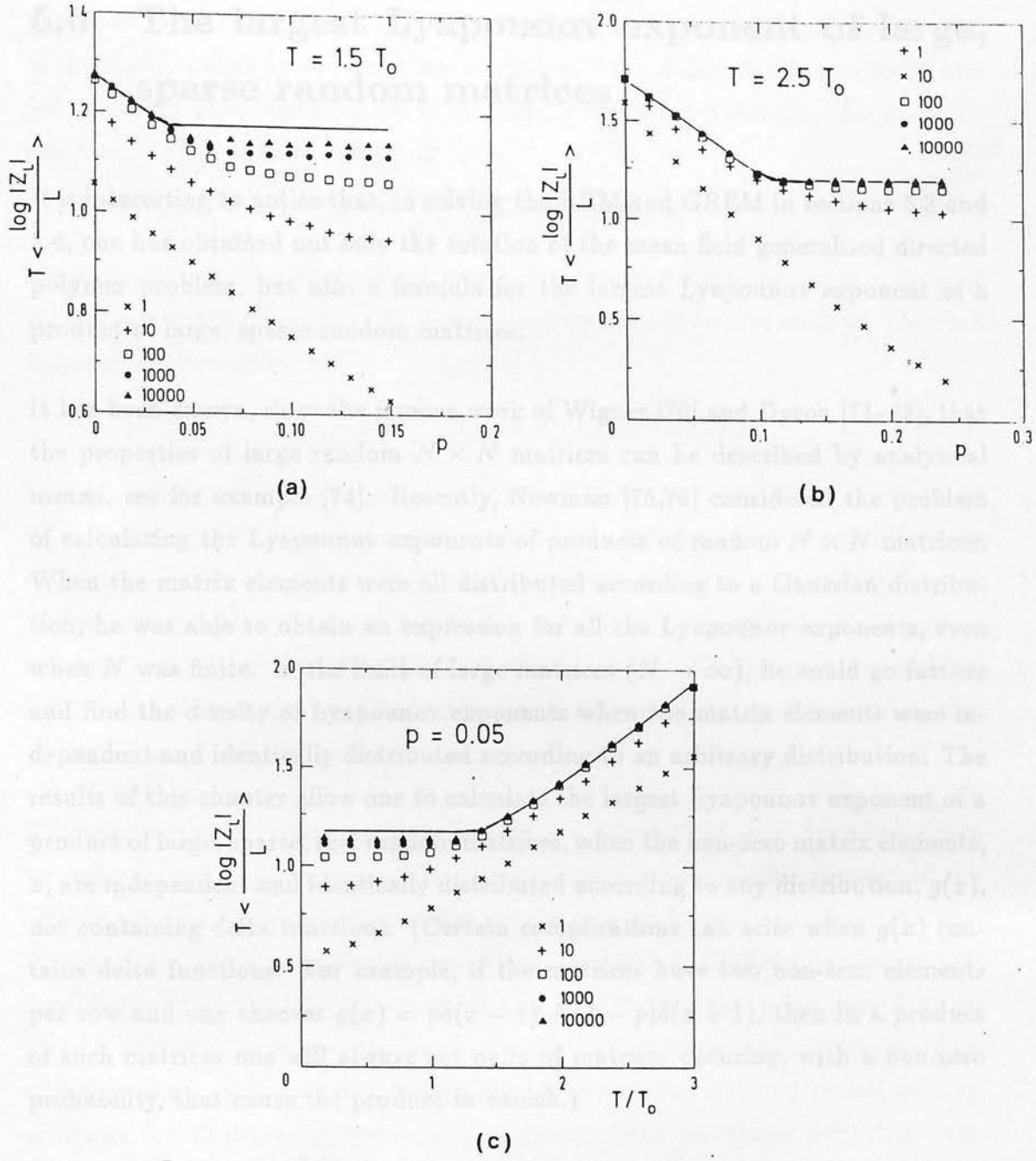

Figure 5.4: $\langle T \ln |Z_L| \rangle / L$ for the generalised directed polymer problem in the geometry of figure 3.7, with $K = 2$ and Gaussian bonds, along three lines on the phase diagram. The lines explored are (a) $T = 1.5T_0$ and p varied, (b) $T = 2.5T_0$ and p varied and (c) $p = 0.05$ and T varied. The solid curves show the analytic predictions, eqs(5.62)–(5.64), and the points are the results of numerical simulations for $N = 1$, $N = 10$, $N = 100$, $N = 1000$ and $N = 10000$.

5.6 The largest Lyapounov exponent of large, sparse random matrices

It is interesting to notice that, in solving the REM and GREM in sections 5.3 and 5.4, one has obtained not only the solution of the mean field generalised directed polymer problem, but also a formula for the largest Lyapounov exponent of a product of large, sparse random matrices.

It has been known, since the famous work of Wigner [70] and Dyson [71–73], that the properties of large random $N \times N$ matrices can be described by analytical means, see for example [74]. Recently, Newman [75,76] considered the problem of calculating the Lyapounov exponents of products of random $N \times N$ matrices. When the matrix elements were all distributed according to a Gaussian distribution, he was able to obtain an expression for all the Lyapounov exponents, even when N was finite. In the limit of large matrices ($N \to \infty$), he could go further and find the density of Lyapounov exponents when the matrix elements were independent and identically distributed according to an arbitrary distribution. The results of this chapter allow one to calculate the largest Lyapounov exponent of a product of large, sparse, real random matrices, when the non-zero matrix elements, x, are independent and identically distributed according to any distribution, $g(x)$, not containing delta functions. (Certain complications can arise when $g(x)$ contains delta functions. For example, if the matrices have two non-zero elements per row and one chooses $g(x) = p\delta(x-1) + (1-p)\delta(x+1)$, then in a product of such matrices one will always get pairs of matrices occuring, with a non-zero probability, that cause the product to vanish.)

To see the link between the largest Lyapounov exponent of a product of large, sparse random matrices and the problem with which this chapter began, that of generalised directed polymers, consider the directed polymer problem of section 5.1 in the geometry of figure 3.7. (This has already been briefly mentioned in section 5.5.) One has a series of L layers, each layer being composed of N points. The points will be labelled by integers, n ($n = 1, 2, \ldots, N$). Suppose that each point in layer l is connected to K points in layer $l+1$, these K sites being chosen at random from the N possible points. There are then KN bonds between layer l

and layer $l+1$. One places a random energy, ϵ_{ij}, and a random sign, S_{ij}, on each of the chosen bonds ij and one then considers all the walks that pass through one point in each plane that can be formed using the selected bonds. The partition function, $Z_L(n)$, is then defined as

$$Z_L(n) = \sum_w \prod_{ij \in w} (S_{ij} \exp(-\epsilon_{ij}/T)) \tag{5.69}$$

the sum running over all walks of length L emanating from the point n in layer L, and the product including all bonds that are visited by the walk w. One can then write a recursion for Z_L

$$Z_{L+1}(n) = \sum_{m=1}^{N} S_{nm} \exp(-\epsilon_{nm}/T) Z_L(m). \tag{5.70}$$

One can see that the vector $\{Z_{L+1}\}$ is obtained from $\{Z_L\}$ by multiplication by an $N \times N$ matrix with K non-zero random elements per row. As was pointed out in section 5.5, when one allows N to become large in this geometry, whilst keeping K fixed, the problem begins to resemble a tree with branching ratio K. Hence, as one is interested in calculating $\langle \ln |Z_L| \rangle$, the mean field directed polymer problem can be thought of in terms of finding the largest Lyapounov exponent of a product of large, sparse random matrices.

The generalised polymer problem chooses the energy and sign distributions to be independent of each other. However, as was shown in the solution of the GREM, section 5.4, it is still possible to solve the problem if one allows the sign distribution to be energy-dependent. If one does this, the REM and GREM will continue to have identical free energies and so it is possible to infer the formula for the largest Lyapounov exponent of a product of large, real, sparse random matrices, the non-zero elements of which are independent and distributed with an arbitrary distibution $g(x)$ (provided that distributions containing delta functions are excluded).

In terms of the distribution, $g(x)$, the largest Lyapounov exponent, γ, of random $N \times N$ matrices, with K non-zero real elements per row, is given, in the limit $N \to \infty$ with K fixed, by

$$\gamma = \gamma_{II} \qquad \text{if } \Lambda_{\min} \leq 1 \tag{5.71}$$

$$\gamma = \max(\gamma_I, \gamma_{II}) \qquad \text{if } 1 \leq \Lambda_{\min} \leq 2 \tag{5.72}$$

$$\gamma = \max(\gamma_I, \gamma_{III}) \qquad \text{if } 2 \leq \Lambda_{\min} \tag{5.73}$$

where

$$\gamma_I = \ln\left[K\left|\int_{-\infty}^{+\infty} g(x)\, x\, dx\right|\right] \tag{5.74}$$

$$\gamma_{II} = \mathcal{G}(\Lambda_{\min}) \tag{5.75}$$

$$\gamma_{III} = \mathcal{G}(2) \tag{5.76}$$

$$\mathcal{G}(\Lambda) = \frac{1}{\Lambda}\ln\left[K\int_{-\infty}^{+\infty} g(x)|x|^{\Lambda} dx\right] \tag{5.77}$$

and $\Lambda_{\min}$ is the value of Λ that minimises $\mathcal{G}(\Lambda)$.

Again it is possible to compare these theoretical predictions with numerical simulations. Here, three different distributions, $g(x)$, are considered:

$$\text{Example 1: } g(x) = 1 \quad \text{if } a \le x \le 1+a$$
$$= 0 \quad \text{otherwise} \tag{5.78}$$

$$\text{Example 2: } g(x) = a x^{-(a+1)} \quad x \ge 1$$
$$0 \quad x < 1 \tag{5.79}$$

$$\text{Example 3: } g(x) = \frac{1}{2} a |x|^{-(a+1)} \quad |x| \ge 1$$
$$0 \quad |x| < 1 \tag{5.80}$$

These distributions are sketched in figure 5.5.

For each of these examples, the largest Lyapounov exponent was calculated for three matrix sizes $N = 1, 100, 10000$ by performing the product of 5.10^5 (for $N = 1$), 5.10^4 (for $N = 100$), and 5.10^3 (for $N = 10000$) random matrices. The number of non-zero elements per row was chosen to be $K = 4$.

The positions of the K non-zero elements in each row were chosen at random. When two elements were placed at the same location they were added.

The results of the simulations for these examples are shown in figure 5.6, together with the analytical expressions for γ, obtained from eqs.(5.71)–(5.77).

For example 1, see eq.(5.78), one sees in figure 5.6a that there is a transition at $a = -1/3$. Below this value of a, the numerical results converge towards γ_{III}, whereas above it they converge to γ_I. This agrees with the theoretical prediction.

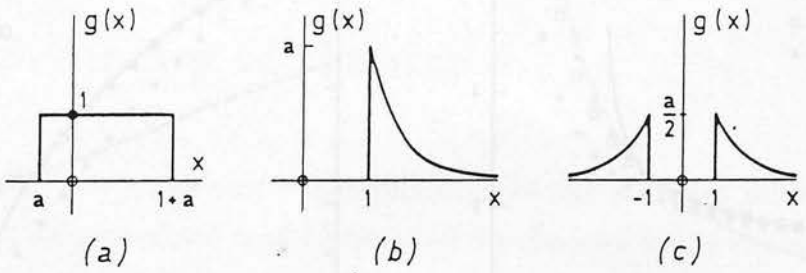

Figure 5.5: The distributions, $g(x)$, used to calculate the largest Lyapounov exponent in the numerical simulations shown in figure 5.6, (a) eq.(5.78), (b) eq.(5.79) and (c) eq.(5.80).

For this choice of $g(x)$, eq.(5.78), one always finds that $\Lambda_{\min} > 2$ and so one expects to observe only cases I and III.

To observe case II, one has to chose a distribution $g(x)$ that can give $\Lambda_{\min} < 2$, eqs.(5.79) and (5.80). In the case of the distribution of eq.(5.79), eqs.(5.71)–(5.77) predict a transition between γ_{II} and γ_I as a is increased. This can clearly be seen from the numerical data in figure 5.6b, where the analytic expressions eq.(5.74) and (5.75) are also shown. For large values of a the results converge rapidly towards γ_I, and below $a \simeq 1.37$ the results converge towards γ_{II}, although the convergence rate is notably poorer in this case.

Lastly a power law distribution, symmetric about $x = 0$ was considered, see eq.(5.80). Clearly one does not expect to observe case I now, as from eq.(5.74) one sees that $\gamma_I = -\infty$. The numerical results are shown in figure 5.6c, together with the analytic expressions for γ_{II} and γ_{III}, eqs.(5.75) and (5.76). For large enough a the numerical data converge rapidly towards γ_{III}, whereas below $a \simeq 2.74$ they converge towards γ_{II} with a slower convergence rate.

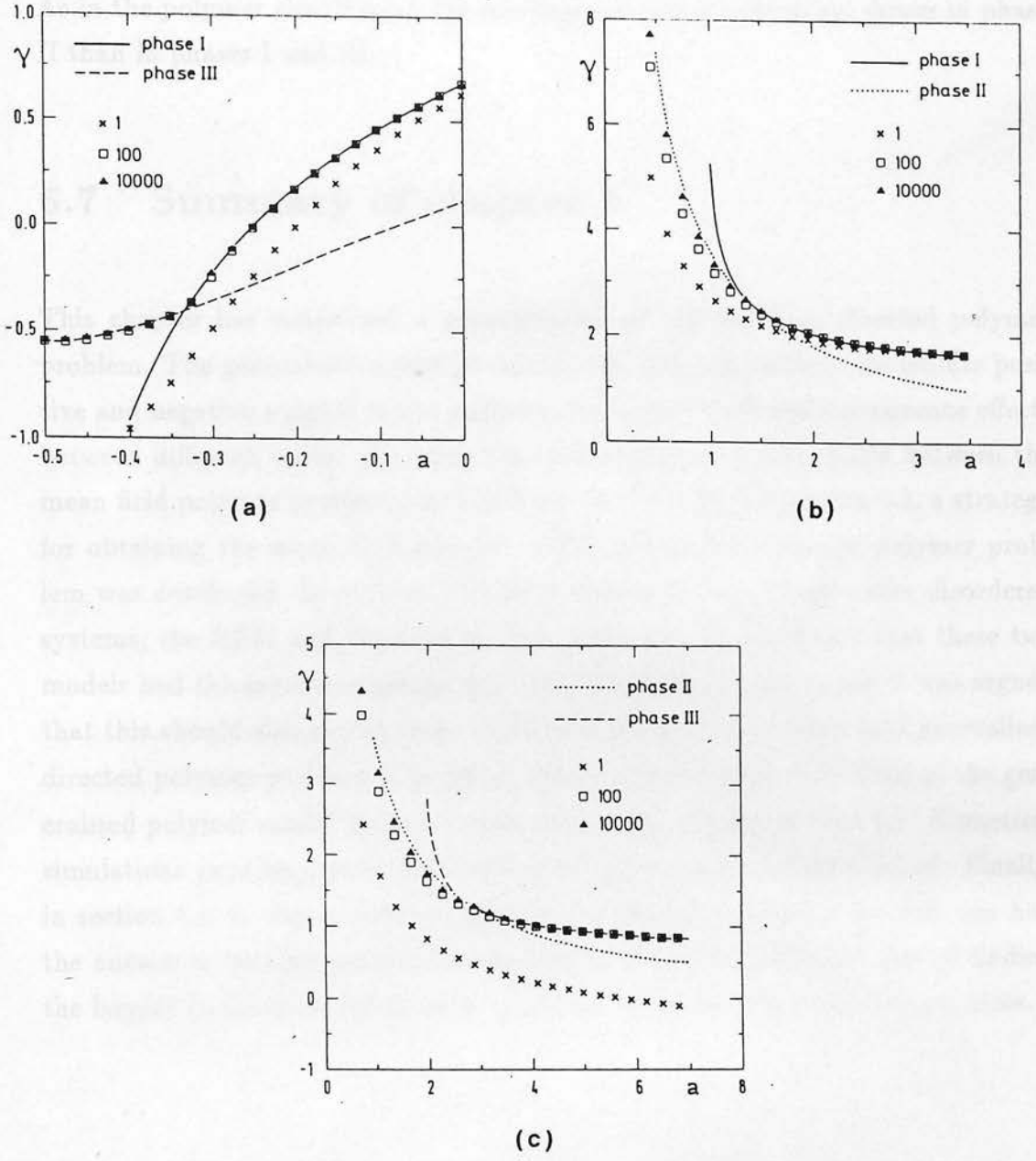

Figure 5.6: The largest Lyapounov exponent, γ, plotted against the parameter a, for the distributions $g(x)$ in (a) fig. 5.5a, (b) fig. 5.5b and (c) fig. 5.5c. The curves show the analytical results (—— γ_I eq.(5.74), • • • • γ_{II} eq.(5.75) and - - - - - γ_{III} eq.(5.76)) and the points show the numerical data for system sizes $N = 1$, $N = 100$ and $N = 10000$.

So, the simulations again provide good confirmation of the analytical predictions. As in the polymer simulations, the convergence rate is noticeably slower in phase II than in phases I and III.

5.7 Summary of chapter 5

This chapter has considered a generalisation of the standard directed polymer problem. The generalised model permitted the directed walks to contribute positive and negative weights to the partition sum, and so allowed interference effects between different walks. By using the close relationship that exists between the mean field polymer problem, the REM and the GREM, see section 5.2, a strategy for obtaining the mean field solution of this generalised directed polymer problem was developed. In sections 5.3 and 5.4 the solutions to two other disordered systems, the REM and the GREM, were obtained. It was found that these two models had the same free energy over the entire phase diagram and it was argued that this should also be the same as the free energy of the mean field generalised directed polymer problem. The phase diagram of the mean field limit of the generalised polymer model defined in section 5.1 was given in section 5.5. Numerical simulations gave very good confirmation of these analytical predictions. Finally, in section 5.6, it was mentioned that, in the results of sections 5.3–5.5, one had the answer to another problem in the field of disordered systems: that of finding the largest Lyapounov exponent of a product of large, sparse random matrices.

Appendix A

The n-tree approximation to the d-dimensional lattice is a tree structure consisting of branches of a number of types. For example, the 2-tree consists of two types of branches, those which are formed by only one path and those which are made up of two paths (see fig. 3.2b). This appendix shows how one can calculate the fraction of each type of branch used by a typical walk on an n-tree. This quantity is needed in the calculation of the overlaps in section 3.2.4.

To see how one can evaluate these fractions, let us consider the simpler problem of directed walks on a tree, with branching ratio K, when one has a discrete distribution of energies. Suppose that the probability of choosing a bond with energy ϵ_i is given by ρ_i, the ϵ_i forming a discrete set $\{\epsilon_i\}$

$$\rho(\epsilon) = \sum_i \rho_i \delta(\epsilon - \epsilon_i). \tag{A.1}$$

The free energy per unit length of the system is then given by eq.(3.12)

$$\begin{aligned} F(T) &= -G(\gamma_{\min}) \qquad T \leq T_c \\ &= -G(1/T) \qquad T \geq T_c \end{aligned} \tag{A.2}$$

where

$$G(\gamma) = \frac{1}{\gamma} \ln \left[K \sum_i \rho_i e^{-\gamma \epsilon_i} \right] \tag{A.3}$$

and $\gamma_{\min}$ is the unique solution of

$$\left. \frac{dG(\gamma)}{d\gamma} \right|_{\gamma_{\min}} = 0. \tag{A.4}$$

Let N_i denote the number of branches of type i in the walks. One can then write the partition function Z_L as

$$Z_L = \sum_{N_1=0}^{L} z_L(N_1) \mathrm{e}^{-\epsilon_1 N_1/T} \tag{A.5}$$

where $z_L(N_1)$ is a partial partition function for all walks of length L containing exactly N_1 steps on bonds of type 1. The aim is to calculate the average number of steps in direction 1

$$\left\langle \overline{N_1} \right\rangle = \left\langle Z_L^{-1} \sum_{N_1=0}^{L} N_1 z_L(N_1) \mathrm{e}^{-\epsilon_1 N_1/T} \right\rangle \tag{A.6}$$

where $\overline{\cdots}$ denotes a thermal average. Comparing eqs.(A.6) and (A.5) one sees that the average of N_1 can be obtained as a derivative of the free energy

$$\left\langle \overline{N_1} \right\rangle = -T \frac{\partial}{\partial \epsilon_1} \langle \ln Z_L \rangle \tag{A.7}$$

and so, from eqs.(A.2)–(A.4), it follows that

$$\left\langle \overline{N_1}/L \right\rangle = \frac{\partial F}{\partial \epsilon_1} = \frac{\rho_1 \mathrm{e}^{-\gamma \epsilon_1}}{\sum_i \rho_i \mathrm{e}^{-\gamma \epsilon_i}} \tag{A.8}$$

where $\gamma = \gamma_{\min}$ for $T \leq T_c$ and $\gamma = 1/T$ for $T \geq T_c$.

This idea can be extended to continuous distributions and used to calculate the average fraction of each type of branch used by walks on an n-tree. As the simplest example consider the 2-tree, although the extension to the n-tree is easy. From eqs.(3.42) and (3.43), the free energy per unit length of the 2-tree is given in the low temperature phase by

$$F_2(T) = -\frac{1}{2\gamma_{\min}} \ln \left[d \left\langle \mathrm{e}^{-\epsilon \gamma_{\min}} \right\rangle^2 + \frac{d(d-1)}{2} \left\langle \left(\mathrm{e}^{-(\epsilon_1+\epsilon_2)/T} + \mathrm{e}^{-(\epsilon_3+\epsilon_4)/T} \right)^{T\gamma_{\min}} \right\rangle \right] . \tag{A.9}$$

where $\gamma_{\min}$ is defined by eqs.(3.44) and (3.42). To calculate the overlap for the 2-tree (see section 3.2.4) one needs to know the typical fraction of branches used in a walk on the 2-tree which consist of two paths with energies $\epsilon_1 + \epsilon_2$ and $\epsilon_3 + \epsilon_4$ on the constituent links. Extending eq.(A.8) to continuous distributions and effective bonds, one can see, from eq.(A.9), that this fraction is given in the low temperature phase by

$$\frac{\frac{d(d-1)}{2} \left(\mathrm{e}^{-(\epsilon_1+\epsilon_2)/T} + \mathrm{e}^{-(\epsilon_3+\epsilon_4)/T} \right)^{T\gamma_{\min}} \rho(\epsilon_1)\rho(\epsilon_2)\rho(\epsilon_3)\rho(\epsilon_4)}{d \left\langle \mathrm{e}^{-\epsilon \gamma_{\min}} \right\rangle^2 + \frac{d(d-1)}{2} \left\langle \left(\mathrm{e}^{-(\epsilon_1+\epsilon_2)/T} + \mathrm{e}^{-(\epsilon_3+\epsilon_4)/T} \right)^{T\gamma_{\min}} \right\rangle} . \tag{A.10}$$

This is the result quoted in eq.(3.78). This method can easily be extended to calculate the average fraction of its length spent by a walk on any type of branch on the n-tree.

Appendix B

This appendix discusses some of the properties of the function

$$f(t,\lambda) = \int_{-\infty}^{+\infty} \frac{du}{(2\pi)^{1/2}} \exp\left[-\frac{1}{2}u^2 - te^{\lambda u}\right]. \tag{B.1}$$

It is organized as follows. First the radius of convergence of the series expansion of $f(t,\lambda)$ about $t = 0$ is considered. Next the various asymptotic expansions of $f(t,\lambda)$ for large λ are derived. Lastly the method of obtaining the low temperature expansions used in chapter 4 is presented.

B.1 Radius of Convergence

It is stated in section 4.3.3 that the series expansion of $f(t,\lambda)\ln f(t,\lambda)$ about $t = 0$ has a zero radius of convergence. This can easily be verified by considering the form of the Taylor series for $f(t,\lambda)$ about $t = 0$:

$$f(t,\lambda) = \sum_{k=0}^{\infty} \frac{t^k}{k!} f^{(k)}(0,\lambda). \tag{B.2}$$

The derivatives of $f(t,\lambda)$ evaluated at $t = 0$ are

$$f^{(k)}(0,\lambda) = (-1)^k \int \exp\left[k\lambda u - \frac{1}{2}u^2 - te^{\lambda u}\right] \frac{du}{(2\pi)^{1/2}}\bigg|_{t=0} = (-1)^k e^{k^2\lambda^2/2}. \tag{B.3}$$

Hence, the coefficients of the series expansion about $t = 0$ increase with k faster than any exponential, and so the series in eq.(B2) has a zero radius of convergence. As $f(t,\lambda)$ has a zero radius of convergence, then the same must be true for

$f(t,\lambda)\ln f(t,\lambda)$. The fact that the derivatives of $f(t,\lambda)$ with respect to t, evaluated at $t=0$, have such a simple form allows the integer moments, eq.(4.110), and overlaps $\langle Q(2+p)\rangle$, eqs.(4.92),(4.97) and (4.98), to be calculated relatively easily.

B.2 Asymptotic Expansion

The asymptotic expansion (large λ, which corresponds to the low temperature limit) of the function $f(t,\lambda)$ will now be considered.

The asymptotic form of $f(t,\lambda)$ depends upon the range of t considered. It is necessary to consider three cases (i) $\ln t \sim \lambda$, (ii) $\ln t \sim \lambda^2$ with $\ln t > 0$ and (iii) $-p\lambda^2 < \ln t < -(p-1)\lambda^2$ with p a positive integer. These three cases will now be considered separately and the relevant asymptotic form of $f(t,\lambda)$ obtained.

B.2.1 $\ln t \sim \lambda$

Consider making the change of variable $t = \exp(\lambda z)$. If now, the derivative of $f(z,\lambda)$ with respect to λ is considered, it is found to have the form

$$\frac{df}{d\lambda}(z,\lambda) = -\int_{-\infty}^{\infty} \frac{du}{(2\pi)^{1/2}}(u+z)\exp\left\{\lambda(u+z) - \frac{1}{2}u^2 - \exp[\lambda(u+z)]\right\} \quad \text{(B.4)}$$

and so only the immediate region of $u=-z$ contributes substantially to the integral. So, letting $u = -z + v/\lambda$, eq.(B4) becomes

$$\frac{df}{d\lambda}(z,\lambda) = -\frac{\exp(-z^2/2)}{\lambda^2}\int \frac{dv}{(2\pi)^{1/2}} v \exp\left[v + \frac{zv}{\lambda} - \frac{v^2}{2\lambda^2} - \mathrm{e}^v\right]. \quad \text{(B.5)}$$

Expanding the exponentials in powers of v/λ and noting that

$$\int_{-\infty}^{\infty} v^p \exp\left[v - \mathrm{e}^v\right] dv = \Gamma^{(p)}(1) \quad \text{(B.6)}$$

(where $\Gamma^{(k)}(1)$ is the k^{th} derivative of the gamma function evaluated at 1) one finds

$$\frac{df}{d\lambda}(z,\lambda) = -\frac{\mathrm{e}^{-z^2/2}}{(2\pi)^{1/2}\lambda^2}\left[\Gamma^{(1)}(1) + \frac{z}{\lambda}\Gamma^{(2)}(1) + \frac{1}{2\lambda^2}(z^2-1)\Gamma^{(3)}(1) + O\left(\frac{1}{\lambda^3}\right)\right]. \quad \text{(B.7)}$$

Hence one sees that $f(t,\lambda)$ can be written as

$$f(t,\lambda) = \int_{\ln t/\lambda}^{\infty} \frac{du}{(2\pi)^{1/2}} e^{-u^2/2} + \frac{\exp(-\ln^2 t/2\lambda^2)}{(2\pi)^{1/2}} \times \left[\frac{\Gamma^{(1)}(1)}{\lambda} + \frac{\Gamma^{(2)}(1)}{2\lambda^2}\frac{\ln t}{\lambda} + \frac{\Gamma^{(3)}(1)}{6\lambda^3}\left(\frac{\ln^2 t}{\lambda^2} - 1\right) + \cdots \right] \quad \text{(B.8)}$$

where it has been noted that

$$f(z,\infty) = \int_z^{\infty} \frac{du}{(2\pi)^{1/2}} e^{-u^2/2}. \quad \text{(B.9)}$$

It will be useful to define

$$F(z) = \int_z^{\infty} \frac{du}{(2\pi)^{1/2}} e^{-u^2/2}. \quad \text{(B.10)}$$

B.2.2 $\ln t \sim \lambda^2$ with $\ln t > 0$

To derive the asymptotic form of $f(t,\lambda)$ in this case, consider the change of variable $z = te^{\lambda u}$. This converts eq.(B1) into

$$f(t,\lambda) = \frac{1}{(2\pi)^{1/2}\lambda} \exp\left(-\frac{\ln^2 t}{2\lambda^2}\right) \int_0^{\infty} dz\, z^{(\ln t)/\lambda^2 - 1} \exp\left[-z - \frac{\ln^2 z}{2\lambda^2}\right]. \quad \text{(B.11)}$$

The integrand is exponentially damped for large z, so it is valid to expand the final exponential for small arguments to obtain

$$\begin{aligned} f(t,\lambda) &= \frac{1}{(2\pi)^{1/2}\lambda} \exp\left(-\frac{\ln^2 t}{2\lambda^2}\right) \\ &\times \int_0^{\infty} dz\, z^{(\ln t)/\lambda^2 - 1} \left[1 - \frac{\ln^2 z}{2\lambda^2} + O\left(\frac{1}{\lambda^4}\right)\right] e^{-z} \\ &= \frac{1}{(2\pi)^{1/2}\lambda} \exp\left(-\frac{\ln^2 t}{2\lambda^2}\right) \\ &\times \left[\Gamma\left(\frac{\ln t}{\lambda^2}\right) - \frac{1}{2\lambda^2}\Gamma^{(2)}\left(\frac{\ln t}{\lambda^2}\right) + O\left(\frac{1}{\lambda^4}\right)\right]. \end{aligned} \quad \text{(B.12)}$$

B.2.3 $-p\lambda^2 < \ln t < -(p-1)\lambda^2$ with p a positive integer

It has been shown for a very similar integral (see the appendix of [64]) that, for this range of t, the asymptotic form of $f(t,\lambda)$ is

$$f(t,\lambda) = 1 - te^{\lambda^2/2} + \frac{t^2}{2!}e^{2\lambda^2} + \cdots + (-1)^{p-1}\frac{t^{p-1}}{(p-1)!}e^{(p-1)^2\lambda^2/2}$$

$$+ \frac{1}{(2\pi)^{1/2}\lambda} e^{-\ln^2 t/2\lambda^2} \left[\Gamma\left(\frac{\ln t}{\lambda^2}\right) - \frac{1}{2\lambda^2}\Gamma^{(2)}\left(\frac{\ln t}{\lambda^2}\right) + O\left(\frac{1}{\lambda^4}\right)\right]. \quad \text{(B.13)}$$

B.3 The low temperature expansions

Having obtained the asymptotic forms of $f(t,\lambda)$, let us now consider how to obtain the low temperature expansions stated in eqs.(4.65), (4.94), (4.95), (4.113), (4.114) and (4.115). In each case it is necessary to calculate an integral over the variable t with an integrand which is a product of some power of t and a simple function of $f(t,\lambda)$. It has just been shown that $f(t,\lambda)$ has different asymptotic forms depending upon the range of t. Hence, to evaluate the required integrals one must first determine which of the asymptotic forms of $f(t,\lambda)$ it is necessary to use. For all the integrals required, the integrand is sharply peaked in one of the three regions of t considered above. Hence it is only necessary to use one of the three possible asymptotic forms of $f(t,\lambda)$ for the calculation of the integrals. So, the low temperature expansions fall into three classes, depending upon which range of t dominates the integrand. Each class of expansion will be dealt with separately.

B.3.1 Class a

In the low temperature expansions of free energy eq.(4.65), $\langle q \rangle$ eq.(4.94), $\langle q(m) \rangle$ eq.(4.95), and moments with $\mu = 0$ eq.(4.115), the integrals are dominated by t in the range $\ln t \sim \lambda$. Consider the calculation of the free energy as an example of this class, in which one needs to consider the integral

$$\int_0^\infty \frac{dt}{t} f(t,\lambda) \ln f(t,\lambda) = \int_{-\infty}^\infty d(\ln t) f(t,\lambda) \ln f(t,\lambda). \quad \text{(B.14)}$$

Consider first case (i) i.e. $\ln t \sim \lambda$. Then setting $\ln t = \lambda z$, the integrand behaves as

$$f(t,\lambda) \ln f(t,\lambda) \sim F(z) \ln F(z)$$

where $F(z)$ is defined in eq.(B10).

Now take case (ii), $\ln t \sim \lambda^2$, where the integrand has the behaviour

$$f(t,\lambda)\ln f(t,\lambda) \sim -\frac{1}{\lambda}e^{-\ln^2 t/2\lambda^2}\left(\frac{\ln^2 t}{2\lambda^2}+\ln\lambda\right).$$

This has its extremal value near $(\ln t)/\lambda^2 = 0$, which is the boundary of region (ii), and that means that the range of t which dominates the integral is elsewhere. Finally let us consider case (iii). For $-p\lambda^2 < \ln t < -(p-1)\lambda^2$

$$\begin{aligned} f(t,\lambda)\ln f(t,\lambda) &\simeq -te^{\lambda^2/2} && \text{for } p>1 \\ &\simeq \frac{1}{(2\pi)^{1/2}\lambda}e^{-\ln^2 t/2\lambda^2}\Gamma\left(\frac{\ln t}{\lambda^2}\right)+\cdots && \text{for } p=1. \end{aligned}$$

Each of these terms is exponentially small i.e. $\sim \exp(-\text{const.}\lambda^2)$ and so the integrand is very much smaller for this range of t than for case (i). Hence the integral in eq.(B14) is dominated by $\ln t \sim \lambda$. Similar consideration shows that this is also true for the integrals in eqs.(4.94), (4.95) and (4.115), when $\mu/T \to 0$.

Now it just remains to evaluate eq.(B14) using the appropriate asymptotic form of $f(t,\lambda)$, eq.(B8):

$$\begin{aligned} \int_0^\infty \frac{dt}{t}f(t,\lambda)\ln f(t,\lambda) &= \lambda\int_{-\infty}^{\infty}dz\left\{F(z)\ln F(z)+\frac{1}{\lambda}\frac{e^{-z^2/2}}{(2\pi)^{1/2}}\Gamma^{(1)}(1)[1+\ln F(z)]\right. \\ &+ \frac{1}{2\lambda^2}\left[\frac{ze^{-z^2/2}}{(2\pi)^{1/2}}\Gamma^{(2)}(1)[1+\ln F(z)]+\frac{e^{-z^2}}{2\pi}\frac{\Gamma^{(1)^2}(1)}{F(z)}\right] \\ &+ \frac{1}{\lambda^3}\left[\frac{(z^2-1)}{2}\frac{e^{-z^2/2}}{(2\pi)^{1/2}}\frac{\Gamma^{(3)}(1)}{3}[1+\ln F(z)]\right. \\ &+ \left.\left.\frac{ze^{-z^2}}{4\pi}\frac{\Gamma^{(1)}(1)\Gamma^{(2)}(1)}{F(z)}-\frac{e^{-3z^2/2}}{(2\pi)^{3/2}}\frac{\Gamma^{(1)^3}(1)}{6F^2(z)}\right]\right\}. \end{aligned} \tag{B.15}$$

Hence, via eq.(4.64), one obtains

$$\begin{aligned} F_n = \varepsilon\left[-K_1\sum_{i=1}^{n-1}\frac{1}{2^{i/2}}+\left(\frac{\Gamma^{(1)^2}(1)-\Gamma^{(2)}(1)}{2}\right)K_1T^2\sum_{i=1}^{n-1}\frac{1}{2^{3i/2}}\right. \\ + \left.\left\{-\frac{\Gamma^{(3)}(1)}{3}+\Gamma^{(1)}(1)\Gamma^{(2)}(1)-\frac{2\Gamma^{(1)^3}(1)}{3}\right\}K_2T^3\sum_{i=1}^{n-1}\frac{1}{4^i}+O(T^4)\right] \end{aligned} \tag{B.16}$$

where K_1 and K_2 are as given in eqs.(4.66) and (4.67).

The low temperature expansions of $\langle q\rangle$, $\langle q(m)\rangle$ and the moments with $\mu = 0$ are obtained in exactly the same manner.

B.3.2 Class b

The integrals contained in the expression for the negative moments of the partition function and the overlaps $\langle Q(2+\mu)\rangle$ with $\mu < -2$ are dominated in the low temperature limit by t in the range $\ln t \sim +\lambda^2$. As an example, consider the negative moments, eqs.(4.108) and (4.113), for which one must evaluate the integral

$$\int_0^\infty dt \frac{t^{-\mu-1}}{\Gamma(-\mu)} f(t,\lambda) \ln f(t,\lambda) = \int_{-\infty}^\infty \frac{d(\ln t)}{\Gamma(-\mu)} t^{-\mu} f(t,\lambda) \ln f(t,\lambda). \qquad \text{(B.17)}$$

First let us show that the integrand is sharply peaked for $\ln t \sim +\lambda^2$ and then eq.(4.113) will be derived. For $\ln t \sim \lambda$ let us again make the change of variable $\ln t = \lambda z$ to see that the integrand behaves as

$$t^{-\mu} f(t,\lambda) \ln f(t,\lambda) \sim \mathrm{e}^{-\mu\lambda z} F(z) \ln F(z).$$

For case (ii), with $\ln t \sim +\lambda^2$, the integrand has the form

$$t^{-\mu} f(t,\lambda) \ln f(t,\lambda) \sim -\frac{\mathrm{e}^{-\mu \ln t}}{\lambda} \mathrm{e}^{-\ln^2 t/2\lambda^2} \left[\frac{\ln^2 t}{2\lambda^2} + \ln \lambda\right].$$

This has an extremum near $\ln t = -\mu\lambda^2$ and at this point it takes a value of the order $\lambda \exp(\mu^2\lambda^2/2)$.

Lastly, for case (iii), $-p\lambda^2 < \ln t < -(p-1)\lambda^2$,

$$\begin{aligned} t^{-\mu} f(t,\lambda) \ln f(t,\lambda) &\sim -\mathrm{e}^{-\mu \ln t} t \mathrm{e}^{\lambda^2/2} && \text{for } p > 1 \\ &\sim \mathrm{e}^{-\mu \ln t} \frac{1}{(2\pi)^{1/2}\lambda} \mathrm{e}^{-\ln^2 t/2\lambda^2} \Gamma\left(\frac{\ln t}{\lambda^2}\right) && \text{for } p = 1. \end{aligned}$$

Again all these terms are exponentially small, $\sim \exp(-\text{const.}\lambda^2)$. Hence the integrand is seen to be peaked for $\ln t \sim +\lambda^2$.

Now one can evaluate eq.(B17) using the asymptotic form of $f(t,\lambda)$ for case (ii), eq.(B12). Using the change of variable $t = \mathrm{e}^{\lambda^2 z}$, one obtains

$$\begin{aligned} &\int_0^\infty dt \frac{t^{-\mu-1}}{\Gamma(-\mu)} f(t,\lambda) \ln f(t,\lambda) \\ &= \frac{\lambda}{\Gamma(-\mu)} \frac{1}{(2\pi)^{1/2}} \int_{-\infty}^\infty dz\, \mathrm{e}^{-\mu\lambda^2 z} \mathrm{e}^{-\lambda^2 z^2/2} \left[-\Gamma(z) \ln[(2\pi)^{1/2}\lambda]\right. \\ &- \left.\frac{\lambda^2 z^2}{2}\Gamma(z) + \Gamma(z)\ln\Gamma(z) + \frac{z^2}{4}\Gamma^{(2)}(z) + \cdots\right]. \qquad \text{(B.18)} \end{aligned}$$

This can be simplified by making the change of variable, $y = z + \mu$, and then expanding the gamma functions for small y, the exponential damping out any contribution from large y. Then, performing the remaining integrals, one obtains, using eq.(4.106),

$$\langle Z_{n+1}^{\mu} \rangle - \langle Z_n^{\mu} \rangle^2 = \varepsilon \exp\left(\frac{\mu^2 2^{n-1}}{T^2}\right) \left\{ -\frac{2^{n-1}\mu^2}{T^2} - \ln\left(\frac{(2\pi)^{1/2} 2^{n/2}}{T}\right) + \frac{\mu\Gamma^{(1)}(-\mu)}{\Gamma(-\mu)} + \ln\Gamma(-\mu) - \frac{1}{2} \right\}. \tag{B.19}$$

The low temperature expansion of the overlaps $\langle Q(2+\mu) \rangle$ with $\mu < -2$ is obtained in the same manner.

B.3.3 Class c

Lastly, in the low temperature expansions of the positive moments, eq.(4.114), and the overlaps $\langle Q_n(2+\mu) \rangle$ for $\mu > -2$, the integrals are dominated by t in the range $-(p-1)\lambda^2 > \ln t > -p\lambda^2$. As an example, consider the low temperature expansion of the positive moments with $m > \mu > m-1$. Here one needs to evaluate the integral

$$\begin{aligned} &\int_0^{\infty} dt\, t^{m-\mu-1} (-1)^m \frac{d^m}{dt^m} \left[f(t,\lambda) \ln f(t,\lambda) \right] \\ &= \int_{-\infty}^{\infty} d(\ln t) \mathrm{e}^{(m-\mu)\ln t} (-1)^m \frac{d^m}{dt^m} \left[f(t,\lambda) \ln f(t,\lambda) \right]. \end{aligned} \tag{B.20}$$

For $\ln t \sim \lambda$, with $t = \mathrm{e}^{\lambda z}$, the integrand behaves, for large λ, as

$$t^{m-\mu} \frac{d^m}{dt^m} \left[f(t,\lambda) \ln f(t,\lambda) \right] \sim \mathrm{e}^{-\mu \ln t}.$$

Secondly let us look at $\ln t \sim \lambda^2$, then the integrand behaves as

$$t^{m-\mu} \frac{d^m}{dt^m} \left[f(t,\lambda) \ln f(t,\lambda) \right] \sim \mathrm{e}^{-\mu \ln t} \mathrm{e}^{-\ln^2 t/2\lambda^2}$$

which is of the form $\exp(-\mathrm{const.}\lambda^2)$.

Lastly consider $-p\lambda^2 < \ln t < -(p-1)\lambda^2$. In this range of t the integrand has the form

$$t^{m-\mu} \frac{d^m}{dt^m} \left[f(t,\lambda) \ln f(t,\lambda) \right] \sim \mathrm{e}^{-\mu \ln t} \mathrm{e}^{-\ln^2 t/2\lambda^2}.$$

This has a maximum when $-\lambda^2\mu = \ln t$, when it takes the value $e^{\mu^2\lambda^2/2}$. This is much greater than the value of the integrand in either of the other regions. So, the correct form of $f(t,\lambda)$ to use is that for t in the range $-m\lambda^2 < \ln t < -(m-1)\lambda^2$. Having determined the dominant range of t it is now straightforward to evaluate the low temperature expansion for the positive moments from eq.(4.109), using the same approach to evaluating the integrals as explained for the treatment of eq.(B18). This yields the results of eq.(4.114). The overlaps $\langle Q_n(2+\mu)\rangle$ for $\mu > -2$ can be evaluated by the same method.

References

[1] M. Mézard , G. Parisi and M. A. Virasoro, "*Spin Glass Theory and Beyond* " (World Scientific, Singapore, 1987).

[2] M. Kardar, G. Parisi and Y. C. Zhang, *Phys. Rev. Lett.* **56** 889 (1986).

[3] M. Kardar and Y. C. Zhang, *Phys. Rev. Lett.* **58** 2087 (1987).

[4] D. A. Huse and C. L. Henley, *Phys. Rev. Lett.* **54** 2708 (1985).

[5] D. A. Huse, C. L. Henley and D. S. Fisher, *Phys. Rev. Lett.* **55** 2924 (1985).

[6] M. Eden, in "*Proceedings of the IV Berkeley Symposium on Mathematical Statistics and Probability* ", F. Neyman, ed. (University of California Press, Berkeley, CA, 1961) Vol.4 p.223.

[7] M. J. Vold, *J. Colloid Interface Sci.*, **18** 684 (1963).

[8] M. Plischke and Z. Rácz, *Phys. Rev. Lett.* **53** 415 (1984).

[9] F. Family and T. Viscek, *J. Phys. A* **18** L75 (1985).

[10] S. F. Edwards and D. R. Wilkinson, *Proc. R. Soc. Lond. A* **381** 17 (1982).

[11] J. Krug and H. Spohn, in "*Solids far from Equilibrium: Growth, Morphology and Defects* ", C. Godrèche, ed. (1990).

[12] J. M. Burgers, "*The Nonlinear Diffusion Equation* " (D. Reidel, Dordrecht, Holland, 1974).

[13] S. Zaleski, *Physica D* **34** 427 (1989).

[14] B. Derrida and H. Spohn, *J. Stat. Phys.* **51** 817 (1988).

[15] D. Sherrington and S. Kirkpatrick, *Phys. Rev. Lett.* **35** 1792 (1975).

[16] G. Parisi, *J. Phys. A* **13** 1101 (1980).

[17] G. Parisi, *J. Phys. A* **13** 1887 (1980).

[18] N. Sourlas, *Europhys. Lett.* **1** 189 (1986).

[19] D. A. Huse and D. S. Fisher, *J. Phys. A* **20** L997 (1987).

[20] D. S. Fisher and D. A. Huse, *Phys. Rev. B* **38** 386 (1988).

[21] A. J. Bray and M. A. Moore, *J. Phys. C* **12** 79 (1979).

[22] C. de Dominicis and I. Kondor, *J. Physique Lett.* **46** L1037 (1985).

[23] W. van Saarloos, *Phys. Rev. A* **37** 211 (1988) and references therein.

[24] W. van Saarloos, *Phys. Rev. A* **39** 6367 (1989) and references therein.

[25] J. M. Hammersley, *Ann. Prob.* **2** 652 (1974).

[26] Y. Shapir and X. R. Wang, *Europhys. Lett.* **4** 1165 (1987).

[27] V. L. Nguyen, B. Z. Spivak and B. I. Shklovskii, *J.E.T.P. Lett.* **41** 42 (1985).

[28] V. L. Nguyen, B. Z. Spivak and B. I. Shklovskii, *Sov. Phys. J.E.T.P.* **62** 1021 (1985).

[29] M. Kardar, *Nucl. Phys. B* **290** 582 (1987).

[30] J. Krug, *Phys. Rev. A* **36** 5465 (1987).

[31] E. Medina, T. Hwa, M. Kardar and Y. C. Zhang, *Phys. Rev. A* **39** 3053 (1989).

[32] D. Forster, D. R. Nelson and M. J. Stephen, *Phys. Rev. A* **16** 732 (1977).

[33] T. Halpin-Healy, *Phys. Rev. Lett.* **62** 442 (1989).

[34] T. Nattermann, Jülich preprint (1989).

[35] T. Halpin-Healy, *Phys. Rev. A* in press.

[36] D. E. Wolf and J. Kertész, *Europhys. Lett.* **4** 651 (1987).

[37] J. M. Kim and J. M. Kosterlitz, *Phys. Rev. Lett.* **62** 2289 (1989).

[38] B. M. Forrest and L. H. Tang, *Phys. Rev. Lett.* **64** 1405 (1990).

[39] B. Derrida and O. Golinelli, *Phys. Rev. A* **41** 4160 (1990).

[40] G. Parisi, Rome preprint ROMF2 -89/24 (1989).

[41] M. Mézard, Ecole Normale Supérieure, Paris preprint (1990).

[42] W. Renz, private communication.

[43] J. Z. Imbrie and T. Spencer, *J. Stat. Phys.* **52** 609 (1988).

[44] J. Cook and B. Derrida, *J. Stat. Phys.* **57** 89 (1989).

[45] J. Cook and B. Derrida, *Europhys. Lett.* **10** 195 (1989).

[46] J. Cook and B. Derrida, *J. Phys. A* **23** 1523 (1990).

[47] B. Derrida and R. B. Griffiths, *Europhys. Lett.* **8** 111 (1989).

[48] J. Cook and B. Derrida, Saclay preprint S Ph T 90/055 (1990).

[49] E. W. Montroll and B. J. West, in "*Fluctuation phenomena* ", E. W. Montroll and J. L. Lebowitz, eds. (North-Holland, Amsterdam, 1979) p.61.

[50] B. Derrida, *Physica A* **163** 71 (1990).

[51] B. Derrida and E. Gardner, *J. Phys. C* **19** 5783 (1986).

[52] M. Bramson, "*Convergence of solutions of the Kolmogorov equation to travelling waves* ", (Memories of the American Mathematical Society, No. 285, 1983).

[53] G. Parisi, *Phys. Rev. Lett.* **50** 1946 (1983).

[54] M. Mézard, G. Parisi, N. Sourlas, G. Toulouse and M. A. Virasoro, *J. Phys.* (Paris) **45** 843 (1984).

[55] J. Blease, *J. Phys. C* **10** 925 (1977).

[56] M. E. Fisher and R. R. P. Singh, in "*Disorder in Physical Systems* ", eds. G.

Grimmett and D. J. A. Welsh.

[57] D. Dhar, *Phys. Lett. A* **130** 308 (1988).

[58] A. N. Berker and S. Ostlund *J. Phys. C* **12** 4961 (1979).

[59] M. Kaufmann and R. B. Griffiths, *Phys. Rev. B* **24** 496 (1981).

[60] M. Kaufmann and R. B. Griffiths, *Phys. Rev. B* **30** 244 (1984).

[61] D. Andelman and A. N. Berker, *Phys. Rev. B* **29** 2630 (1984).

[62] B. Derrida and E. Gardner, *J. Phys. A* **17** 3223 (1984).

[63] E. Gardner, *J. Phys.* (Paris) **45** 1755 (1984).

[64] B. Derrida, *Phys. Rev. B* **24** 2613 (1981).

[65] B. Derrida, *J. Physique Lett.* **46** L401 (1985).

[66] E. Medina, M. Kardar, Y. Shapir and X. R. Wang, *Phys. Rev. Lett.* **62** 941 (1989).

[67] Y. C. Zhang, *Phys. Rev. Lett.* **62** 979 (1989).

[68] Y. C. Zhang, *Europhys. Lett.* **9** 113 (1989).

[69] Y. C. Zhang, *J. Stat. Phys.* **57** 1123 (1989).

[70] E. P. Wigner, *Ann. Math.* **62** 548 (1955).

[71] F. J. Dyson, *J. Math. Phys.* **3** 140 (1962).

[72] F. J. Dyson, *J. Math. Phys.* **3** 157 (1962).

[73] F. J. Dyson, *J. Math. Phys.* **3** 166 (1962).

[74] M. L. Mehta, "*Random Matrices and the Statistical Theory of Energy Levels* ", (Academic Press, New York, 1967).

[75] C. M. Newman, *Commun. Math. Phys.* **103** 121 (1986).

[76] C. M. Newman, *Contemporary Mathematics* **50** 121 (1986).